AL/EQ-TR-1993-0034

CATALYTIC DESTRUCTION OF CHLORINATED VOLATILE ORGANIC COMPOUNDS

Howard L. Greene

Chemical Engineering Department
University of Akron
Akron OH 44325

ENVIRONICS DIRECTORATE
139 Barnes Drive, Suite 2
Tyndall AFB FL 32403-5323

August 1993

Final Technical Report for Period October 1988 - July 1992

AIR FORCE MATERIEL COMMAND
TYNDALL AIR FORCE BASE, FLORIDA 32403-5323

NOTICES

This report was prepared as an account of work sponsored by an agency of the United States Government. Neither the United states Government nor any agency thereof, nor any employees, nor any of their contractors, subcontractors, or their employees, make any warranty, expressed or implied, or assume any legal liability or responsibility for the accuracy, completeness, or usefulness of any privately owned rights. Reference herein to any specific commercial product, process, or service by trade name, trademark, manufacturer, or otherwise, does not necessarily constitute or imply its endorsement, recommendation, or favoring by the United States Government or any agency, contractor, or subcontractor thereof. The views and opinions of the authors expressed herein do not necessarily state or reflect those of the United States Government or any agency, contractor, or subcontractor thereof.

When Government drawings, specifications, or other data are used for any purpose other than in connection with a definitely Government-related procurement, the United States government incurs no way supplied the said drawings, specifications, or other data, is not to be regarded by implication, or otherwise in any manner construed , as licensing the holder or any other person or corporation; or as conveying any rights or permission to manufacture, use, or sell any patented invention that may in any way be related thereto.

This technical report has been reviewed by the Public Affairs Office (PA) and is relasable to the National Technical Information Service, where it will be available to the general public, including foreign nationals.

This report has been reviewed and is approved for publication.

Edward G. Marchand

EDWARD G. MARCHAND, Capt, USAF,
Project Officer

Robert G. LaPoe

ROBERT G. LaPOE, Maj, USAF
Chief, Site Remediation
R&D Division

Neil J. Lamb

NEIL J. LAMB, Col, USAF
Director,
Environics Directorate

REPORT DOCUMENTATION PAGE

Form Approved
OMB No. 0704-0188

1. AGENCY USE ONLY (Leave blank)	2. REPORT DATE	3. REPORT TYPE AND DATES COVERED
	August 1993	Final; Oct 1988 - Jul 1992

4. TITLE AND SUBTITLE

Catalytic Destruction of Chlorinated Volatile Organic Compounds

5. FUNDING NUMBERS

USEPA Contract
CR-815095-02

6. AUTHOR(S)

Greene, Howard L.

7. PERFORMING ORGANIZATION NAME(S) AND ADDRESS(ES)

Chemical Engineering Department
University of Akron
Akron OH 44325

8. PERFORMING ORGANIZATION REPORT NUMBER

9. SPONSORING/MONITORING AGENCY NAME(S) AND ADDRESS(ES)

AL/EQW
139 Barnes Dr, Suite 2
Tyndall AFB FL 32403-5323
Environics Directorate, Armstrong Lab

10. SPONSORING/MONITORING AGENCY REPORT NUMBER

AL/EQ-TR-1993-0034

11. SUPPLEMENTARY NOTES

Joint US Air Force/Environmental Protection Agency effort.

12a. DISTRIBUTION/AVAILABILITY STATEMENT

Distribution Unlimited

12b. DISTRIBUTION CODE

13. ABSTRACT *(Maximum 200 words)*

This report gives test results for 14 different cation-modified zeolite catalysts, all of which were prepared in our laboratories. Three different dilute vapor phase feeds (trichloroethylene, carbon tetrachloride, and methylene chloride) were investigated in detail for catalytic destruction characteristics over a temperature range from 175-600 °C. Long term catalyst thermal stability studies were carried out at high temperature (600 °C), while deactivation by coking was investigated at temperatures as low as 175 °C. It was found that the most active catalysts for destruction of One-carbon VOCs were cobalt exchanged Y-zeolites, while for two-carbon VOCs, the presence of chromium in the catalyst was highly desirable, preferably in the impregnated form. Thus the most versatile active catalyst for the destruction of mixed feeds was shown to be a cobalt exchanged, chromium impregnated Y-zeolite known as Co-Y/CA.

14. SUBJECT TERMS	15. NUMBER OF PAGES
Catalysts, zeolites, chlorinated organics, destruction, volatile organics, vapor treatment, catalytic oxidation	97
	16. PRICE CODE

17. SECURITY CLASSIFICATION OF REPORT	18. SECURITY CLASSIFICATION OF THIS PAGE	19. SECURITY CLASSIFICATION OF ABSTRACT	20. LIMITATION OF ABSTRACT
UNCLASSIFIED	UNCLASSIFIED	UNCLASSIFIED	SAR (UL)

(Reverse of this pg blank)

PREFACE

This report was prepared by the Chemical Engineering Department, University of Akron, Akron OH 44325, EPA Contract No. CR-815095-02, for the U.S. Environmental Protection Agency (EPA) and the Armstrong Laboratory Environics Directorate (AL/EQ), Suite 2, 139 Barnes Drive Tyndall Air Force Base, Florida 32403-5323.

This final report describes the development, characterization and evaluation of potentially superior modified zeolite catalysts for chlorinated volatile organic compound (CVOC) oxidation. The metrics used to measure successful catalysts were high activity at low temperatures (300-350 °C), high selectivity to complete oxidation products, and superior thermal stability. Catalysts from this laboratory effort can now be tested in the field to treat vapor streams containing these CVOCs.

The work was performed between October 1988 and July 1992. The AL/EQW project officer was Captain Edward G. Marchand. EPA project managers were Chester Vogel and Carlos Nunez of the Air & Energy Engineering Research Laboratory, Research Triangle Park, NC 27711.

(The reverse of this page is blank)

EXECUTIVE SUMMARY

Interest in catalytic destruction of chlorinated volatile organic compounds (CVOCs) has increased significantly over the past four years. Currently, supported catalysts containing transition metal oxides and/or noble metals appear to be the only configurations available in the marketplace. While performance may be acceptable by today's standards, major concerns as to limitations in activity, selectivity and stability still remain. In an effort to improve on these types of catalysts, a new approach, utilizing cation exchanged/impregnated large pore zeolites was initiated by our research group over the past three years.

The objectives of the present study have been to develop, characterize and evaluate performance of potentially superior modified zeolite catalysts for CVOC oxidation. The criteria for success are high activity at low temperatures (300°-350°C), high selectivity to complete oxidation products, and superior thermal stability.

This report gives test results for 14 different cation-modified zeolite catalysts, all of which were prepared in our laboratories. Three different dilute vapor phase CVOC feeds (trichloroethylene, methylene chloride, carbon tetrachloride) were investigated in detail for catalytic destruction characteristics over a temperature range from 175°-600°C. Long term catalyst thermal stability studies were carried out at high temperature (600°C), while deactivation by coking was investigated at temperatures as low as 175°C.

It was found that the most active catalysts for destruction of one-carbon CVOCs were cobalt exchanged Y-zeolites, while for two-carbon CVOCs, the presence of chromium in the catalyst was highly desirable, preferably in the impregnated form. Thus, the most versatile active catalyst for the destruction of mixed feeds was shown to be a cobalt exchanged, chromium impregnated Y-zeolite known as Co-Y/CA. This result correlates well with abundant chemisorption of both oxygen and CVOC feeds on the catalyst surface as measured by thermogravimetric analysis.

Zeolite catalyst selectivities did not vary significantly with cation addition, generally producing deep oxidation products (HCl, CO, CO_2, H_2O). No detectable higher chlorinated CVOCs were found. When chromium was present in the catalyst, however, 10-100 ppm of chlorine were generally found in the product spectrum. Addition of water vapor to the reaction mixture greatly diminished Cl_2 formation.

Catalyst stability was tested for both low temperature (< 300°C) reversible coke formation and high temperature (600°C) irreversible thermal degradation. For all feeds, coking was

negligible at temperatures of 325°C or above. Thermal degradation at 600°C was found to occur more readily with impregnated versus exchanged chromium catalysts.

TABLE OF CONTENTS

Section	Title	Page
I	INTRODUCTION	1
	A. OBJECTIVES	1
	B. BACKGROUND	1
	C. SCOPE	2
II	EXPERIMENTAL AND ANALYTICAL FRAMEWORK	5
	A. ZEOLITE CATALYST CONFIGURATION	5
	1. Supports	5
	2. Cation Exchange and Impregnation	5
	B. CHLORINATED HYDROCARBON FEEDS	6
	C. REACTOR CONFIGURATION	6
	D. ANALYTICAL QUANTIFICATION	8
	E. CATALYST CHARACTERIZATION	10
	1. Chemical Composition	10
	2. Surface Area Determination	10
	3. Adsorption Characteristics	10
	4. Catalyst Acidity Determination	11
	F. QA/QC EFFORTS	11
	1. Introduction	11
	2. Data Quality Indicators	11
	3. Sampling Procedures	12
	4. System and Performance Audit Plans	14
	5. Corrective Action Procedures	14
III	OXIDATIVE CATALYSIS OF CHLORINATED HYDROCARBONS BY METAL LOADED ACID CATALYSTS	16
	A. STUDY OF WASHCOATED CORE CATALYSTS USING METHYLENE CHLORIDE	16
	1. Results	16
	2. Discussion	22
	B. COMPARISON OF WASHCOATED CORE CATALYST PERFORMANCE USING THREE FEEDS (METHYLENE CHLORIDE, CARBON TETRACHLORIDE AND TRICHLOROETHYLENE)	26
	1. Results	26
	2. Discussion	37

TABLE OF CONTENTS
(Concluded)

Section	Title	Page
	C. IN DEPTH STUDY OF COMBINED EXCHANGED/ IMPREGNATED CATALYST PELLETS . . .	42
	1. Results	42
	2. Discussion	51
IV	DEACTIVATION OF METAL LOADED ACID CATALYSTS . .	58
	A. REVERSIBLE LOSS OF ACTIVITY BY COKING . . .	58
	1. Results	58
	2. Discussion	69
	B. IRREVERSIBLE LOSS OF ACTIVITY BY THERMAL INSTABILITY	75
	1. Results	75
	2. Discussion	76
V	CONCLUSIONS	79
VI	RECOMMENDATIONS	81
	REFERENCES	82

LIST OF FIGURES

Figure	Title	Page
1	Schematic of the Reactor	7
2	Corrective Action Procedure	15
3	$MeCl_2$ Conversion vs. Temperature for Runs without Water Addition	19
4	$MeCl_2$ Conversion vs. Temperature for Runs with 27000 ppm Water Addition	19
5	Arrhenius Plot for Runs without Water . . .	20
6	Arrhenius Plot for Runs with Water . . .	20
7	$MeCl_2$ Conversion vs. Temperature Plot with Various Catalysts	31
8	TCE Conversion vs. Temperature Plot with Various Catalysts	31
9	CCl_4 Conversion vs. Temperature Plot with Various Catalysts	33
10	TCE Conversion vs. Temperature Plot with Various Catalysts	33
11	NH_3 Desorption vs. Temperature Plot with Cation-Exchanged Zeolite Powders . . .	36
12	NH_3 Desorption vs. Temperature Plot with Various Zeolite Pellets	36
13	NH_3 TPD Plot for Acidity Comparison of Different Exchanged/Impregnated and Exchanged Catalysts	46
14	NH_3 TPD Plot for Several Co-Y/CA Catalysts .	46
15	$MeCl_2$ Conversion vs. Temperature Plot with Various Catalysts	49
16	TCE Conversion vs. Temperature Plot with Various Catalysts	49
17	Deactivation of Modified Co-Y Pellets during TCE Conversion at Different Temperatures .	60

LIST OF FIGURES
(Concluded)

Figure	Title	Page
18	Product Spectrum Obtained during Regeneration of Deactivated Modified Co-Y Pellets at 450°C	60
19	Coke Deposition in Modified Co-Y during TCE Oxidation at Different Temperatures	62
20	Deactivation of Modified Co-Y Pellets during $MeCl_2$ Oxidation at Different Temperatures	62
21	Coke Deposition in Modified Co-Y Pellets during $MeCl_2$ oxidation at Different Temperatures	63
22	Rate of Weight Gain vs. Time Plot during Coking of Modified Co-Y Pellets with TCE and $MeCl_2$	64
23	Deactivation of Modified Co-Y/Silbond Catalyst during TCE Oxidation at Various Temperatures	64
24	Deactivation of Modified Co-Y/Silbond Catalyst during $MeCl_2$ and CCl_4 Oxidation	65
25	Deactivation of High Co Loaded Modified Co-Y Catalyst during TCE Oxidation	67
26	Deactivation of Modified Co-M Catalyst during TCE Oxidation at Various Temperatures	67
27	Effect of Space Velocity on Deactivation of Modified Co-Y Catalyst during TCE Oxidation at 275°C	68
28	Stability of Catalysts for TCE Conversion at 275°C after Aging at 600°C	77
29	Chromia Content of Different Catalysts after Aging at 600°C	77

LIST OF TABLES

Table	Title	Page
1	SAMPLING PROCEDURES FOR CRITICAL MEASUREMENTS .	13
2	RESULTS OF CATALYTIC EXPERIMENTS ALONG WITH THEIR CHLORINE AND CARBON BALANCES . . .	17
3	ACTIVATION ENERGIES OF ZEOLITE CATALYSTS FOR METHYLENE CHLORIDE OXIDATION . . .	21
4	COMPARISON OF FEED CONVERSION, OXYGEN PICKUP AND ACIDITY OF DIFFERENT ZEOLITE CATALYSTS .	22
5	THE CHEMICAL COMPOSITION OF VARIOUS CATALYSTS .	27
6	COMPARISON OF THE PROPERTIES OF THE VARIOUS CATALYSTS	30
7	CVOC ADSORPTION RESULTS ON CATALYSTS AFTER HALF HOUR	39
8	THE CHEMICAL COMPOSITION AND PROPERTIES OF VARIOUS CATALYSTS	44
9	COMPARISON OF PROPERTIES OF VARIOUS CATALYSTS .	58
10	TOTAL COKE FORMATION (MG/G) IN CATALYSTS AFTER 1000 MINUTES OF CHLORINATED VOC OXIDATION	63

ACRONYMS

CCl_4	Carbon Tetrachloride
CO	Carbon Monoxide
CO_2	Carbon Dioxide
CH_2Cl_2	Methylene Chloride
C_2HCl_3	Trichloroethylene
CVOC	Chlorinated Volatile Organic Compound
E	Activation Energy
FCA	Fractional Cation Availability
GC/MS	Gas Chromatograph/Mass Spectrometer
GS	Graduate Student
HCl	Hydrogen Chloride
K	True Rate Constant
K_{obe}	Observed Reaction Rate
$MeCl_2$	Methylene Chloride
MSA	Mine Safety Appliances
PI	Principal Investigator
QAO	Quality Assurance Officer
RGA	Residual Gas Analyzer
TCE	Trichloroethylene
TGA	Thermogravimetric Analyzer
TMO	Transition Metal Oxide
VOC	Volatile Organic Compound
XRF	X-Ray Fluorescence

ZEOLITE CATALYSTS:

H-Y	Hydrogen Y Zeolite
Cr-Y	Chromium Exchanged Y Zeolite
Ce-Y	Cerium Exchanged Y Zeolite
Mn-Y	Manganese Exchanged Y Zeolite
Co-Y/CA	Cobalt Exchanged Y Zeolite Impregnated with Chromium from a Chromic Acid Solution
Co-Y1 - Co-Y6	Cobalt Exchanged Y Zeolite with Different Cobalt wt percent Loading
Co-Y/CA1 - Co-Y/CA8	Cobalt Exchanged Y Zeolite Impregnated with Different wt percent Chromium Loading from a Chromic Acid Solution

TRADE NAMES

Air-Cadet
Alphagaz
Ametek
Chlorhydrol
Cole-Parmer
Cordierite
Corning
Corning Ion Analyzer
DuPont
Dycor
Eurotherm
Fiberfrac
Fisher
Hamilton
Hewlett-Packard
Lindberg
LZ-Y62
LZ-Y82
Mine Safety Appliances
Omega
Philips
Platinel II
Porter
Quantasorb Jr.
Samox
Samplair
Silbond
Superior
Thermolyne

(The reverse of this page is blank)

SECTION I

INTRODUCTION

A. OBJECTIVES

The development of catalysts for low-temperature (250°C-350°C) oxidation of chlorinated VOCs (Volatile Organic Compounds) to non toxic compounds has been the main objective of this study. Initial experimentation with cation exchanged zeolite catalysts for this purpose proved fruitful. Consequently, all available resources were geared towards developing modified metal-loaded zeolite catalysts which would possess superior activity and selectivity for the oxidation of the chlorinated VOCs.

Another significantly important catalyst characteristic, catalyst deactivation/stability, was also investigated. Coking was found to be the major cause of reversible catalytic deactivation, while thermal instability caused irreversible loss of catalytic activity.

B. BACKGROUND

The increased production and application of chlorinated VOCs such as methylene chloride (CH_2Cl_2), carbon tetrachloride (CCl_4) and trichloroethylene (C_2HCl_3) have caused increased concerns over proper disposal and control of these hazardous waste materials. Among the available waste disposal processes, catalytic combustion may be the most economically advantageous method for dilute halocarbon destruction because of its low temperature (250°C-350°C) of operation, low energy consumption and reduction in noxious by-product formation.

A large number of articles are available regarding catalytic oxidation of chlorinated hydrocarbons over various metal and metal oxide catalysts. The desired reaction is the complete oxidation of the chlorinated VOC to produce HCl and CO_2; however, an excess of chlorine over hydrogen atoms in the parent molecule hinders complete oxidation, and chlorine gas is produced as a reaction by-product (1). Although noble metals have found widespread application as automotive exhaust catalysts (2) and as other industrial gas treatment catalysts (3), the deactivation and volatilization of the noble metals by chlorine and HCl renders them ineffective for chlorinated VOC oxidation (4-8). Transition metal oxide (TMO) catalysts, on the other hand, have been found highly active and much more resistant to chlorination and HCl poisoning. A detailed review of VOC oxidation catalysts and mechanisms was compiled by Spivey (9), who reported that the most active catalysts for a variety of complete oxidation reactions are usually the oxides of V, Cr, Mn, Fe, Co, Ni and Cu. Further studies (10-13) have suggested that the elemental

chlorine produced by the classical Deacon reaction (14) during VOC oxidation can cause chlorination, hence, deactivation of the TMO catalyst. Therefore, catalysts less efficient for the Deacon reaction are more suitable for chlorocarbon oxidation. Addition of water to the reactants has also been found to inhibit the Deacon reaction and thus improve the catalyst stability by preventing direct chlorination.

Much less consideration has been given to investigating the suitability of cation-exchanged zeolites as potential catalysts for chlorinated VOC oxidation. The unique features of shape selectivity and high Brönsted acidity caused by their regular crystalline structures have made them essential for numerous industrial catalytic processes, while the presence of multivalent cations within the zeolite matrix has been found to increase the activity for various reactions by creating highly acidic centers through hydrolysis of charged cations (15).

Some investigations on the oxidation of hydrocarbons (viz. ethanol, propylene, toluene) over metal loaded zeolite catalysts have been reported (16-22) in recent years. The high activity of transition metal exchanged zeolites as catalysts for deep oxidation as well as partial oxidation reactions has been noticed. Kubo et al. (23) reported that oxygen chemisorption capacity and hence the activity of zeolite catalysts for CO oxidation increased with the presence of transition metal ions such as Cr^{3+}, Co^{3+}. Aparicio et al. (22) further suggested that the activity of a metal loaded zeolite catalyst in CO oxidation increased with the ease of oxidation of the metal cation to higher valence states. They found that Cr-Y showed the maximum activity due to the ability of the Cr ion to be oxidized from +3 to +5. The application of zeolite catalysts for selective oxidation of chlorocarbons to form HCl and CO_2 was reported in a patent issued to Dow Chemical Co.(24). Even without the presence of any transition metal cations, zeolites of type Y as well as mordenite produced complete oxidation of $CHCl_3$ and CCl_4 between 200°C and 300°C. The potential of metal exchanged zeolites for chlorocarbon destruction was briefly suggested in several other existing patents (25).

In view of the notable activity of the zeolite catalysts in oxidation reactions, it seems highly probable that suitable cation-exchanged zeolites can be effective alternatives to the metal and metal oxide catalysts currently available for halocarbon destruction.

C. SCOPE

Various cation-exchanged zeolite catalysts were prepared and the activities and selectivities of those catalysts were determined by performing reactor experiments. The catalytic activity of cation-exchanged washcoated core catalysts for the oxidation of CH_2Cl_2 was investigated using three different catalysts, namely H-Y, Cr-Y and Ce-Y. Conversions varied from 17

to 99 percent, with the catalytic activity decreasing in the order: Cr-Y > H-Y > Ce-Y. The oxygen chemisorption and the acidity values of the catalysts showed similar trends. Differences in oxidizability to higher valence states (Cr-Y > Ce-Y) and cation sizes (Ce^{3+} > Cr^{3+}) were probable reasons behind the higher activity of the Cr-Y. A dual-site mechanism for the oxidation process, involving adsorption of the chlorocarbon at the Brönsted sites and adsorption of oxygen at the cationic sites, was found feasible. The presence of water (about 27,000 ppm) in the feed stream reduced conversion between 10 and 60 percent, depending upon the catalyst and the temperature and appeared to temporarily deactivate the catalysts. The selectivities among the catalysts were quite similar, with HCl and CO being the major products (26).

Comparisons of activities and selectivities were also made using exchanged/impregnated zeolite catalysts for the oxidation of three different chlorinated VOCs (CH_2Cl_2, CCl_4 and C_2HCl_3). The reactions were carried out under atmospheric pressure with temperatures varying from 150°C to 400°C and with the addition of about 13,000 ppm of water. Primarily, three different cordierite supported (washcoated) zeolite catalysts (Co-Y, Cr-Y and Mn-Y) were prepared and tested, with Co-Y appearing to be the catalyst superior in activity and selectivity. Although complete conversions of methylene chloride and carbon tetrachloride could be obtained at temperatures of 350°C and 200°C, respectively, no significant conversion of trichloroethylene could be noticed at temperatures below 400°C. Incorporation of transition metal oxide within the zeolite matrix by Cr_2O_3 impregnation of the cation-exchanged zeolites produced a substantial improvement in trichloroethylene conversion with over 90 percent destruction obtained at only 325°C (64). An unsupported chromia-impregnated 1/16-inch pelletized Co-Y catalyst showed even better activity results for chlorocarbon oxidation than the supported catalysts (27).

Since the cobalt exchanged and chromia-impregnated Y zeolite catalyst (Co-Y/CA) showed good activity and selectivity for the destruction of the above mentioned CVOCs, the effects of cobalt and chromia compositions on the catalytic properties were investigated (28). Higher cobalt exchange increased the acidity and the oxygen adsorption capacity of the Co-Y zeolite without affecting the surface area, whereas increasing Cr_2O_3 impregnation caused increased dealumination and consequent loss of acidity. Higher loading of Cr_2O_3 also reduced catalyst surface area by a combination of structural loss and pore/channel blockage. Increasing Co exchange produced improved conversion of methylene chloride, while higher loading of impregnated Cr_2O_3 was detrimental for methylene chloride conversion due to the associated loss of surface area and acidity. Methylene chloride conversion appeared to be primarily controlled by carbonium ion formation at the acidic sites followed by oxidation with the oxygen adsorbed at the cationic sites. Conversely, trichloroethylene oxidation was primarily determined by the

impregnated Cr_2O_3 sites; low or no Cr_2O_3 produced poor conversion while increasing Cr_2O_3 loading increased the conversion. However, an optimum impregnation level of about 5 percent seemed necessary to avoid poor activity either due to lack of sites or to structural damage by overloading. Additionally, increasing Co exchange level in the Co-Y/CA catalysts also showed improved trichloroethylene conversion probably due to the increasing acidity. Therefore, trichloroethylene conversion seemed to be controlled by the initial adsorption at the Cr_2O_3 sites with subsequent reactions which may involve the acidic and/or cationic sites.

Reversible deactivation of the modified cation-exchanged zeolite catalysts was studied during the complete oxidation of the above mentioned VOCs. Two different types of zeolites, (1) Y zeolite with the larger pore diameter and (2) mordenite with a medium pore diameter, were used for the preparation of the catalysts used for the deactivation study. The deactivation rates for the different VOCs were determined and compared. Also, the effects of temperature and space velocity on the deactivation rate were analyzed. Coking was found to be the cause of reversible deactivation, and, based on the above results, a mechanism for coking was proposed with CO as the possible reaction intermediate leading to the formation of coke (29).

Irreversible loss of activity due to thermal instability was also studied. The catalysts were characterized by determination of their specific surface areas (BET), chemical compositions (XRF), acidities (TGA) and also their capacities to adsorb oxygen and VOCs (TGA). Four catalysts (Cr-Y, Cr-Y/Co, Co-Y/CA and a commercial Cr_2O_3 catalyst) were tested for their long term activity. The Cr-Y catalyst showed good stability and so did the commercial Cr_2O_3 catalyst. But the commercial Cr_2O_3 catalyst showed a significant drop in chromia content over the period of time the catalyst was tested. A relatively poor performance by the Co-Y/CA catalyst may be attributed to the loss of crystallinity during impregnation of chromia, due to the highly acidic nature of the chromic acid solution. Also, the results suggested that chromia in the form of exchanged cation in the zeolite was not as easily removable as the chromia impregnated on the catalyst.

SECTION II
EXPERIMENTAL AND ANALYTICAL FRAMEWORK

A. ZEOLITE CATALYST CONFIGURATION

1. Supports

Some of the catalysts used for the various studies were prepared by loading the powdered zeolites using binders (Silbond or Chlorhydrol), onto low-surface-area (0.5-1.0 m^2/g) honeycomb cordierite supports obtained from Corning Co. These honeycomb supports had 400 cells/in^2 and weighed approximately 14g each.

The other type of catalysts was prepared by the cation exchange and impregnation of Y zeolites received as 1/16 inch extruded pellets (LZ-Y62) from Union Carbide Co.

2. Cation Exchange and Impregnation

Cation Exchange: The H-Y zeolite in the form of powder was obtained from Union Carbide Co. as low-soda ammonium-exchanged LZ-Y82. H-Y was prepared by calcining the ammonium-exchanged LZ-Y82 at 500°C for 10-12 hours, in air.

Approximately 2 wt percent of metal ions were loaded onto the LZ-Y82 zeolite by well-known exchange procedures (30). Cation exchange was carried out in two steps. In the first step, NH_4^+ exchange of the LZ-Y82 was carried out by dissolving 89.77 grams of NH_4Cl in 745 ml of distilled water (the ratio being 120.5 grams of salt in 1 liter of water) and slurrying 74.5 grams of Linde LZ-Y82 powder in it. The slurry was heated to about 100°C and an even mixing was accomplished by stirring it for 2 hours. The exchanged powder was filtered hot and washed with distilled deionized water during filtration.

The second step was the metal loading process. In the case of Cr^{3+} exchange, a $Cr(NO_3)_3$ solution was prepared with 0.33 wt percent of the salt in distilled deionized water. The NH_4^+-exchanged and filtered zeolite powder was then added to the dilute solution of the exchanged salt and the resulting mixture was continuously stirred. To establish an exchange equilibrium, stirring of the mixture was continued over 12-15 hours. After the required time period, the slurry was filtered and washed with distilled deionized water to remove all traces of soluble salts. The filtered zeolite powder was dried at 125°C for 2 hours, then calcined at 550°C over 10-12 hours. For the cation exchange of the 1/16 inch Y zeolite pellets, the same procedure was followed, except that filtration was unnecessary.

The resulting exchanged zeolite agglomerate was crushed to a fine powder and washcoated onto the honeycomb cordierite support from a slurry of the zeolite, usually in perhydrolyzed ethyl orthosilicate binder. Approximately 25 wt percent (based on the binder volume) of the zeolite powder was slurried in 200 ml of silica binder. The slurry was kept well mixed by continuous stirring. Leached and dried cordierite cores were dipped into the slurry and then taken out. The cordierite channels were cleared by blowing compressed air through them. The above procedure was repeated three more times with the same core. Finally, the washcoated cores were dried at 200°C followed by calcination at 550°C for 12-15 hours. Generally the cores showed a weight gain of about 15-20 percent after completion of the washcoating procedure. The actual exchanged zeolite constituted approximately 50-60 percent of the total washcoat after calcining.

Impregnation: After completion of the cation exchange, some of the zeolite washcoated cores were further impregnated, usually with Cr_2O_3 in order to enhance their catalytic properties. Cr_2O_3 impregnation was carried out with a solution of a chromium salt containing about 10 wt percent of Cr_2O_3. The washcoated cores were kept immersed in the chromium salt solution for 2-4 hours and then dried at 200°C for 2 hours followed by calcination at 500°C for 10-12 hours. This would typically result in approximately 1-1.5 percent Cr_2O_3 loading on the washcoated catalyst. Metal impregnation was also carried out in the same way with the Y zeolite pellets.

B. CHLORINATED HYDROCARBON FEEDS

Chlorinated volatile organic compounds, generally CH_2Cl_2, CCl_4 and C_2HCl_3 with a vapor-phase concentration range of 1000-1500 ppm, were used as feeds to the reactor system. The VOCs were received as liquids having a purity of >99.9 percent, from Fisher Scientific Corporation.

C. REACTOR CONFIGURATION

The reactor used in catalytic experiments was a vertical pyrex tube, 28 mm O.D. and 1 meter in length. A schematic of the whole reactor system is shown in Figure 1. The glass reactor passed through two furnaces. Both the furnaces were Lindberg 55035 hinged tube type. The top furnace served the purpose of heating the reactor zone while the lower one was utilized as a preheater for the incoming gases. The section in between the furnaces was heated by a Thermolyne Briskheat (Standard Insulation Samox type) heating tape to maintain an isothermal temperature profile throughout the reactor. Two Omega 6100 temperature controllers were used in conjunction with chromel-alumel (type K) thermocouples for maintaining the reactor and the preheater temperatures within ± 2°C of the setpoint. The heating tape temperature was controlled by using a Superior Electric Company Powerstat. Four chromel-alumel thermocouples

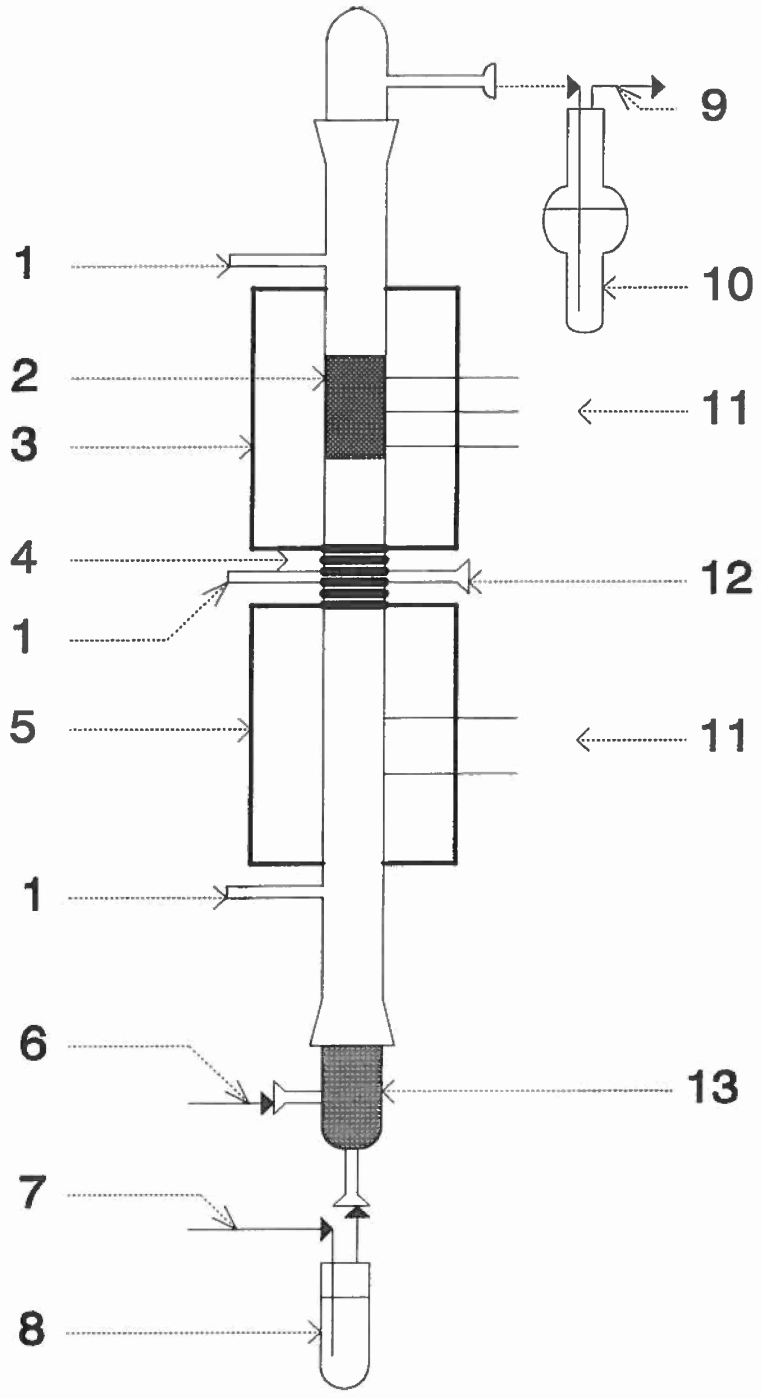

1. Sampling Ports
2. Catalyst Section
3. Reactor Furnace
4. Heat Tape & Insulation
5. Preheater Furnace
6. Main Air Inlet to the Reactor
7. N_2 to the CVOC Bubbler
8. CVOC Bubbler
9. Outlet to Vacuum Pump
10. HCl Scrubber
11. Thermocouples
12. Manometer Tap
13. Glass Wool

Figure 1. Schematic of the Reactor

were used to check the isothermality of the catalytic section, preheater section and also the heat tape. Their temperatures were read by an Omega digital thermometer (Model 115KC).

The zeolite catalyst, washcoated on a honeycomb cordierite support was kept inside the top catalytic section. The support was wrapped with Fiberfrac insulation (about 1 mm) to prevent any bypass of reactant gases through the annular space between the support and the reactor wall. In the case of catalyst pellets, a thin layer of glass wool was used to hold the bed in place. The chlorinated hydrocarbon feed was introduced into the reactor by connecting a glass bubbler to the bottom and passing air through it. The desired flow rate of dry compressed air was passed through the bubbler for achieving proper feed concentration (approximately 1500-2000 ppm). The excess oxygen required for deep oxidation was supplied by passing 450 cc/min of dry compressed air through the side part. Addition of water as a hydrogen source was accomplished by connecting a water bubbler between the reactor and the main air flow so that the main air carried entrained moisture droplets along with it. Both the feed and the main air flow rates were measured by rotameters (Porter Instrument Co.), which were calibrated prior to use. The dry grade air supply from the Linde compressed air cylinder was passed through a tube containing anhydrous $CaCl_2$ and Drierite before being used in the reactor. A separate line was maintained for purging the catalyst with nitrogen before and after experiments and also for the optional addition of water.

Two sample ports were used during the experiments for feed and product sample collection. The sample ports were covered by rubber septa which minimized leakage during sampling.

Since HCl could not be detected in the GC/MS, gravimetric methods were used for HCl analysis. For this purpose, the product HCl was collected in a distilled water trap by passing the effluent gases through a water sparger. This water sparger (or the HCl trap) caused excess pressure buildup inside the reactor and a Cole Parmer Air Cadet vacuum pump had to be connected to the trap outlet for maintaining atmospheric pressure inside the reactor. A surge vessel was positioned between the vacuum pump and the HCl trap to prevent any liquid being pulled directly into the pump. This surge vessel also helped in monitoring pressure fluctuations by means of a vent valve situated on top of it. A water manometer connected between the surge vessel and the reactor midsection indicated the pressure situation inside the catalytic reactor.

D. ANALYTICAL QUANTIFICATION

The primary analytical equipment used in the reactor experiments was a Hewlett-Packard 5890 Gas Chromatograph with a Hewlett-Packard 5970B Mass Selective Detector (GC/MS). The uniqueness of this GC/MS system was the dual capability of identification and quantification of compounds. The GC was

equipped with a fused silica column for the separation of the components. The GC/MS had a dedicated 9133 Chem Station Computer with a capability of identifying 40,000 chemical compounds by comparing the sample mass spectra with that available in its data base.

Quantification of any known sample was achieved by using response factors obtained from calibrating the GC/MS with a known amount of a similar sample. The calibration procedure involved sample injection from a pre-analyzed gas mixture obtained from Alphagaz Inc. Once the response factors were obtained, the GC/MS could be used to quantify CO_2, CH_2Cl_2, CCl_4, $CHCl_3$ and similar other chlorinated components.

Two major products of the catalytic oxidation reactions were CO and HCl. The GC/MS could quantify neither one of them. For CO measurements, the capillary column present in the GC was unable to separate it from other components of air. Moreover, since its mass was identical to that of N_2 and almost 80 percent of the gas sample was made up of N_2, it was impossible to distinguish between CO and N_2 peaks in the MS. The problem with HCl quantification was also a result of poor separation in the column. The general purpose column used in the GC/MS was unable to produce a distinct peak for HCl. The HCl peak showed severe tailing which affected integration results. This problem was further intensified by the presence of Cl_2 in the product spectrum. During ionization in the MS, Cl_2 combined with H_2O to produce HCl and thus interfered with HCl quantification. Therefore, neither HCl nor Cl_2 could be properly measured in the GC/MS. Alternative methods were utilized for proper quantification of CO, HCl and Cl_2.

CO, Cl_2 and $COCl_2$ measurements were carried out by using a MSA Samplair pump along with appropriate MSA detector tubes. The CO tubes could detect 50-3000 ppm, the Cl_2 tubes were able to go from 0.5-100 ppm and the $COCl_2$ tubes measured a range of 0-10 ppm.

HCl data were evaluated by analyzing the samples collected in the HCl trap. A Corning Ion Analyzer 255 pH meter with General Purpose Combination electrode was used in determining the acid concentration. The pH meter was calibrated at two different pH levels(pH 2.0 and 3.0) prior to its use for sample measurements. After obtaining the pH reading, the actual HCl concentration was calculated by using a simple program in the Lotus 1-2-3 software.

For the deactivation studies, the feed and product samples from the reactor were continuously monitored by an on-line Ametek Dycor M200MDEF residual gas analyzer (RGA).

E. CATALYST CHARACTERIZATION

1. Chemical Composition

The prepared catalysts were characterized using several analytical techniques, then subjected to catalytic activity and selectivity experiments. The final metal loadings of the prepared catalysts were obtained using a Philips PV9550 X-ray Fluorescence (XRF) spectrometer. The Si/Al ratios of the different zeolite pellets were also determined from the compositional data obtained using the XRF. The percent cation exchange of each exchanged zeolite was calculated based on the corresponding final metal loading, the Si/Al ratio and the unit cell composition of Y zeolite (i.e., $H_{56}(AlO_2)_{56}(SiO_2)_{136}$).

2. Surface Area Determination

The surface areas of the catalysts were determined using the Quantasorb Jr. BET surface area analyzer. The Quantasorb Jr. determines the surface area of a sample by employing the technique of adsorbing gas from a flowing mixture of adsorbate and an inert non-adsorbable carrier gas. The processes of adsorption and desorption were monitored by measuring the change in the thermal conductivity of the gas mixture. Liquid nitrogen was used as the coolant when nitrogen was used as the adsorbate. The adsorption peak was produced by the change in the thermal conductivity of the gas mixture resulting from the decrease in adsorbate concentration due to adsorption on the sample surface. Adsorption was completed when there was no longer any difference in the thermal conductivities of the gas entering and leaving the sample cell. Desorption was initiated by the removal of the coolant from the sample cell. During the desorption process the gas leaving the sample cell was richer in adsorbate. Therefore, the signal would be opposite in polarity to that obtained during the adsorption process. Both the adsorption as well as the desorption peak areas are recorded by a meter. After the desorption was over a known amount of adsorbate was introduced into the flow stream in order to calibrate the desorption signal. Since the adsorption signals are sometimes accompanied by non-Gaussian tailing curves, particularly on porous samples at the high nitrogen concentrations, it was always preferable to work with the desorption signals. From the values of the desorption peak area, the calibration peak area and the weight of the sample, and utilizing the BET equation, the sample specific surface area (area per gram) was calculated.

3. Adsorption Characteristics

Adsorption experiments with O_2 and the reactor feeds (CH_2Cl_2, CCl_4 and C_2HCl_3) were carried out to characterize the catalysts, using a Dupont Model 2100 Thermal Analyst with Model 2950 Thermogravimetric Analyzer (TGA).

The TGA was used to detect weight changes that occur due to adsorption on the sample. The sensitivity of the instrument was sufficient to detect weight changes in the order of a microgram. The catalyst sample was placed in the pan inside the TGA furnace and brought to the desired temperature. Typically, a catalyst sample would be degassed at 500°C in a N_2 atmosphere to remove any moisture and other impurities from its surface and then cooled down to the temperature desired for the adsorption. After achieving steady state of temperature, the adsorbate was passed into the chamber for adsorption to begin. The total amount adsorbed was determined after the sample weight had again stabilized with time. However, this weight change measurement was affected by instrument buoyancy effects associated with temperature change from the degassing temperature to the adsorption temperature, as well as by gas change from N_2 to O_2 (or VOC in N_2). Therefore, an identical volume of crushed glass beads was used as inert sample, and the experiment repeated in the TGA in order to quantify the weight change from buoyancy effects. This weight change was incorporated in the actual oxygen adsorption experiment to obtain the final adsorption data.

4. Catalyst Acidity Determination

Ammonia was used as a probe molecule to determine the Brönsted acidity of the catalysts. The powdered sample was degassed by heating at 250°C for 2 hours. The degassed sample was then subjected to NH_3 adsorption at 25°C for about 8 hours. The adsorbed NH_3 was then quantitatively desorbed in the TGA. For NH_3 desorption, the sample was first equilibrated at 100°C for 1.5 hours in order to remove any physisorbed NH_3 from the sample, then the rest of the NH_3 was desorbed by using a 10°C/min temperature ramp to heat the sample from 100°C to 550°C. The NH_3 desorbed above 100°C was considered as chemisorbed NH_3 and used for acidity determination.

F. QA/QC EFFORTS

1. Introduction

Quality assurance and quality control have been very important factors utilized in all the experimentation that was carried out. The significance and importance of experimental results carry no meaning if the data collected are not accurate. Considerable effort was used to ensure that (1) the experimental procedures followed were proper and that (2) the analytical measurements were accurate and precise.

2. Data Quality Indicators

The experimental work primarily involved measurement of vapor-phase concentrations of chlorinated organic feeds and reaction products, as well as reactor temperatures, gas flow rates and surface area measurements of the developed catalysts.

The relative standard deviation was used for the precision values shown in Table 1. The values for accuracy were defined as the relative difference, expressed as percent, between the numerical average of successive readings and a known standard, or in some cases, a calibrated value derived from a linear regression equation for the best-fit curve. Since percent of relative standard deviation and accuracy at low concentration were relatively high compared to those values at high concentration, the data quality indicators were reported in two concentration ranges for the reactor gas measurements. Completeness was defined as the percentage of the total data set which was accepted as valid.

3. Sampling Procedures

Gas samples for analysis were retrieved through sampling ports with rubber septa covers to allow penetration by the syringe needle while minimizing leakage. Hamilton constant-rate syringes were used for transferring the samples from the reactor to the GC/MS. These syringes reduced the errors due to differences in operator technique. The syringe was cleaned prior to each sample collection by plugging it into a Hamilton syringe cleaner for 5 minutes. Four sets of samples were alternately collected from bottom and top ports of the reactor during a given experiment and immediately injected into the GC/MS. All the chlorinated VOCs and CO_2 were calibrated in the GC/MS from a calibration gas mixture cylinder containing known concentrations of the gases.

An MSA Samplair pump was used to determine the concentrations of CO, Cl_2 and $COCl_2$ using appropriate MSA detector tubes. The detector tubes had been factory calibrated to ensure accurate readings.

For the quantification of HCl, the reactor outlet gases were sparged into a known quantity of distilled water for a known time. The pH of this solution was measured by a Corning ion analyzer to calculate the HCl concentration.

Temperature control in the reactor was accomplished by a Lindberg Mini-Mite tube furnace with Eurotherm digital controllers using a Platinel II thermocouple. Three chromel-alumel(Type K) thermocouples were placed axially along the reactor to check axial isothermality of the catalyst bed, while one chromel-alumel (Type K) thermocouple was placed in the preheater furnace to obtain the temperature of the preheater section. The temperatures from the thermocouples were read by an Analog Devices digital thermometer.

The pressure inside the system was monitored by watching the manometer which was connected to the middle section of the reactor. A Cole-Parmer Air Cadet vacuum pump was used to maintain atmospheric pressure inside the reactor during the sparging of the reactor effluents in distilled water for HCl

TABLE 1: SAMPLING PROCEDURES FOR CRITICAL MEASUREMENTS

Measurement	Sampling Location	Sampling Method	Sampling Frequency	Reference
Concentrations: Dichloromethane Chloroform Carbon Tetrachloride Trichloroethylene Perchloroethylene Carbon Dioxide	Bottom and top sample ports on reactor	200 μl constant rate syringe collection	Four times during each reactor run	
Concentrations: Carbonyl Chloride Carbon Monoxide	Top sample port on reactor	Samplair Pump	Duplicate measurement during each reactor run	MSA Manual
Concentration: Chlorine	Top Sample port on reactor	20 μl constant rate syringe collection	Five times during each reactor run	
Concentration: Hydrogen Chloride	Outlet of reactor	Bubbler trap collection	One time per reactor run	
Catalyst Surface Area	Support with or without catalyst	Grab sample	One time per catalyst	
Reactor Temperature	Top furnace and bottom furnace on reactor	Thermocouples	Continuous	Instruction Manual
Reactor Pressure	Middle port of reactor	Manometer	Continuous	Instruction Manual
Flow Rate	Inlet and outlet of reactor	Rotameter	Continuous	
Oxygen Pickup	Catalyst	TGA	Triplicate Measurement	TGA Manual

quantification. All flows were metered and controlled by rotameters and mass flow controllers.

4. System and Performance Audit Plans

System audits were conducted by on-site inspection of the laboratory apparatus and review of the quality assurance methods used for the total measurement system for each monitoring sensor. Specific systems to be audited included the Hewlett Packard GC/MS, Quantachrome surface area analyzer, and the DuPont thermogravimetric analyzer.

Performance audits refer to independent checks made to evaluate the quality of the data produced by the total sampling and analysis system. Sampling audits, analysis audits and data processing audits were the three categories of performance audits. System and performance audits were scheduled once during each three month period.

5. Corrective Action Procedures

The corrective action procedure is shown in Figure 2. If problems were uncovered during systems or performance checks, corrective action was initiated immediately. The problems may be identified by the graduate students (GS) or quality assurance officer (QAO). The individual identifying the problem would report directly to the principal investigator (PI), where the problem would be reviewed by the PI, QAO and GS.

If measurement systems or procedures were determined to be unsatisfactory, the GS would proceed to solve the problem. QAO verified the result after it had been rectified by the GS. The verification may include calibration and system or performance audits.

Following solution of the measurement problem and other related action, the PI and QAO would review the questionable data and determine whether specific tests must be repeated.

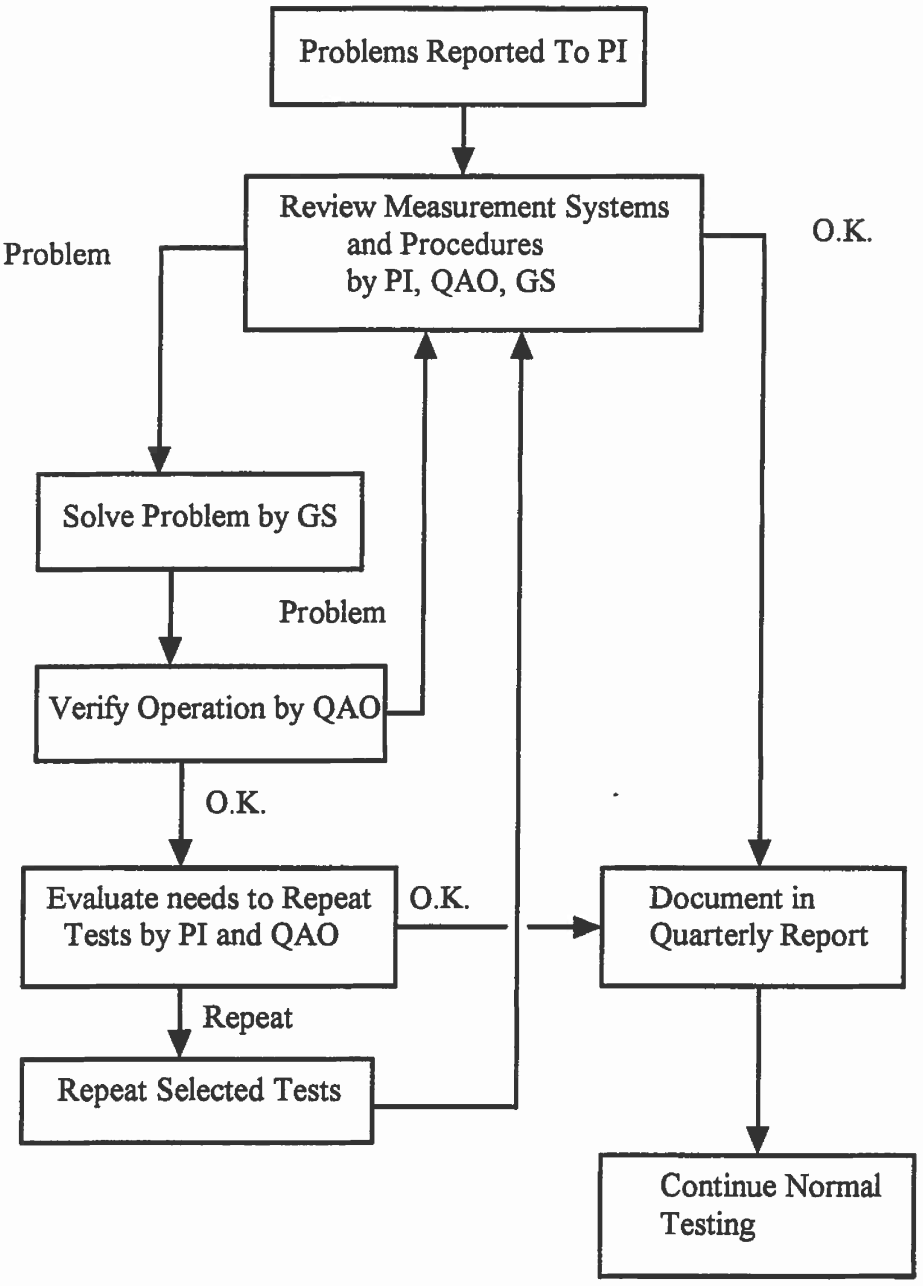

Figure 2. Corrective Action Procedure

SECTION III
OXIDATIVE CATALYSIS OF CHLORINATED HYDROCARBONS BY METAL LOADED ACID CATALYSTS

A. STUDY OF CATION EXCHANGED WASHCOATED CORE CATALYSTS USING METHYLENE CHLORIDE FEED

1. Results

The results from catalytic reactor experiments with the three zeolite washcoated catalysts (H-Y, Cr-Y, and Ce-Y) are summarized in Table 2. "Feed Conc." in the table refers to $MeCl_2$ inlet concentration. Each product selectivity is calculated based on either chlorine or carbon atoms present in that product divided by the total chlorine or carbon atoms present in the feed (expressed as percent).

The catalytic experiments with the H-Y, Cr-Y and Ce-Y catalysts, without water addition to the feed, were carried out at reaction temperatures varying from 300° to 475°C. As shown in Figure 3 and listed in Table 2, $MeCl_2$ conversion with all three catalysts remained above 90 percent. At temperatures below 425°C, $MeCl_2$ conversions with the three catalysts showed the following trend: Cr-Y > H-Y > Ce-Y.

As shown in Figure 4, with addition of about 27,000 ppm of water to the feed, $MeCl_2$ conversions with all three catalysts were significantly reduced for temperatures below 400°C. For example, at 350°C conversion for the H-Y catalyst went from about 70 to 20 percent; for Cr-Y from about 91 to 78 percent; and for Ce-Y from about 56 to 48 percent. Thus, the effect of water addition on conversion was variable, being greatest for the H-Y and least for the Ce-Y.

A previously developed integral reactor model (31) for a porous walled reactor was used to fit the data to a pseudo first order rate equation, from which the observed reaction rate constants (K_{obs}) and activation energies (E) were determined. K_{obs} was defined as the product of the effectiveness factor (η) and the true rate constant (K). The true reaction rate constants based on surface area could not be separated out due to well known inaccuracies in determining appropriate surface areas for zeolitic washcoated catalysts by standard BET methods. Therefore, during modeling calculations, the geometric surface area of a single cordierite channel (3.05 cm^2) was used instead. Figures 5 and 6 show the Arrhenius plots for all three catalysts with or without water being present as a co-feed. The activation energies as calculated from these plots are listed in Table 3.

Table 2: RESULTS OF CATALYTIC EXPERIMENTS, ALONG WITH THEIR CHLORINE AND CARBON BALANCES

Run No.	Feed Conc. (ppm)	Water Conc. (ppm)	Temp. (°C)	Conv. (%)	% Cl to HCl	% Cl to Cl_2	% C to CO	% C to CO_2	Chlorine Balance	Carbon Balance
					H-Y Catalyst					
574	1297		350	71.6	65.9	N.D.	23.1	5.8	94.4	57.4
575	1225	30611	350	24.8	1.6	N.D.	8.2	3.4	76.9	86.9
576	1380		400	91.6	81.9	N.D.	58.0	3.2	90.3	69.7
577	1637	29676	400	79.0	89.7	N.D.	36.7	1.8	110.8	59.5
578	1599		425	99.2	118.1	N.D.	50.0	6.6	118.9	57.4
579	1322	30849	425	92.5	72.7	N.D.	60.5	1.3	80.2	69.2
580	1497		450	99.1	93.5	N.D.	53.4	7.7	94.5	62.0
581	1485	27803	450	98.5	53.5	N.D.	53.9	1.9	55.0	57.3
582	1482		475	99.7	81.7	N.D.	54.0	7.0	82.0	61.4
583	1600	27934	475	99.3	53.4	N.D.	50.0	0.2	54.2	50.9
584	1667		375	89.0	74.8	N.D.	48.0	2.2	85.9	61.2
585	1610	28713	375	62.2	32.3	N.D.	24.8	5.4	70.1	68.0
586	1772		410	98.8	81.0	N.D.	56.4	5.7	82.2	63.4
587	1517	32742	410	91.4	95.9	N.D.	52.7	2.6	104.5	63.9
588	1433		325	69.4	63.4	N.D.	42.3	6.4	94.0	79.4
589	1104	24588	325	25.3	6.5	N.D.	9.1	3.8	81.2	87.6
590	1440		400	96.7	103.5	N.D.	55.6	6.6	106.7	65.5
591	1662	25613	400	86.6	65.7	N.D.	48.1	0.5	79.0	62.0
608	1728		400	98.1	86.2	N.D.	69.5	0.9	88.1	72.3
609	1388		400	98.0	70.4	N.D.	72.1	7.2	72.4	81.3
610	1493		425	98.0	84.9	N.D.	67.0	6.2	86.9	75.2
611	1806		450	98.4	70.5	N.D.	55.4	6.4	72.1	63.3
					Cr-Y Catalyst					
592	1454		325	73.5	78.8	1.5	55.0	3.5	106.8	85.0
593	1336	23247	325	50.1	32.4	N.D.	44.9	1.9	82.3	96.8
594	1601		350	92.2	107.8	1.6	75.0	4.3	117.2	87.2
595	1375	23825	350	77.8	86.7	N.D.	72.7	5.2	108.9	100.2
596	1829		375	93.7	97.4	N.D.	65.6	10.1	103.7	82.0
597	1749	23300	375	79.5	71.8	0.3	57.2	6.2	92.6	83.9
598	1794		400	97.0	106.7	5.0	66.9	10.8	114.7	80.7
599	1606	24048	400	92.3	90.4	1.2	74.7	8.8	99.3	91.2

Table 2: RESULTS OF CATALYTIC EXPERIMENTS, ALONG WITH THEIR CHLORINE AND CARBON BALANCES (CONCLUDED)

Run No.	Feed Conc. (ppm)	Water Conc. (ppm)	Temp. (°C)	Conv. (%)	% Cl to HCl	% Cl to Cl_2	% C to CO	% C to CO_2	Chlorine Balance	Carbon Balance
					Cr-Y Catalyst					
600	1785		425	96.2	103.4	6.2	67.2	15.1	113.4	86.1
601	1574	22854	425	94.6	93.8	1.0	76.3	9.1	100.1	90.8
602	1735		300	76.0	69.9	N.D.	46.1	3.1	93.9	73.2
603	1603	28440	300	37.4	27.1	N.D.	24.9	0.3	89.7	87.9
604	1769		360	98.2	93.8	N.D.	67.8	7.8	95.6	77.4
605	1736	27649	360	84.5	67.5	N.D.	69.1	2.6	83.1	87.3
606	1550		450	98.9	97.3	N.D.	77.4	14.5	108.8	93.2
					Ce-Y Catalyst					
643	1939		300	31.7	20.8	N.D.	20.6	2.8	89.1	91.8
644	1680	25440	300	23.0	4.7	N.D.	11.9	1.2	81.7	90.1
645	1779		325	48.6	27.8	N.D.	22.5	1.4	79.3	75.3
646	1485	25637	325	22.5	13.1	N.D.	13.5	0.5	90.6	90.0
647	1919		350	57.5	32.6	N.D.	42.1	3.5	74.8	87.7
648	1665	26097	350	48.4	26.9	N.D.	48.0	0.4	78.6	100.1
649	1899		375	78.3	57.1	N.D.	63.2	1.2	78.8	86.1
650	1541	26227	375	67.6	55.5	N.D.	51.9	0.6	87.9	84.9
651	1771		400	90.9	82.4	N.D.	79.0	5.5	91.5	93.6
652	1382	26124	400	85.2	67.1	N.D.	72.4	0.9	81.9	88.0
653	1774		425	96.9	92.9	N.D.	78.9	7.7	96.0	89.7
654	1760	27536	425	95.6	13.5	N.D.	68.2	0.6	17.9	73.2
655	2100		450	98.0	80.5	N.D.	76.2	7.9	82.5	86.0
656	1573	27295	450	97.4	101.9	N.D.	76.3	2.7	104.5	81.5

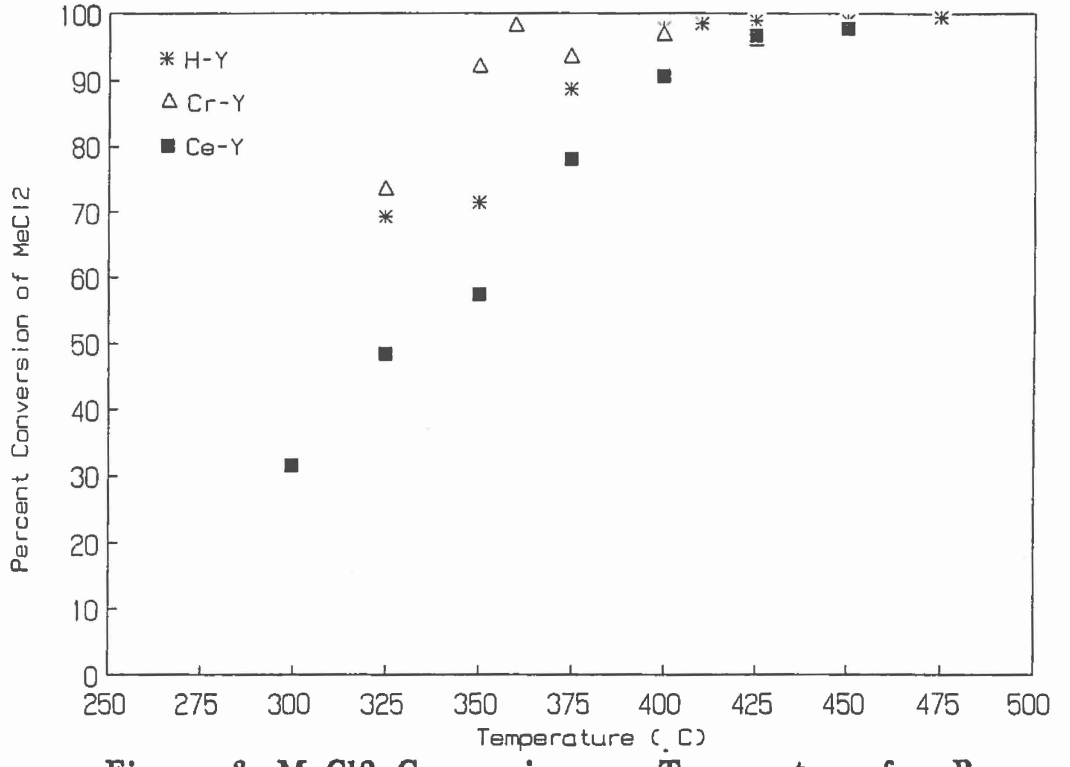

Figure 3. MeCl2 Conversion vs. Temperature for Runs without Water Addition

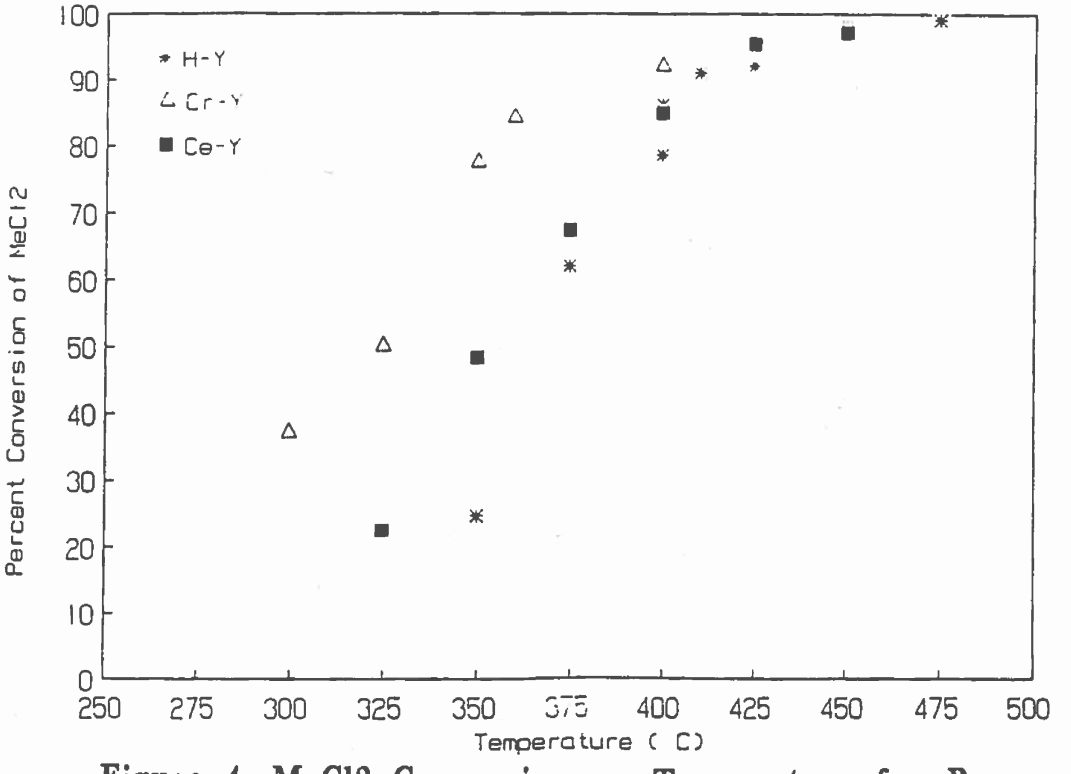

Figure 4. MeCl2 Conversion vs. Temperature for Runs with 27000 ppm Water Addition

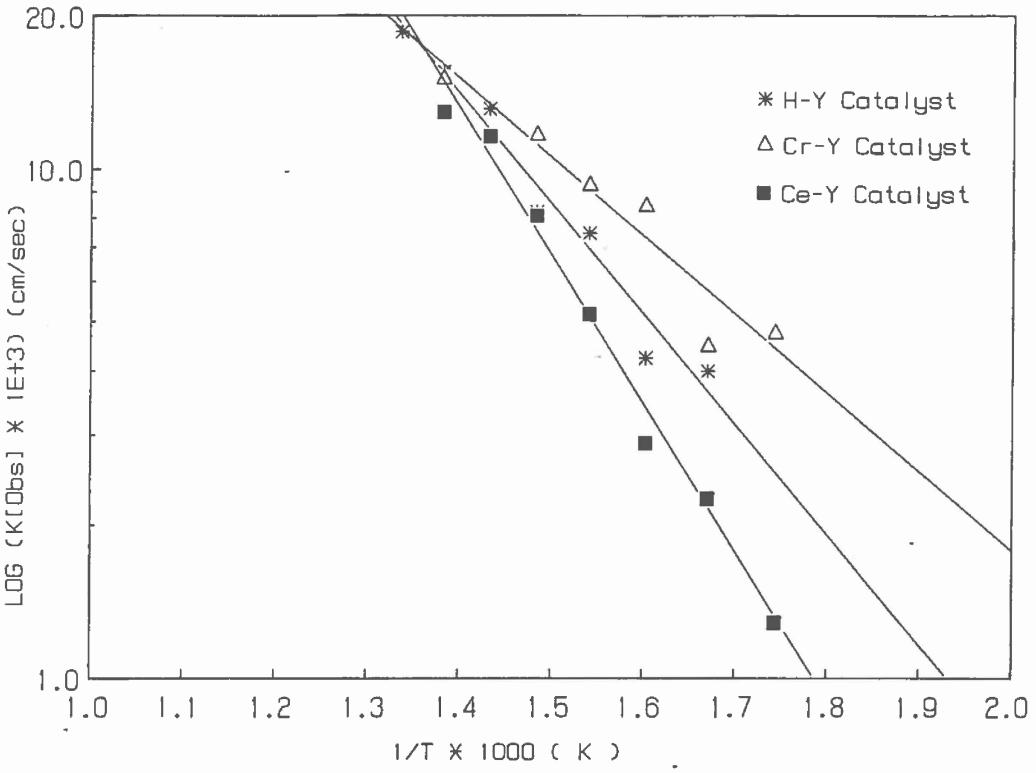

Figure 5. Arrhenius Plot for Runs without Water

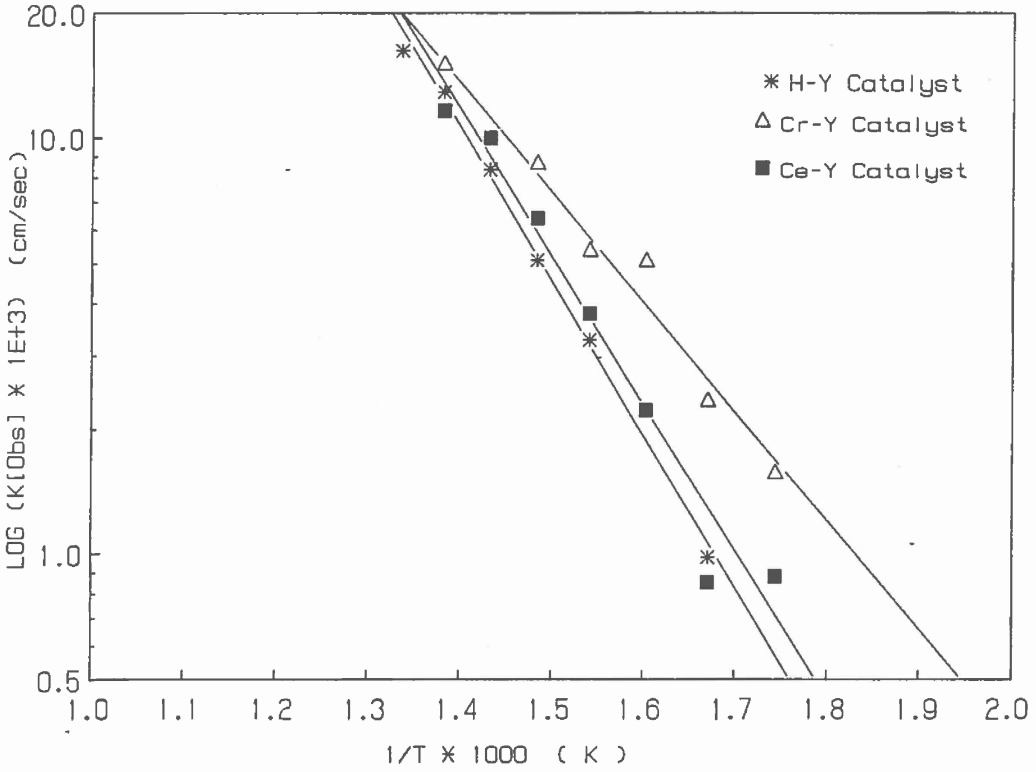

Figure 6. Arrhenius Plot for Runs with Water

TABLE 3: ACTIVATION ENERGIES OF ZEOLITE CATALYSTS FOR METHYLENE CHLORIDE OXIDATION

Water Addition	Catalyst		
	H-Y	Cr-Y	Ce-Y
	Activation Energies (Kcal)		
Without Water	9.92	7.08	13.28
With Water	19.92	12.01	16.16

For runs without water addition, the results showed that the observed rate constants (K_{obs}) of the catalysts increased in the order of Cr-Y > H-Y > Ce-Y, corroborating the fact that Cr-Y was the most active one.

However, with water addition and corresponding reduction in activity, the trend in rate constants was modified to Cr-Y > Ce-Y > H-Y. The resulting losses in activity are confirmed by the observed increases in activation energies. The effect of water addition was found to be temporary, however, as soon as water was removed from the feed, the catalysts regained their prior activity.

The product selectivity data for the zeolite catalysts without water addition to the feed did not show any detectable formation of undesirable higher chlorinated compounds as a result of partial oxidation reactions, as shown in Table 2. Only oxidation products such as HCl, CO and CO_2 were obtained in the product spectrum. However, small amounts of Cl_2 (1-6 percent) were formed with the Cr-Y catalyst, suggesting the occurrence of the Deacon reaction (14), whereby HCl and oxygen are converted to Cl_2 and H_2O. The low CO_2/CO product ratios (about 0.1) for all three catalysts, suggest that the zeolites generally favor the formation of CO over CO_2.

Water addition to the feed appeared to substantially reduce the catalytic selectivity toward CO_2 in the case of H-Y and Ce-Y, but only modestly with Cr-Y. Water addition also almost completely eliminated Cl_2 formation with the Cr-Y catalyst.

Table 4 lists the oxygen adsorption (or pickup) capacities of the three catalysts at 450°C along with their no-water feed conversions (at 350°C) and acidity values. Unfortunately, comparisons of oxygen pickup with feed conversions

for each catalyst at 450°C would be meaningless since all conversions were >95 percent. The comparisons in Table 4 suggest that feed conversion is possibly enhanced by an increase in catalyst oxygen pickup and/or acidity (based on mmole of desorbed NH_3 per gram of catalyst). However, this is not conclusive and should be further investigated.

TABLE 4: COMPARISON OF FEED CONVERSION, OXYGEN PICKUP AND ACIDITY OF DIFFERENT ZEOLITE CATALYSTS

Catalyst	Feed Conversion (%) [at 350°C]	O_2 Pickup (μg/g) [at 450°C]	Acidity mmol/g NH_3 [at 25°C]
H-Y	71.6	62.37	5.42
Cr-Y	92.2	104.70	6.49
Ce-Y	57.5	43.68	5.09

The "fractional cation availability" defined as the ratio of metal cations that are active for chemisorbing oxygen to the total number of metal cations present, was calculated by combining the oxygen pickup data and the catalyst metal loading obtained from X-ray fluorescence (XRF) data. The number of cations available for oxygen pickup was obtained from the oxygen adsorption data, arbitrarily assuming a 1:1 ratio between cations and adsorbed oxygen atoms. The total number of metal cations present in the zeolite was calculated from the metal loading (about 2 percent) of the chromium and cerium zeolites as measured by the XRF. The results showed that the fractional cation availability (FCA) for Cr-Y was 0.017 while for Ce-Y it was 0.022. This fraction implies that only about 2 of every 100 metal cations present in the zeolite structure are nominally accessible for 1:1 oxygen pickup.

The acidity values of the zeolite catalysts, based on mmole of desorbed NH_3 per gram of catalyst, followed the same trend as the oxygen pickup capacities. Cr-Y, the most active catalyst, showed the highest acidity; next was the H-Y, followed by the least active Ce-Y.

2. Discussion

The results indicate that the catalytic activity of the different zeolites was largely determined by the respective cations present in the Y zeolite matrix. The transition metal ion Cr^{3+} was present in Cr-Y while the rare earth ion Ce^{3+} occupied the cationic sites within the Ce-Y. By contrast, only H^+ ions (with small amounts of unexchanged Na^+) and no metal ions, were present in the H-Y. It is probable that these cations

influenced the acidity, oxygen adsorption capacity and ultimately the activity of the catalysts by virtue of properties including electronic structure, ionization potential, atomic radius, cation zeolite bond strength and site occupancy (or accessibility) within the zeolite.

The primary catalytic property for predicting activity in oxidative reactions is usually the oxygen adsorption capacity of the catalyst. In the case of cation-exchanged zeolites, the oxygen adsorption capacity of a zeolite is believed to increase with the highest available oxidation state change (22, 23). Thus, comparing Cr-Y and Ce-Y, the Cr ion could be oxidized to a valence state (Cr^{3+} to Cr percent^{+})(32, 22) higher than that of the Ce ($Ce^{3+}$to Ce^{4+}) ion (33).

Also unfavorable for Ce-Y activity, it is noted that to an incoming ligand, the rare earth Ce^{3+} ion presents essentially a noble gas atom outer electronic arrangement with the 4f orbitals and the electrons occupying them being effectively unavailable, whereas the partially filled d orbitals of the Cr^{3+} transition metal ion make Cr-Y much more reactive. Furthermore, the larger size of the Ce^{3+}ion ($\simeq$1.03 Å) vs Cr^{3+}($\simeq$ 0.63 Å) minimizes the covalent interaction with ligands and thus electrostatic interactions are reduced (34) over what they might be for a typical 3+ charge. As a result, the Ce^{3+} ion is susceptible to form far fewer addition complexes than the Cr^{3+}.

In addition to the poor reactivity of the Ce cations, their inaccessibility due to migration from zeolite supercages toward the smaller β cages (35) at elevated calcination temperature (550^{0}C) could also have caused lower oxygen pickup and activity of Ce-Y as compared to the Cr-Y. Although the FCA for the Ce-Y was higher than for the Cr-Y, its oxygen pickup capacity was substantially less. This is reasonable since the FCA was calculated, based on the total number of metal ions present in the zeolites and Cr-Y had almost three times the number of exchangeable metal ions that Ce-Y did. Hence it could be argued that the ions exchanged on the Ce-Y occupied fewer sites which were on average more accessible to oxygen atoms than with the Cr-Y, where cation exchange continued even after oxygen accessible sites were filled.

In contrast to the Cr-Y and the Ce-Y catalysts, the H-Y catalyst did not have an exchanged metal ion, yet showed slightly higher oxygen pickup than did the Ce-Y. At this point, it is not clear whether the adsorbed oxygen was directly associated with the framework Al atoms or somehow bonded to the Brönsted acid sites in the H-Y catalyst. It seems evident however, that cerium exchange must have blocked or interfered with more original H-Y sites than were created during the exchange process.

Even though the absence of any exchanged metal ions in the H-Y could make it appear to be a blank catalyst and lead us

to accept the results obtained with the H-Y as baseline experiments, it was apparently not the case. Under the existing conditions, no detectable homogeneous reactions of $MeCl_2$ occurred at temperatures below 400°C. This, therefore, suggests that, in spite of the absence of any exchanged metal ions, the H-Y catalyst did have some activity which was considerably higher than the homogeneous conversion results.

As suggested by Gentry et al. (17), oxidation of a hydrocarbon with a cation exchanged zeolite can involve two primary steps: (a) hydrocarbon adsorption as a secondary carbonium ion at the Brönsted acid sites, (b) oxygen adsorption at cationic sites. In subsequent steps, this adsorbed oxygen reacts with the carbonium ion to yield final oxidation products. Therefore, both the acidity and the oxygen pickup can influence the catalytic activity for hydrocarbon oxidation with zeolite catalysts.

The catalyst acidity values showed the same trend as oxygen pickup (Cr-Y > H-Y > Ce-Y). It is known that replacement of monovalent ions by polyvalent ones in Y zeolites improves activity by creating highly acidic centers through hydrolysis of charged cations (16). This is represented by the scheme

$$Me^{n+} + xH_2O \quad \Leftrightarrow \quad Me(OH)_x^{(n-x)} + xH^+$$

Thus, Cr-Y would show acidity higher than that of H-Y due to enhanced cation hydrolysis of the trivalent chromium ion. Further, the above reaction equilibrium is known to move toward the right with decreasing cation radius and increasing electrostatic field potential of the cation (36, 37). Therefore, in the present experiment, the lower electronegativity and larger ionic radius of cerium ions would be expected to produce lower acidity in the Ce-Y than in the Cr-Y or the H-Y. Hence, both the oxygen adsorption and the acidity results tend to support the observed catalytic activity for $MeCl_2$ oxidation in the absence of water.

Water addition ($\simeq$ 27,000 ppm) during vapor phase $MeCl_2$ oxidation with all the zeolite catalysts resulted in a sudden significant reversible drop in activity. Similar results were also reported by Petunchi and Hall (38) during CO oxidation with Cu-Y. The possible reason for such an occurrence could have been the blockage of cationic sites by water molecules. As explained by Breck (39), when water molecules enter inside the Y zeolite cavity they are localized near the cationic sites. Non-framework water and cations behave as a concentrated electrolyte. At higher temperatures, this localization is prevented and the zeolite does not undergo any structural changes during this process. Results obtained during the present experiments tend to support this approach. Thus, as the reaction temperature was gradually increased from 300 to 400°C, the deactivation effect of water addition diminished accordingly.

The following kinetic scheme can be proposed for the present reaction system:

(Note that { } and [ ] represent two different catalytic sites.)

1. $CH_2Cl_2 + \{\ \} \Leftrightarrow \{CH_2Cl_2\}$
2. $O_2 + [\ ] \Leftrightarrow \}[O_2]$
3. $[O_2] + [\ ] \Leftrightarrow 2[O]$
4. $\{CH_2Cl_2\} + [O] \Leftrightarrow [CO] + 2\{HCl\}$
5. $2\{HCl\} + [O] \Leftrightarrow [H_2O] + \{Cl_2\}$
6. $[CO] + [O] \Leftrightarrow [CO_2]$
7. $[CO] \Leftrightarrow CO + [\ ]$
8. $\{HCl\} \Leftrightarrow HCl + \{\ \}$
9. $[CO_2] \Leftrightarrow CO_2 + [\ ]$
10. $\{Cl_2\} \Leftrightarrow Cl_2 + \{\ \}$

As depicted in the above mechanism, the first three steps involve reactant adsorption either at Brönsted acid sites (CH_2Cl_2) or at the metal ion sites (O_2). Step 4 is the probable dual site reaction of the feed while Step 5 shows the Deacon by-product reaction proceeding between the product HCl and the adsorbed oxygen. Step 6 represents the formation of product CO_2. Steps 7, 8, 9, and 10 represent desorption of products (CO_2, CO, HCl and Cl_2).

Additional experiments are obviously needed to ascertain the validity of the dual site reaction mechanism in this case. However, since HCl, Cl_2, CO and CO_2 were the only compounds present (other than unconverted $MeCl_2$) in the product spectrum from the three zeolite catalysts, the oxidation of $MeCl_2$ did not appear to violate the above mechanism. Even if any intermediate chlorinated by-products were formed, they were converted to these final products and thus remained undetected.

Although the effects of diffusion might be expected to become significant at higher conversions in the case of a zeolite catalyst, the Arrhenius plots for the H-Y, Cr-Y and Ce-Y catalysts did not show any curvature at high temperatures suggesting diffusion limitations. If this effect were true the small size of the $MeCl_2$ molecule (4.75 Å), as compared to the entrance ($\simeq$ 8 Å) to the large faujasite supercages would have played a significant role. However, a detailed investigation of the potential for diffusion limitations has not yet been carried out.

The presence of Cl_2 only in the product spectrum of the Cr-Y suggested the occurrence of the Deacon reaction only with this catalyst. Addition of water retarded the Deacon reaction on this catalyst and competed for sites occupied by Deacon reactants (i.e., HCl and O_2).

The reduction in CO_2/CO ratio with water addition for all three catalysts suggests that CO (which may need to be desorbed and then re-adsorbed in order to form CO_2) receives increased competition for active sites from the added water. If we speculate that the active site is an adsorbed oxygen, this is consistent with the concomitant loss in CH_2Cl_2 oxidative activity, which we believe also requires adsorbed oxygen to proceed.

B. COMPARISON OF WASHCOATED CORE CATALYST PERFORMANCE USING THREE FEEDS(METHYLENE CHLORIDE, CARBON TETRACHLORIDE AND TRICHLOROETHYLENE)

1. Results

The catalytic experiments were carried out with 10 different catalysts. Three of these catalysts were metal exchanged zeolites washcoated on cordierite cores. The metals selected for exchange were cobalt (Co), chromium (Cr) and manganese (Mn). In this report, these catalysts are referred to as Co-Y, Cr-Y and Mn-Y respectively. Three more catalysts were prepared by chromia impregnation of the previously washcoated metal exchanged zeolites. These are listed here as Co-Y/CA, Cr-Y/CA and Mn-Y/CA respectively. A separate catalyst was prepared by washcoating the cordierite with Silbond alone (no zeolite), then impregnating it with chromia. This is referred to as the Silbond/CA catalyst. Two separate washcoated Co-Y and Co-Y/CA catalysts were prepared with an alumina-based binder (Chlorhydrol) instead of silica-based Silbond. These catalysts were used to compare the effects of binders on catalyst properties. Finally, another Co-Y/CA catalyst was prepared from 1/16 inch diameter Na-Y extrudates. This catalyst, listed here as Co-Y/CA pellets, was prepared by Co exchange of the Na-Y extrudates followed by chromia impregnation.

After completion of catalyst preparation, the compositions of the washcoated cores, as well as the pellets, were determined using XRF techniques. In addition to the actual catalyst cores, the base metal exchanged powdered zeolites (viz., Co-Y, Cr-Y and Mn-Y) were also analyzed to obtain information about levels of metal exchange. To determine the effect of chromia impregnation on washcoated cores, the Silbond binder and the Chlorhydrol binder were calcined to powder form and then impregnated with chromia and calcined. These catalyst forms, referred to as Silbond/CA powder and Chlorhydrol/CA powder respectively, were also analyzed in the XRF. Table 5 lists the results of the X-ray analyses.

TABLE 5: THE CHEMICAL COMPOSITION OF VARIOUS CATALYSTS

Catalyst	Composition						
	Al_2O_3	MgO	Fe_2O_3	SiO_2	Co_3O_4	Cr_2O_3	MnO_2
Co-Y (Powder)	23.56	0.00	0.00	75.67	0.74	0.00	0.00
Co-Y (Core)	26.73	8.68	0.30	63.72	0.15	0.00	0.00
Co-Y (Core) Chlorhydrol	44.17	7.30	0.27	47.74	0.22	0.00	0.00
Co-Y/CA (Core)	24.64	8.57	0.35	64.67	0.09	1.46	0.00
Co-Y/CA (Core) Chlorhydrol	38.22	8.20	0.33	51.02	0.15	2.20	0.00
Co-Y/CA (Pellet)	34.24	0.00	0.03	58.10	1.05	5.98	0.00
Cr-Y (Powder)	25.66	0.14	0.05	72.89	0.00	1.20	0.00
Cr-Y/CA (Core)	25.98	8.96	0.34	63.18	0.00	1.30	0.00
Mn-Y (Powder)	27.91	0.42	0.07	64.07	0.00	0.00	7.50
Mn-Y (Core)	29.54	9.69	0.34	59.44	0.00	0.00	0.64
Mn-Y/CA (Core)	28.56	9.87	0.40	59.42	0.00	1.56	0.30
Silbond/CA (Core)	27.72	10.14	0.34	60.26	0.00	1.04	0.00
Silbond/CA (Powder)	2.09	0.00	0.00	92.30	0.00	5.58	0.00
Chlorhydrol/CA (Powder)	85.59	1.44	0.00	2.95	0.00	9.69	0.00

The cordierite support used for washcoating metal exchanged zeolite was mostly made up of alumina ($\simeq$ 35 percent), magnesia ($\simeq$ 13 percent) and silica ($\simeq$ 50 percent). Besides these, trace amounts (<1 percent) of oxides of iron, calcium and titanium were also present.

Cobalt exchange with the LZ-Y82 powder produced 0.74 wt percent cobalt loading on the unsupported Co-Y zeolite. After washcoating with Silbond, the resulting Co loading on the washcoated core was only 0.07 percent. The cobalt content was thus low as a result of the large quantity of inert support material ($\simeq$ 80 percent) that now made up the total catalyst. The Co loading corresponded to approximately 60 percent zeolite in the final calcined washcoat. However, the alumina based Chlorhydrol washcoated Co-Y produced higher Co loading (0.13 percent) partly as a result of increased zeolite content of the final washcoat. Chromia impregnation of the two different washcoated catalysts also showed a difference in Cr_2O_3 loading. While the Chlorhydrol washcoated Co-Y/CA showed 1.73 percent Cr_2O_3 content, the Silbond washcoated Co-Y/CA contained only 1.26 percent Cr_2O_3.

XRF analysis of the chromia impregnated Co-Y/CA cores also showed a drop in Co concentrations following the impregnation step. With both the Silbond and Chlorhydrol washcoats, a 50-80 percent drop in Co concentration was noticed.

This reduction was much more than that expected as a result of 1-2 percent Cr_2O_3 loading, suggesting a probable structural loss due to Cr_2O_3 impregnation.

The 1/16 inch diameter Co-Y/CA pellets, conversely, showed higher cobalt ($\simeq$ 1 percent) and chromia ($\simeq$ 6 percent) loading than both the washcoated catalysts. The Silbond and Chlorhydrol washcoated catalysts also showed differences in silica and alumina content. The silica-based Silbond catalyst showed higher overall silica content ($\simeq$ 64 percent) while alumina-based Chlorhydrol catalyst showed increased overall alumina content ($\simeq$ 40 percent).

Cr and Mn exchange of the LZ-Y82 zeolite produced 1.2 percent and 7.5 percent loading of the respective metals in the powdered zeolite. As with the Co-Y cores, the approximate 50-60 percent powdered zeolite content of the calcined washcoat produced less than 1 percent overall Cr_2O_3 or MnO_2 content of the washcoated cores. Since the bulk of the washcoated catalyst was made up of the inert cordierite core, the diluent effect of the core produced the lower overall Cr_2O_3 or MnO_2 content. Cr_2O_3 impregnation further reduced the exchanged metal concentration in the washcoated catalysts and this was much more severe than that expected by the addition of 1-2 percent of impregnated Cr_2O_3. This effect was more prominent in the case of Mn-Y/CA than Cr-Y/CA, since in the later case, both impregnated and exchanged metal salts were Cr_2O_3.

The chromia-impregnated Silbond washcoated (no zeolite) cordierite supported catalyst showed approximately 1 percent overall chromia loading, similar (1.2 percent) to that obtained with the earlier Silbond washcoated Co-Y/CA core. The unsupported Silbond/CA and Chlorhydrol/CA powders, prepared by CA impregnation of calcined Silbond and Chlorhydrol binders respectively, showed a significant difference in Cr_2O_3 content between the two binders. As seen earlier with the Co-Y/CA cores, alumina-based Chlorhydrol/CA gave higher Cr_2O_3 loading (9.6 percent) than the Silbond/CA (5.5 percent).

The BET surface areas of the various washcoated cores and the metal exchanged zeolite powders are shown in Table 6. As can be seen, all the metal exchanged zeolite powders had much higher surface area (500-600 m^2/g) than the washcoated cores (85-115 m^2/g). The inherent low surface area (0.5-1 m^2/g) of the inert support material (cordierite) that comprised almost 80 percent of the total washcoated catalyst was primarily responsible for this decrease in surface area. Conversely, it was the high surface area of the zeolite present in the washcoat that determined the total surface area of the washcoated catalysts. Following Cr_2O_3 impregnation, the surface areas of the washcoated cores were further reduced to about 15-40 m^2/g. Similar to the washcoated catalyst cores, the exchanged and impregnated 1/16 inch pellets also showed a drop in surface area following the chromia impregnation. The original surface area of

about 570 m^2/g with the Co-Y was reduced to 325 m^2/g with approximately 6 percent of chromia loading.

As mentioned above, the surface areas of the washcoated catalysts were mostly dependent on the zeolite content and hence the differences between the two different types of washcoats could not be distinguished from these data. However, the pure Silbond/CA and Chlorhydrol/CA powders were completely free from any zeolite and were able to show a clear difference in the surface area between these two binders. Chlorhydrol appeared to be of much higher surface (160 m^2/g) area than Silbond (2 m^2/g).

Table 6 shows the oxygen pickup capacities of the metal exchanged zeolite powders and the metal-exchanged 1/16 inch diameter zeolite pellets. The unit mg/g signifies mg of oxygen adsorbed per gram of catalyst used. Among the various metal exchanged zeolites, O_2 pickup increased from Co-Y to Cr-Y to Mn-Y. The "fractional cation availability", defined as the ratio of metal cations which are active for chemisorbing oxygen to the total number of metal cations present, was calculated by combining the oxygen pickup data and the metal loading of the zeolites. Among the metal exchanged zeolites, Co-Y showed the highest FCA of 0.86, i.e., 86 percent of the cobalt ions present within the zeolite matrix were available for oxygen adsorption in a one-to-one ratio. The FCA ratios for the other two metal-exchanged zeolites were relatively lower, with 0.60 for Cr-Y and 0.15 for Mn-Y. However, it is possible that, since both Cr-Y and Mn-Y had larger concentrations of respective metal ions than Co-Y (Mn-Y: 10 times more metal atoms than Co-Y; Cr-Y: 2 times as many as Co-Y), so that even if the total number of sites for O_2 adsorption were similar, different FCA numbers would be obtained with Cr-Y and Mn-Y.

The effect of Cr_2O_3 treatment on oxygen adsorption capacity of the zeolite catalysts is evidenced by comparing the 1/16 inch diameter Co-Y and Co-Y/CA pellets. The O_2 pickup capacity of the Co-Y pellet dropped sharply from 2.78 mg/g to 1.365 mg/g following the Cr_2O_3 impregnation. This could have been a consequence of the combination of drop in surface area and loss of Co from the zeolite, caused by Cr_2O_3 impregnation. Conversely, comparing the oxygen adsorption of the Cr_2O_3 impregnated calcined Silbond and Chlorhydrol powders revealed that the higher surface alumina binder produced much better oxygen adsorption than the silica based one. Normalizing the O_2 pickup based on Cr_2O_3 content, revealed that the Chlorhydrol/CA picked up 0.355 g of oxygen per gram of Cr_2O_3 while the same for the Silbond/CA was only 0.027 g per gram of Cr_2O_3. This difference in results suggests a much better dispersion of Cr_2O_3 sites on the alumina based binder than the silica one.

TABLE 6: COMPARISON OF THE PROPERTIES OF THE VARIOUS CATALYSTS

Catalyst	Cation Loading (as wt. % TMO)	Surface Area (m^2/g)	O_2 Pickup (mg/g)	FCA
H-Y (Pellet)	0.00	574		
Co-Y (Powder)	0.74	540	1.27	0.86
Co-Y (Pellet)	3.00	576	2.78	1.05
Co-Y/CA (Pellet)	1.05	325	1.37	
Co-Y (Core)	0.15	116		
Silbond Co-Y/CA (Core)	0.09	21		
Silbond Co-Y (Core)	0.22	109		
Chlorhydrol Co-Y/CA (Core)	0.15	15		
Chlorhydrol Cr-Y (Powder)	1.20	564	1.5	0.60
Cr-Y/CA (Core)		31		
Mn-Y (Powder)	7.50	619	2.04	0.15
Mn-Y (Core)	0.64	86		
Mn-Y/CA (Core)	0.30	40		
Silbond/CA (powder)		2	0.15	
Chlorhydrol/CA (Powder)		160	3.45	

The catalytic activity data for the various zeolitic catalysts are presented in Figures 7 through 10. The activities of the different catalysts are compared on the basis of actual feed conversion obtained with several chlorinated VOCs. Each graph shows the conversion of a particular VOC with various catalysts as a function of temperature. Unless mentioned as pellets, all the catalysts used were washcoated cordierite cores. Space velocities shown on the graphs were calculated at ambient temperature and based on the catalyst bed volume.

As shown in Figure 7, among all the washcoated catalyst cores, $MeCl_2$ conversion was highest with the Co-Y catalyst. More than 90 percent conversion of $MeCl_2$ could be obtained with the Co-Y at temperatures at and above 350°C. Generally, all the metal exchanged and washcoated catalysts without chromia impregnation produced higher $MeCl_2$ conversions than the impregnated ones. For example, Co-Y/CA produced 10-20 percent lower $MeCl_2$ conversion than the Co-Y under identical conditions. Similar results were obtained with Cr-Y/CA and Mn-Y/CA catalysts. The Co-Y/CA pellets and the washcoated Silbond/CA catalysts were at the extremes of the conversion spectrum; while zeolite-rich Co-Y/CA pellets produced the highest conversion among all the

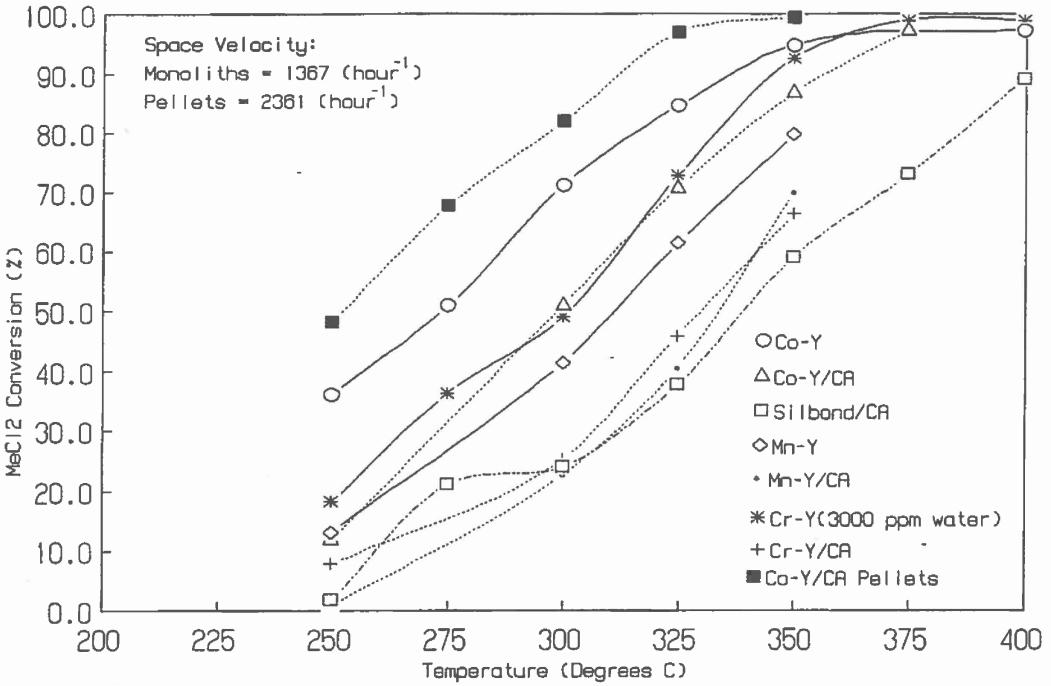

Figure 7. MeCl2 Conversion vs. Temperature plot with Various Catalysts

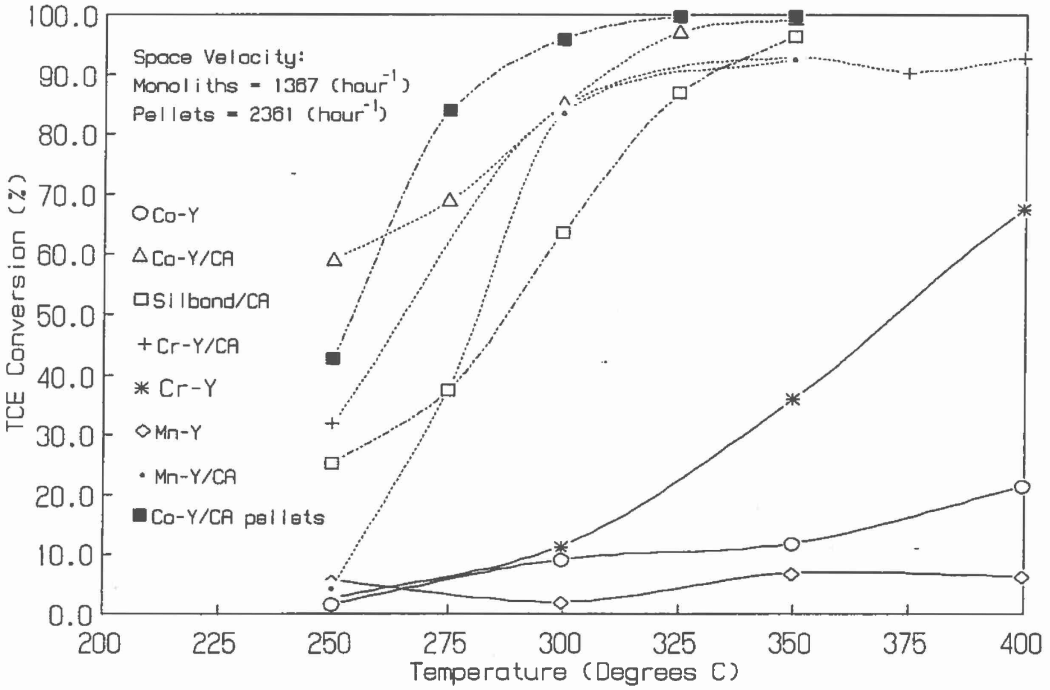

Figure 8. TCE Conversion vs. Temperature plot with Various Catalysts

catalysts, the zeolite-free Silbond/CA was the worst. The Co-Y/CA pellets produced over 90 percent conversion of $MeCl_2$ at temperatures as low as 300°C. This represents about 40°C drop in reaction temperature for similar conversion level as compared to the washcoated Co-Y core. By contrast, the Silbond/CA catalyst needed a minimum temperature of 400°C to produce 90 percent conversion of $MeCl_2$.

Activities of the various catalysts for TCE conversion are compared in Figure 8. The drastic difference between the reactivity of $MeCl_2$ and TCE is indicated by the extremely low conversion of TCE with the Co-Y, Cr-Y and Mn-Y catalysts. Whereas non-chromia-impregnated catalysts produced higher $MeCl_2$ conversions than their chromia-impregnated counterparts, the case was completely reversed with TCE. Without chromia impregnation all three metal exchanged catalysts showed less than 50 percent conversion at temperatures below 350°C. However, among the cation exchanged washcoated catalysts, Cr-Y appeared to show better activity for TCE destruction at 300°C and above. Following impregnation, the same catalysts produced 80 percent and above conversions at temperatures as low as 300°C. The order of activity among the three chromia-impregnated zeolite catalysts was: Co-Y/CA > Cr-Y/CA > Mn-Y/CA. The difference in activity was primarily noticeable at temperatures below 300°C where the Co-Y/CA was much superior to the other two.

In the case of TCE, the Silbond/CA washcoated catalyst cores showed higher activity than the non-chromia-impregnated zeolite cores. However, its activity was still considerably lower than the similar chromia impregnated zeolite cores.

Co-Y/CA pellets, as expected, produced higher activity for TCE conversion compared to the supported washcoated ones. This catalyst was able to produce 90 percent and higher conversions from 250°C upwards. For TCE conversions over 90 percent, this meant almost 60°C reduction of the minimum reaction temperature as compared to the washcoated Co-Y/CA catalyst.

The activity of the various zeolite catalysts for decomposition of CCl_4 is shown in Figure 9. The non-impregnated zeolite catalysts (Co-Y, Cr-Y, etc.) gave much higher conversion of CCl_4 than their chromia-impregnated versions (Co-Y/CA etc.). The Co-Y catalyst was the best, producing almost complete conversion of CCl_4 at temperatures of 175°C and above. The chromia-impregnated Silbond/CA catalyst showed the worst activity with CCl_4. The Co-Y/CA pellets, conversely, showed activity as high as the Co-Y catalyst and produced complete conversion of CCl_4 at temperatures as low as 200°C. Although CCl_4 conversions between Cr-Y and Cr-Y/CA should not be compared, due to the difference in water concentrations, additional unpublished data with Cr-Y and also other such catalysts do show that the activity of the exchanged catalyst is significantly higher for CCl_4 conversion than similar exchanged/impregnated ones (Cr-Y/CA).

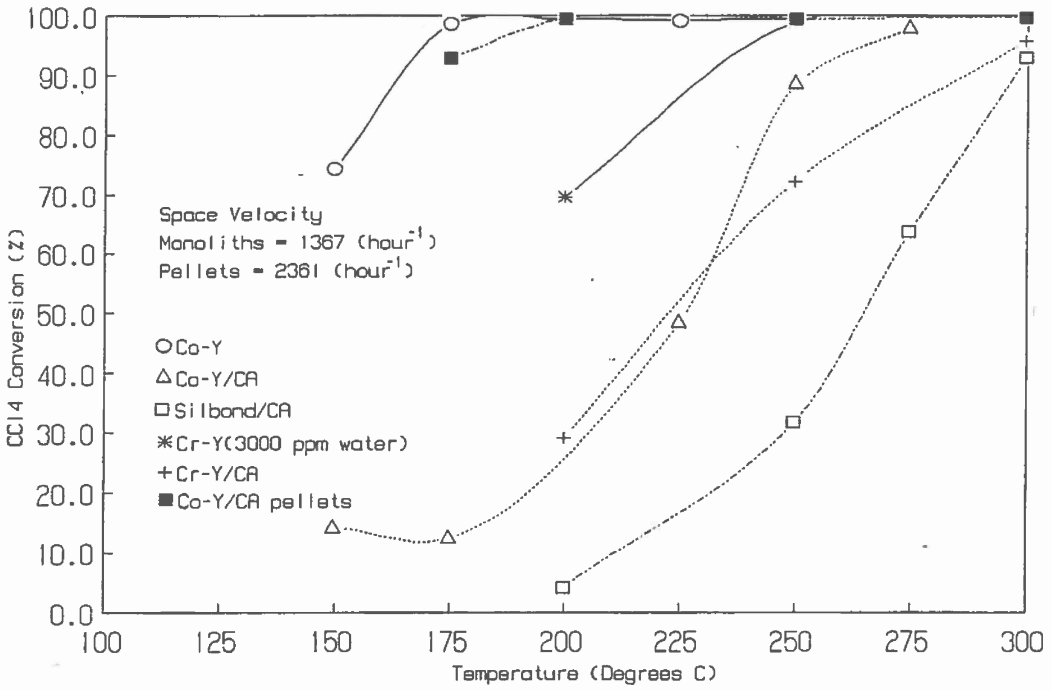

Figure 9. CCl4 Conversion versus Temperature plot with Various Catalysts

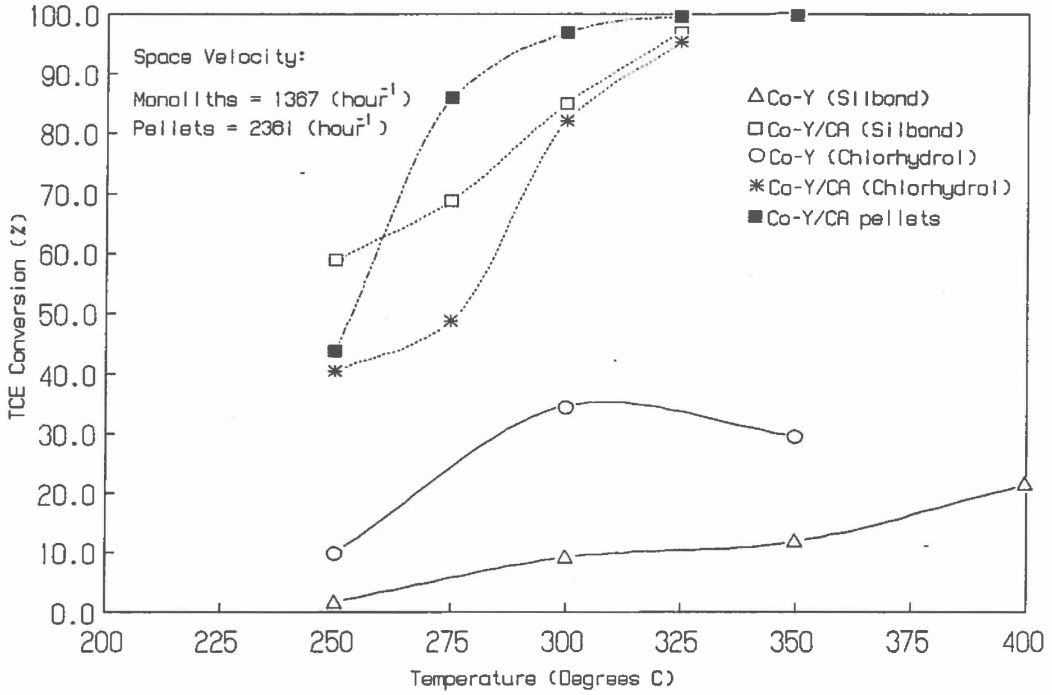

Figure 10. TCE Conversion vs. Temperature plot with Various Catalysts

Since this study incorporated several washcoated metal exchanged zeolite catalysts, the properties of the washcoat and its effect on the overall catalytic activity was also of paramount importance. As mentioned earlier, two different binders, one silica-based (Silbond) and the other alumina-based (Chlorhydrol), were used to washcoat the zeolite powder on the cordierite supports. The loading level of the active zeolite phase on the washcoated support (which depended on the volatility of the binder precursor) significantly affected the activity of the catalyst. Moreover, during chromia impregnation of the washcoated catalysts, the surface area of the washcoat directly affected the loading of Cr_2O_3. Therefore, it was necessary to compare the activity of washcoated catalysts prepared from these binders for CVOC destruction.

Figure 10 compares the TCE oxidation activity of the washcoated Co-Y and Co-Y/CA catalysts, made from these two different binders. Even though both surface area and oxygen pickup capacity of the chromia-impregnated calcined Chlorhydrol powder were much higher than the Silbond/CA powder, Co-Y and Co-Y/CA catalysts prepared with these two binders showed very similar results. Between the two Co-Y catalysts, the Chlorhydrol washcoated one showed modest but slightly higher activity for TCE oxidation than the Silbond washcoated one. Conversely, comparing the Co-Y/CA catalyst cores showed the Silbond washcoated one producing slightly higher conversion than the Chlorhydrol one. However, the unsupported Co-Y/CA pellets, as expected, were still by far the best catalyst for TCE conversion.

As far as product selectivity was concerned, CO, CO_2 and HCl were the major products obtained during the oxidation of the chlorinated VOCs with the zeolite catalysts. The CO_2/CO ratio in the product spectrum was quite similar between $MeCl_2$ and TCE. The CO_2/CO ratio was approximately 0.02-0.05 for non-chromia impregnated catalysts, such as Co-Y, while it increased to 0.2-0.3 following the chromia impregnation (Co-Y/CA, Cr-Y/CA, etc.). It appeared that this increase in CO_2 production was a direct effect of chromia impregnation, since even the Silbond/CA catalyst produced a CO_2/CO ratio similar to the Co-Y/CA and Cr-Y/CA catalysts. By contrast, CO_2 was the only carbon containing product formed during CCl_4 oxidation, with all the catalysts; no detectable amounts of CO were observed.

During oxidation of the chlorinated VOCs, the bulk of the chlorine was converted to HCl, utilizing excess hydrogen from the added water. Small amounts of elemental Cl_2 (1-10 percent) were detected with chromia-impregnated catalysts in the temperature range of 300 to 350°C, suggesting the occurrence of the Deacon reaction. With CCl_4 experiments below 200°C, about 5-10 percent $COCl_2$ was detected. No other undesirable higher chlorinated partial oxidation products could be detected in the product spectra of the various catalysts.

The results from the acidity determination experiments are plotted in Figures 11 and 12. While the abscissa denotes temperature, the normalized NH_3 desorbed per degree temperature increment is indicated in the ordinate. Ammonia is reported to be an excellent probe molecule for acidity determination of zeolites due to its small size and strong basicity. As plotted in Figures 11 and 12, the position of the temperature maximum of the ammonia desorption versus temperature graph is a qualitative indication of the magnitude of the NH_3 desorption activation energy and, consequently, the relative acid strength of the particular sites (26). All the curves displayed a major desorption peak between 150 and 200°C. This peak was indicative of the weak Brönsted sites present in the zeolite catalysts, which were easily accessible to the adsorbing NH_3. Among the three cation-exchanged zeolites (Figure 11), the relative acid strength increased in the order of Mn-Y (167°C) < Co-Y (170°C) < Cr-Y (174°C). Similarly, in the case of the pelletized catalysts (Figure 12), the acidity increased from H-Y (167°C) to Co-Y (170°C) to Co-Y/CA (187°C). This suggested that the acidity of the zeolites increased by cation exchange from the base H-Y value (except with Mn-Y) with Co-Y/CA producing the maximum acid strength among all of them.

Apart from the temperature maximum of the NH_3 desorption curve, the area under the desorption peak is also indicative of the relative number of acid sites present. Comparison of the desorption curves of the different catalysts shows that the apparent number of weak Brönsted sites was almost similar among the three cation-exchanged zeolite powders (Figure 11). However, Figure 12 indicates a significant drop in the number of acid sites in going from H-Y to Co-Y, but, chromia impregnation did not appear to influence the site availability for NH_3 adsorption on the Co-Y/CA, as compared to the Co-Y. This suggested that although the strength of the acid sites was increased by cation exchange, this also produced a loss of the total number of acidic sites.

A second much smaller desorption peak was obtained with the powdered cation exchanged zeolites in the range of 300 to 400°C, indicating the presence of small amounts of strong Brönsted acid sites. Among these stronger acidic sites, a distinct and significant peak was noticed only with Co-Y. The other two zeolites (Cr-Y and Mn-Y) showed much smaller inflection in this region. Although, peak tailing could have affected the results in this region, the data seemed to indicate the presence of a significant amount of stronger Brönsted sites with the Co-Y which were less noticeable with Cr-Y and Mn-Y. Although the relative strength of these strong acid sites could not be clearly distinguished due to tailing of the desorption peaks, it appeared that, similar to the weaker sites, the strength of these strong Brönsted acid sites was also maximum with the Cr-Y.

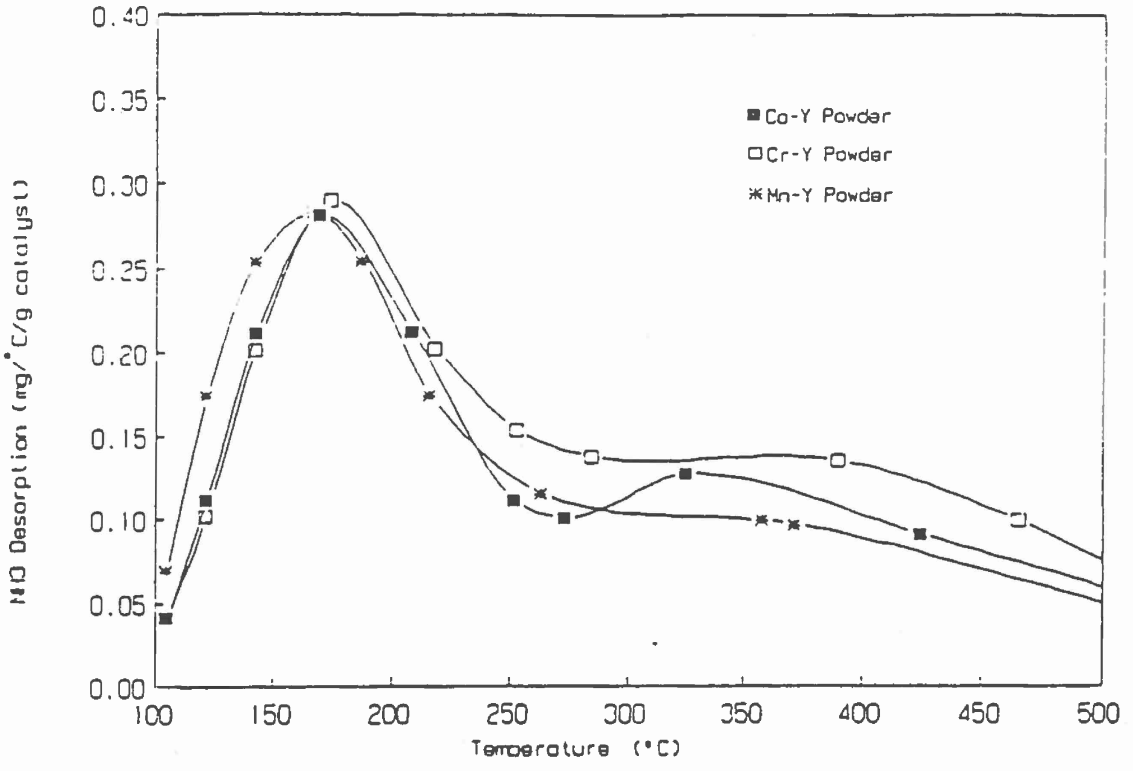

Figure 11. NH3 Desorption versus Temperature plot with Cation-exchanged Zeolite Powders

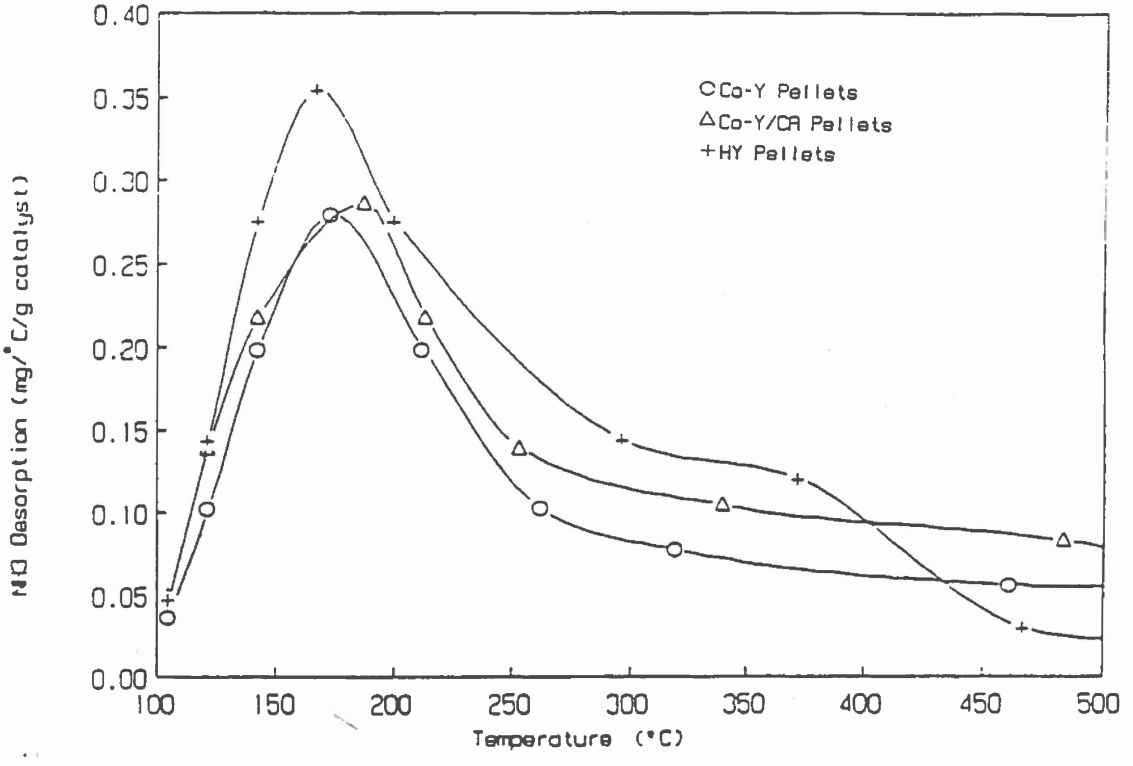

Figure 12. NH3 Desorption versus Temperature plot with Various Zeolite Pellets

2. Discussion

As indicated in the results, the properties of these zeolite/TMO bifunctional catalysts were determined by both the cations present within the zeolite as well as the TMO impregnated on the washcoat. The three different transition metal ions, Co^{2+}, Cr^{3+} and Mn^{2+}, when exchanged into the Y zeolite matrix, played a major role in influencing the catalytic properties for complete oxidation of the chlorinated hydrocarbons.

It is probable that addition of these transition metal ions improved the catalytic properties in two ways. First, since the cationic sites are responsible for oxygen adsorption (26), the presence of transition metal cations with higher available oxidation states and lower ionization potential improved the O_2 pickup capacity of the exchanged zeolite. Secondly, cation hydrolysis of the bi or tri-valent transition metal ions, in the presence of water vapor, increased the Brönsted acidity of the zeolite (41). However, the differences in electronic structure, ionization potential, cation-oxygen bond strength, etc. among the three exchanged cations could be expected to produce variations in catalyst activity.

The oxygen pickup capacity of the three cation-exchanged zeolites was found to decrease from Mn-Y>Cr-Y>Co-Y. However, the total amount of cations present in the respective zeolites also decreased in the same order. Since the transition metal cations are assumed to be primarily responsible for the increased oxygen adsorption capacity of the zeolites at elevated temperatures, the lower cation content could have produced lower O_2 pickup with the Co-Y.

However, the activity of a cation exchanged zeolite for the complete oxidation process is believed to be determined not only by its oxygen adsorption capacity but also by the ionization potential of the cation and the cation-oxygen bond strength. Total oxygen adsorption is controlled by the ease of oxidizability of the cation to higher valence states and, therefore, in the present study Cr (+3 to +5 to +6) and Mn (+2 to +4) could have produced higher oxygen pickup capacity than Co (+2 to +3). However, the ability of an oxide for total oxidation increases with lower ionization potential (42) and with lower heat of formation of cation-oxygen bond (18). Suzuki et al. (18) earlier reported that Co-Y showed lower heat of formation for cation oxygen bonds during ethanol oxidation than either Cr-Y or Mn-Y. Furthermore, the cation oxygen bond strength is smaller (43) with Co (92 kcal/mole) than with Cr (102.6 kcal/mole) or Mn (96.3 kcal/mole). This could have led to the formation of a less stable and weakly bound oxygen species with cobalt, which in turn produced the higher activity of the cobalt exchanged Y zeolite, so noticeable with $MeCl_2$ and CCl_4 oxidation, despite its lower total oxygen pickup.

Besides oxygen pickup and cation-oxygen bond strength, acidity of the zeolite also plays a major role in controlling the activity for chlorocarbon oxidation (26). The acidity results obtained during this study showed a slight increase in the strength of the weak Brönsted sites in the order of Mn-Y<Co-Y<Cr-Y, but the relative amounts of these sites were almost similar among the three catalysts. Although the differences in acidity strength were quite small (3-4°C), the validity of this trend was indicated by similar results obtained with several repetitions of the experiments. It has been reported (36, 37) that acidity due to cation hydrolysis of the cation exchanged zeolites increases with decreasing ionic radius and increasing electronegativity of the cation. In this case, the ionic radius decreased in the order of $Mn^{2+}>Co^{2+}>Cr^{3+}$ while the electronegativity increased as $Cr^{3+}<Mn^{2+}<Co^{2+}$. At this point, it appears that the strength of the weak Brönsted sites was primarily influenced by the size of the exchanging cation with little or no observable effect of the cation electronegativity. Conversely, a different trend was noticed with the stronger Brönsted sites, which contributed the NH_3 desorption peaks at temperatures above 300°C. The data suggested the presence of larger amounts of the stronger Brönsted sites with the Co-Y than both the Cr-Y and the Mn-Y. These stronger acidic sites could have played a major role in determining the catalyst activity for CVOC oxidation, thereby producing higher activity with the Co-Y.

Apart from the composition of the catalysts, the efficiency of the catalytic oxidation process was directly related to the size, structure and composition of the chlorinated VOC used. The presence of four chlorine atoms bonded to a single carbon atom in CCl_4 gives it a perfectly symmetric structure. $MeCl_2$ is also a symmetric molecule with two hydrogen atoms and two chlorine atoms bonded to a single carbon. Unlike these two, TCE is an unsaturated double bonded compound (carbon-carbon double bond) with three chlorine and one hydrogen bonded to two carbon atoms. Therefore, it seems probable that the activity of the cation exchanged zeolites depended directly on the structure of the VOC feed with the surface reaction process being linked to the breaking of the strongest bond within the compound.

To clarify this effect, adsorption of the three chlorinated VOCs on the powdered Co-Y zeolite in a nitrogen atmosphere was carried out using the TGA. Table 7 compares the relative adsorption of the feeds on the Co-Y catalyst after half an hour of exposure to the CVOC/N_2 mixture at different temperatures. It can be seen that, for the Co-Y powder, TCE adsorption was only about 20 percent of the values obtained for the other two feeds. Conversion trends of the three chlorinated feeds with the Co-Y zeolite exactly followed their adsorption patterns. CCl_4 (with maximum adsorption on Co-Y) was easily converted at temperatures as low as 200°C. $MeCl_2$, which showed less adsorption than CCl_4, required a temperature rise to 350°C

for complete conversion while TCE showed the least adsorption and also minimum conversion with the cation exchanged zeolites.

TABLE 7: CVOC ADSORPTION RESULTS ON CATALYSTS AFTER HALF HOUR

Feed	VOC Adsorbed at Different Temperatures (m mole/g catalyst)		
	250° C	300° C	350° C
Co-Y Powder			
TCE	0.004	0.003	
$MeCl_2$	0.020	0.018	0.015
CCl_4	0.025	0.008	
Co-Y/CA Pellets			
TCE	0.025	0.018	
$MeCl_2$	0.037	0.037	
CCl_4		0.019	

In addition to its higher adsorption within the cation-exchanged zeolite, the relative ease of complete conversion of CCl_4 at lower temperatures (in contrast to either $MeCl_2$ or TCE) could also be related to the differences in bond strengths among these molecules. In the chlorinated hydrocarbons, the carbon-chlorine bond is the weakest as compared to the carbon-hydrogen or the carbon-carbon double bonds (43, 44). Bond strength for C-Cl at 25°C in the CCl_4 molecule is only about 73 kcal/mole whereas for the C-H in $MeCl_2$ and the C=C bond in TCE it is about 100 and 172 kcal/mole respectively. If one considers breaking of the strongest bond within the VOC as a probable rate-controlling process, (provided rapid and sufficient adsorption is possible), higher conversion of CCl_4 would be favored as compared to the other two feeds at a given temperature. Similarly comparing between $MeCl_2$ and TCE, the higher adsorption of $MeCl_2$ in the non-impregnated cation-exchanged zeolites (Co-Y, Cr-Y, etc.) along with the lower bond strength of the C-H bond, produced higher conversion of $MeCl_2$ than TCE, with Co-Y, Cr-Y and Mn-Y.

The considerably lower adsorption of TCE within the Co-Y catalyst led to the initial assumption of probable size-exclusion of TCE from the zeolite supercages. However, comparing the reported kinetic diameters for these molecules (45, 46) it was found that the size of the molecules increased in the order of TCE (3.2 Å) < $MeCl_2$ (4.75 Å) < CCl_4 (5.6-5.9 Å). With

TCE apparently having the smallest kinetic diameter, this difference in adsorption did not appear to be caused by a probable size exclusion but perhaps by a difference in adsorption mechanism or due to lack of proper adsorption sites.

The probable size-exclusion theory for TCE was further disproved by the VOC adsorption experiments on the Co-Y/CA pellets. It was noticed that although the zeolite surface area went down as a result of chromia impregnation (576 to 325 m^2/g), adsorption of TCE showed significant (about 50 to 70 percent of $MeCl_2$ adsorption) improvement. This further suggested that instead of size-exclusion, TCE adsorption was limited by the type of adsorption sites present in the zeolite matrix.

In addition to the adsorption changes, catalytic conversion of TCE was also substantially improved (Figure 8) following chromia impregnation of the washcoated cation exchanged zeolite catalysts (Co-Y/CA, Cr-Y/CA, etc.). This change was highly desirable and apparently brought about by the presence of the non-framework Cr_2O_3 along with the metal exchanged cation. Since earlier results (9, 14) have shown good potential for Cr_2O_3 as a deep oxidation catalyst for chlorinated VOCs, this p-type oxide was chosen to form a bi-functional zeolite/TMO catalyst. The chromia impregnation of Co-Y and Cr-Y zeolites appeared to produce a catalyst which had both the acidic properties of the zeolite required for high conversions of CCl_4 and $MeCl_2$, as well as a non-framework deep oxidation catalyst probably required for the initial adsorption and subsequent oxidation of TCE.

During the initial experiments with the chromia-impregnated zeolite catalysts, it appeared as if the non-framework Cr_2O_3 was supported solely on the Silbond washcoat. When later experiments with a plain Silbond/CA catalyst showed a significantly lower TCE conversion compared to Co-Y/CA or the Cr-Y/CA, it seemed probable that the impregnating cation (or the TMO) was also present inside the zeolite cavities, thus producing higher conversions. This was further evidenced by a drop in surface area and O_2 pickup after chromia impregnation of the cation-exchanged catalysts. This result is consistent with a process whereby the impregnated TMO not only may reside inside the zeolitic supercages but may block some of these supercages and/or the connecting channels. However, another possibility for the surface area loss following the Cr_2O_3 impregnation might have been partial structural collapse of the zeolite during the impregnation process. Some dealumination trends were indeed noticed in comparing the silica/alumina weight percent ratios of the Co-Y and Co-Y/CA cores. In going from Silbond washcoated Co-Y to Co-Y/CA cores, the ratio changed from 2.3 to 2.6 and again with Chlorhydrol washcoated ones it changed from 1.0 to 1.3. However, even though this apparent blockage or structural loss caused some reduction in $MeCl_2$ and CCl_4 conversions over non-impregnated counterparts at lower temperatures, the corresponding improvement in TCE conversion was much more significant.

Compared to the washcoated Co-Y/CA catalyst (≃ 10-15 percent zeolite content), the unsupported 1/16 inch diameter Co-Y/CA catalyst pellets were only made out of H-Y zeolite (with small amounts of alumina binder). This additional amount of zeolite in the Co-Y/CA pellets more than compensated for the adverse effects of chromia impregnation and thus produced improved $MeCl_2$, TCE and CCl_4 conversions as compared to the washcoated Co-Y/CA. It is also to be noted that this additional zeolite amount was significant enough to produce higher activity with the Co-Y/CA pellets in-spite of the higher space velocity (≃ 2300 hr^{-1}) used with the catalyst pellets.

The drop in Co content of the Co-Y catalysts that was noticed after Cr_2O_3 impregnation was probably due to some loss of Co during immersion in the chromic acid solution over a period of 8-10 hours. This could be an additional indication of structural loss due to Cr_2O_3 impregnation.

On initially comparing the BET results (Table 6) between the calcined chromia impregnated Chlorhydrol powder (Chlorhydrol/CA) and the calcined chromia impregnated Silbond powder (Silbond/CA), the former appeared to be superior based on its much higher surface area (≃ 160 m^2/g). With this increased surface area, the Chlorhydrol/CA powder was able to incorporate almost twice the amount of Cr_2O_3 loading during impregnation. Further, the additional Cr_2O_3 sites resulted in significantly higher O_2 (more than 20 times) pickup with the Chlorhydrol/CA powder compared to the Silbond/CA.

However, despite these differences between the two chromia-impregnated powders, washcoated Co-Y or Co-Y/CA cores prepared from the Silbond and Chlorhydrol binders did not show any significant difference in surface area (Table 6). Similar trends were also found by comparing the activities for TCE conversion between the Co-Y and Co-Y/CA catalysts prepared from the two different binders. No remarkable difference in activity was noticed between catalysts prepared from the different binders (Figure 10). This similarity in activity between the two washcoated catalysts suggests that the bulk of the catalytic surface area was contributed by the zeolite and not by the binder. Consequently, much of the impregnated Cr_2O_3 was probably present inside the zeolite cages rather than on the outside binder. Therefore, the difference in binder surface area did not affect the catalyst properties in any significant way.

Comparing the product selectivities between the non-impregnated and the chromia-impregnated zeolite catalysts for TCE and $MeCl_2$ conversion, a significant difference in the CO_2/CO ratio was noticed, with chromia impregnation apparently causing a doubling of the CO_2/CO ratio with the washcoated zeolite catalysts. This suggested that the impregnated Cr_2O_3 sites which could be situated either inside the zeolite structure or in the binder were responsible for the further reaction of CO to CO_2.

This was consistent with our previous suggestion (26) that for further conversion to CO_2, CO may need to be desorbed and then re-adsorbed on another active site. In the present case, this second active site was probably obtained from the additional impregnated Cr_2O_3 which thus enhanced CO_2 production.

A peculiar difference between CCl_4 and the other two CVOCs was the complete absence of any CO formation during CCl_4 oxidation. Irrespective of non-impregnated Y zeolites or Cr_2O_3 impregnated ones, no detectable CO was ever observed during CCl_4 oxidation. This indicated a definite difference in the reaction mechanism or the intermediates formed during CCl_4 oxidation as compared to TCE or $MeCl_2$. This was further supported by the presence of $COCl_2$ and significant Cl_2 in the CCl_4 product spectrum at temperatures below 300°C. Most of the Cl_2 production with $MeCl_2$ and TCE feeds, for the chromia impregnated catalysts, occurred at temperatures between 300 and 350°C, apparently as a result of the Deacon reaction (14).

As mentioned in the case of CCl_4, molecular Cl_2 in the amount of 2-6 percent of the total chlorine balance was noticed at temperatures below 300°C, i.e., where the Deacon reaction is not thermodynamically favored. Similarly, small amounts of $COCl_2$ were noticed as a byproduct only with CCl_4 and were not detected with either $MeCl_2$ or TCE feeds. Therefore, it could be speculated that the oxidation of CCl_4 involves an intermediate step producing $COCl_2$ and Cl_2, and this $COCl_2$ (on further reaction with adsorbed oxygen or water vapor) produces CO_2. Conversely, the hydrogen atoms present in $MeCl_2$ and TCE could lead to the formation of intermediates such as COHCl (47). Such an unstable intermediate would immediately dissociate to produce CO and HCl. In this way, CO could be produced from the hydrogen-containing CVOCs as a direct oxidation product. On further oxidation, this CO can form CO_2. Since this type of reaction does not lead to direct Cl_2 production, and the only Cl_2 could be formed from the Deacon reaction with HCl, the amount of Cl_2 formed with either $MeCl_2$ or TCE is usually negligible at temperatures below 300°C.

C. IN DEPTH STUDY OF COMBINED EXCHANGED/IMPREGNATED CATALYST PELLETS

1. Results

The different catalysts prepared for this study can be categorized into three types: cobalt exchanged Y catalysts (Co-Y), Cr_2O_3 impregnated Co-Y (Co-Y/CA) and Co_3O_4 impregnated Co-Y (Co-Y/Co). All were prepared starting with HY pellets. Out of a total of 15 catalysts prepared, 6 were different Co loaded Co-Y catalysts. These Co-Y catalysts were further impregnated with Cr_2O_3 to produce 8 different Co-Y/CA catalysts. Additionally, one Co-Y/Co catalyst was prepared by Co_3O_4 impregnation of the Co-Y, instead of Cr_2O_3. The catalysts are listed in Table 8, according to this nomenclature, along with their compositions, surface areas, and oxygen adsorption

capacities. The properties of the "as obtained" H-Y catalyst are also included as a reference.

As reported earlier (27), although cobalt exchanged Y zeolite showed excellent activity for single carbon CVOC ($MeCl_2$, CCl_4, etc.) oxidation, additional Cr_2O_3 impregnation was necessary for obtaining similar activity for double carbon TCE destruction. The purpose of this study was to investigate the effects of Co exchange and Cr_2O_3 impregnation levels for obtaining the desired activity and selectivity for both single and double carbon CVOC destruction.

Accordingly, several Co-Y catalysts were prepared with Co exchange levels varying from $\simeq$ 1 percent to 5.6 percent. Some of these Co-Y catalysts were further impregnated with chromic acid solution to obtain a Cr_2O_3 loading of about 6-8 percent. These were the Co-Y/CA2 to Co-Y/CA5 catalysts, which were prepared from the Co-Y3 to Co-Y6 pellets respectively, to investigate the effects of varying Co loadings in similarly Cr_2O_3 impregnated Co-Y/CA catalysts. The Co-Y/CA1 catalyst was prepared from an earlier batch of Co-Y pellets, containing about 3 percent Co. The Co-Y/CA6 and the Co-Y/CA7 catalysts were prepared from the same Co-Y2 pellets to find the effects of different Cr_2O_3 loadings, by varying it from a low of 2 percent to a high of about 14 percent. The Co-Y/CA8 catalyst was prepared with a high ($\simeq$ 14 percent) Cr_2O_3 loading from the Co-Y3 pellets to show the effects of both higher Co and Cr_2O_3 loadings. Finally, a Co-Y/Co catalyst was prepared from the Co-Y2 pellets to compare the effects of Cr_2O_3 versus Co_3O_4 impregnation.

Table 8 compares the silica/alumina weight percent ratio and cobalt and chromia loading of the different catalysts. The cobalt loading (represented by Co_3O_4 weight percent) was gradually increased from about 1 percent to 5.6 percent in the different Co-Y catalysts. Comparing with the original H-Y, cobalt exchange caused a slight increase in the silica/alumina ratio from 1.49 to about 1.56. This change, however, was not dependent upon the cobalt loading level of the zeolite since the silica/alumina ratios of the different cobalt loaded Co-Y catalysts were almost identical. This change suggests that some dealumination occurred during the cobalt exchange of the zeolites.

TABLE 8: THE CHEMICAL COMPOSITION AND PROPERTIES OF VARIOUS CATALYSTS

Catalyst	Composition (wt%)			Surface Area	O_2 Pickup
	SiO_2/Al_2O_3	Co_3O_4	Cr_2O_3	(m^2/g)	(mg/g)
H-Y	1.49	0.00	0.00	574	3.10
Co-Y1	1.56	1.12	0.00	560	2.00
Co-Y2	1.57	1.98	0.00	576	2.68
Co-Y3	1.55	3.04	0.00	593	2.75
Co-Y4	1.57	4.28	0.00	609	2.83
Co-Y5	1.55	4.57	0.00	600	2.93
Co-Y6	1.57	5.62	0.00	570	3.13
Co-Y/CA1	1.77	1.21	7.08	325	2.16
Co-Y/CA2	1.66	1.51	5.81	325	2.23
Co-Y/CA3	1.79	1.25	8.75	117	1.93
Co-Y/CA4	1.76	1.42	6.39	214	1.88
Co-Y/CA5	1.77	1.82	5.47	329	1.89
Co-Y/CA6	1.66	0.70	2.02	440	2.18
Co-Y/CA7	1.87	0.66	13.87	115	1.65
Co-Y/CA8	1.90	1.05	13.50	108	2.05
Co-Y/Co	1.58	4.56	0.00	523	2.68

Comparing the different Co-Y/CA catalysts prepared during this study, the Cr_2O_3 loading can be broadly categorized into three different levels: low Cr_2O_3 level of about 2 percent, medium Cr_2O_3 level of about 6-8 percent and high Cr_2O_3 level of about 14 percent. A further increase in the silica/alumina ratio was noticed with all the Co-Y/CA catalysts as compared to the Co-Ys from which they were prepared. The silica/alumina ratio with the Co-Y/CA catalysts varied from $\simeq$ 1.66 with the low Cr_2O_3 level to $\simeq$ 1.77 with the medium Cr_2O_3 level to finally $\simeq$ 1.90 with the high Cr_2O_3 level. Conversely, the silica/alumina ratio of the Co-Y/Co catalyst was almost identical to the original Co-Y catalysts. This result showed that Cr_2O_3 impregnation caused an additional increase in the silica/alumina ratio from the Co-Y and unlike the Co exchange, the Cr_2O_3 impregnation changed the silica/alumina ratio with progressive increase in the loading. This suggested that increased dealumination would correlate with the Cr_2O_3 impregnation step rather than with the Co exchange step.

Some X-ray diffraction studies were carried out to compare the relative dealumination occurring during Co exchange versus Cr_2O_3 impregnation. The initial results supported the

trends noticed with the silica/alumina ratios. Significant dealumination or loss of crystallinity was noticed with Cr_2O_3 impregnation and this was more severe with higher Cr_2O_3 loading. Co exchange, conversely, showed no XRD peak loss or significant crystallinity loss. To follow up on these dealumination effects, a detailed study has been undertaken to investigate the pH effects of impregnation solutions on zeolite crystallinity and framework dealumination and will be reported later when completed.

The BET surface area results of the various catalysts are shown in Table 8. The cation-exchanged Co-Y catalysts showed almost no reduction in surface area compared to the original H-Y. This was true in-spite of the wide variation in the Co exchange levels. However, following the Cr_2O_3 impregnation, a significant drop in catalyst surface area was noticed. This reduction in surface area was directly dependent on the Cr_2O_3 level. Similar to the changes in the silica/alumina ratios, the surface area decreased, going from the low Cr_2O_3 level ($\simeq$ 440 m^2/g) to medium Cr_2O_3 level ($\simeq$ 200-300 m^2/g) to high Cr_2O_3 level ($\simeq$ 100 m^2/g). This result supported the earlier suggestion of increased structural loss with increased Cr_2O_3 loading. Unlike the Co-Y/CA catalysts, the Co-Y/Co showed no significant drop in surface area compared to the Co-Y catalysts. This again suggested that dealumination and hence structural loss was far less significant in the case of Co exchange or Co impregnation.

The catalytic oxygen-adsorption capacity, also listed in Table 8, is believed to be one of the characteristics representing the oxidation capability of the catalyst. In the case of the Co-Y catalysts, the oxygen chemisorption capacities appeared to show a slight increase with increasing Co content. As Co exchange level increased from 1 percent to 5.6 percent, the O_2 pickup at 300°C also increased from 2.00 mg/g to 3.13 mg/g. However, after the Cr_2O_3 impregnation, in-spite of the high Cr_2O_3 content, the O_2 pickup values also dropped, similarly to the surface area results. This again appeared to be the consequence of Co loss from the zeolite framework due to Cr_2O_3 impregnation. Apparently, the exchanged Co played a more significant role in determining the zeolite oxygen chemisorption capacity than the impregnated Cr_2O_3.

Figures 13 and 14 show the NH_3 Temperature Programmed Desorption (TPD) curves for several of the catalysts. The TPD curves for the various Co exchanged Co-Y catalysts are compared along with the H-Y, the Co-Y/Co and the Co-Y/CA1 in Figure 13. As can be seen from the curves, a shift in the TPD peaks from about 170°C to 200°C was noticed with all the Co-Y and Co-Y/CA curves as compared to the H-Y. This indicated an increase in the strength of the acid sites with Co exchange and CA impregnation. Additionally, the area under the TPD curves dropped significantly for all the catalysts compared to the original H-Y, thereby showing an overall loss of the total number of acidic sites with both Co exchange and CA impregnation. The combination of these

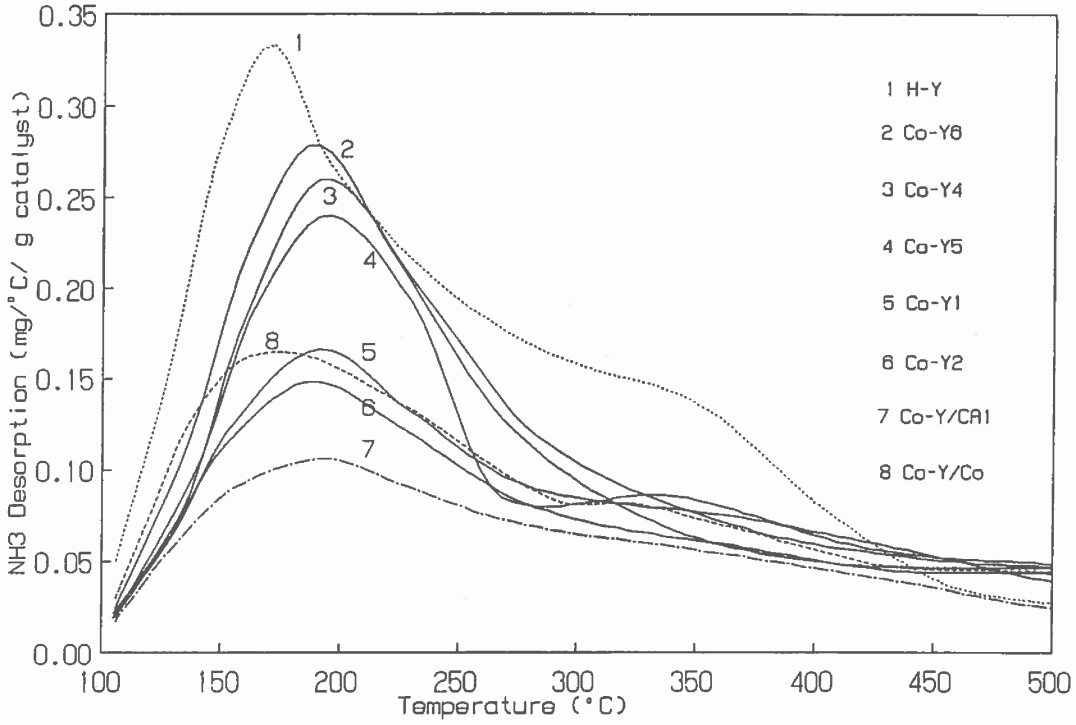

Figure 13. NH3 TPD plot for Acidity Comparison of different Exchanged/Impregnated and Exchanged Catalysts

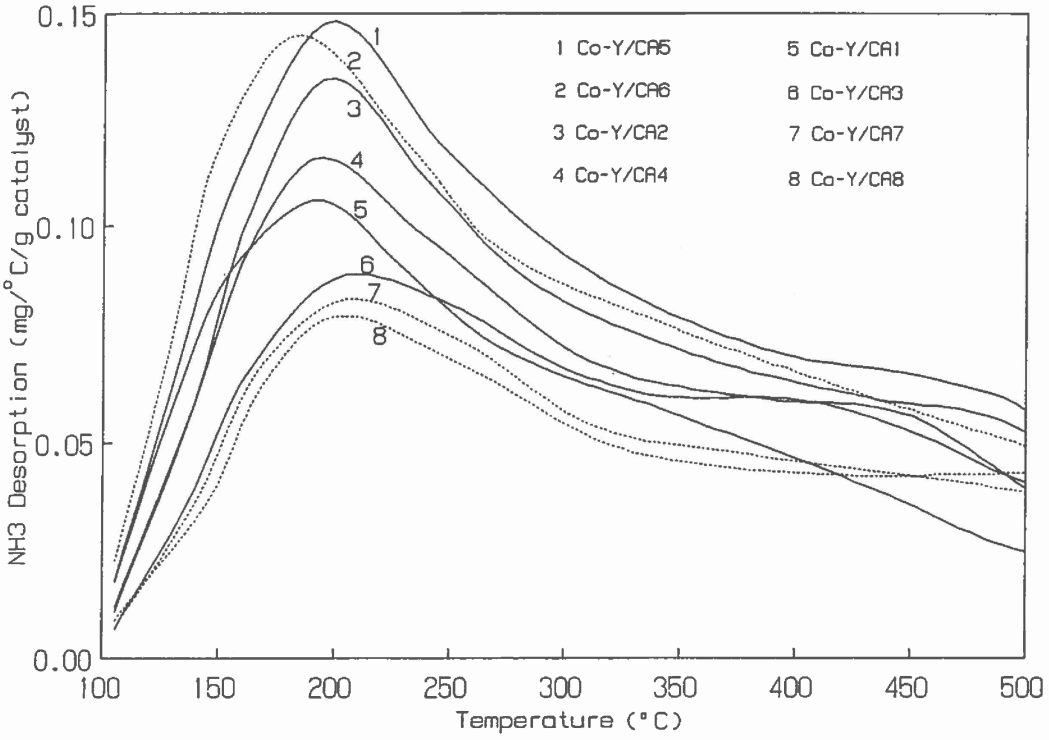

Figure 14. NH3 TPD plot for Several CO-Y/CA Catalysts

two effects suggested some partial dealumination during Co exchange and CA impregnation, which thus caused a partial loss of the weaker acidic sites and increased the strength of the remaining ones.

Comparison of the different Co-loaded Co-Y catalysts, shows that the total number of acid sites increased with increasing Co content. Thus as the Co content of the catalysts increased from about 1 to 5.6 percent, the area under the TPD curves for the respective catalysts gradually increased, with the maximum obtained with the Co-Y6. However, the strength of the acid sites, as denoted by the TPD peak temperatures, did not show any significant changes with increasing Co content. CA impregnation showed a significant drop in the number of acid sites for the Co-Y/CA1 as compared to any of the Co-Y catalysts. The Co-Y/Co, on the other hand, did not show any drop in the number of the acid sites, compared to the original Co-Y2 catalyst, from which it was prepared. This indicated that dealumination was more prevalent with CA impregnation than Co impregnation.

Figure 14 compares the TPD curves of the various Co-Y/CA catalysts. The main trend observable with these curves is the decrease of the total number of acidic sites with increasing Cr_2O_3 content. As the Cr_2O_3 content increased from about 5.5 percent with the Co-Y/CA5 to about 13.5 percent with the Co-Y/CA8, the area under the TPD curves also dropped correspondingly. In addition to that, the increasing Co content probably also controlled the number of the acidic sites to some extent, as evidenced by the higher areas with the Co-Y/CA5, Co-Y/CA2 and Co-Y/CA4, which contained higher Co than the rest of the catalysts. However, in the case of catalysts with similar Co contents, an increase in Cr_2O_3 loading by CA impregnation caused significant decrease in the number of the acidic sites. This can be noticed by comparing the TPD curves for the Co-Y/CA1 and the Co-Y/CA3 catalysts, which both contained about 1.2 percent Co but the increase in Cr_2O_3 amount from 7 to about 8.8 percent showed a significant drop in the number of the acidic sites. Conversely, as the Cr_2O_3 loading was further increased to about 13.5 percent with the Co-Y/CA7 and Co-Y/CA8 catalysts, the difference in Co content (0.66 percent versus 1.0 percent) did not seem to affect the TPD curve at all. The dealumination due to the large Cr_2O_3 content appeared to play the major role in determining the number of acidic sites.

The Co-Y/CA6 catalyst, which contained about 2 percent Cr_2O_3, showed the presence of a large number of acidic sites compared to the other catalysts in Figure 14. This low Cr_2O_3 content seemed to have contributed towards less dealumination with this catalyst, thereby keeping the number of acidic sites relatively high. Additional evidence of the effects of less dealumination was noticed by comparing the TPD peak temperatures of the Co-Y/CA6 catalyst with the others. While the TPD peak temperatures with the higher Cr_2O_3 containing catalysts (5.5 to

13.5 percent) varied from 197 to 205°C, that with the Co-Y/CA6 was about 185°C.

The catalytic activity data for $MeCl_2$ and TCE conversion are plotted in Figures 15 and 16, respectively. For activity purposes, only the Co exchanged and CA impregnated catalysts were utilized and not the unimpregnated Co-Y catalysts. This was because earlier results (27) showed that the Co-Y catalyst was effective only for single carbon VOCs such as $MeCl_2$ and CCl_4 but not at all for TCE. Conversely, the Cr_2O_3 impregnated Co-Y showed a substantial improvement for TCE oxidation without any significant loss in its activity for $MeCl_2$ and CCl_4 conversion. Since the primary objective of this study was to develop a catalyst equally effective for the destruction of both single carbon and double carbon chlorinated feeds, the emphasis was, therefore, more on analyzing the behavior of the Co-Y/CA type catalysts.

Comparing the activities for $MeCl_2$ conversion among the Co-Y/CA1 to Co-Y/CA5 catalysts, which were prepared by CA impregnation of Co-Ys with increasing Co content, the overall trend seemed to indicate that the catalysts that contained more Co in the original Co-Y showed higher conversion also in the Co-Y/CA form. Accordingly, the trend was as follows: Co-Y/CA5 > Co-Y/CA4 > Co-Y/CA3 > Co-Y/CA2, Co-Y/CA1. However, the differences in activity were discernable only at temperatures below 300°C. Above 300°C, almost all the catalysts showed 95 percent and above conversion of $MeCl_2$. To some extent, the trend in activity also followed the Co and Cr_2O_3 content of the Co-Y/CA catalysts. Among Co-Y/CA5, Co-Y/CA4 and Co-Y/CA3, as the Co content increased from 1.25 percent to 1.42 percent to 1.82 percent and the Cr_2O_3 loading decreased from 8.75 percent to 6.39 percent to 5.47 percent, $MeCl_2$ conversion with these catalysts increased correspondingly. $MeCl_2$ conversions with the Co-Y/CA1 and Co-Y/CA2 catalysts were similar and also lower than the Co-Y/CA3 to Co-Y/CA5 catalysts. This was probably due to the reason that they were both prepared from similar Co-Y containing only 3 percent exchanged Co.

The effects of Cr_2O_3 loading on $MeCl_2$ conversion are demonstrated by the Co-Y/A6 to Co-Y/CA7 catalysts. These two catalysts were prepared from the same Co-Y and hence contained similar Co after Cr_2O_3 impregnation. However, the huge difference in Cr_2O_3 loading (2 percent vs. 14 percent) contributed towards the noticeable differences in activity at temperatures below 325°C. It was apparent that the increased (14 percent) Cr_2O_3 loading caused a drop in the catalytic activity for $MeCl_2$ conversion. For example, $MeCl_2$ conversion obtained with Co-Y/CA6 at 275°C was about 55 percent while the same dropped to about 36 percent with the Co-Y/CA7 catalyst.

The activity of the catalysts for TCE conversion, as shown in Figure 16, seemed to be primarily influenced by the Cr_2O_3 loading of the catalysts. The most remarkable difference

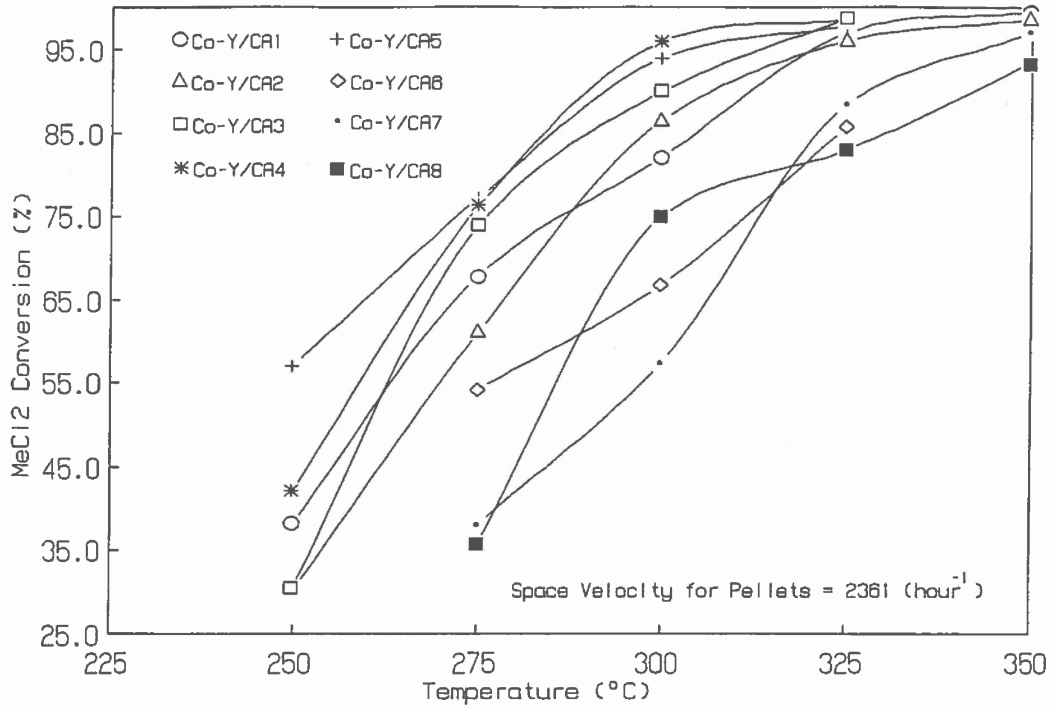

Figure 15. MeCl2 Conversion vs. Temperature Plot with Various Catalysts

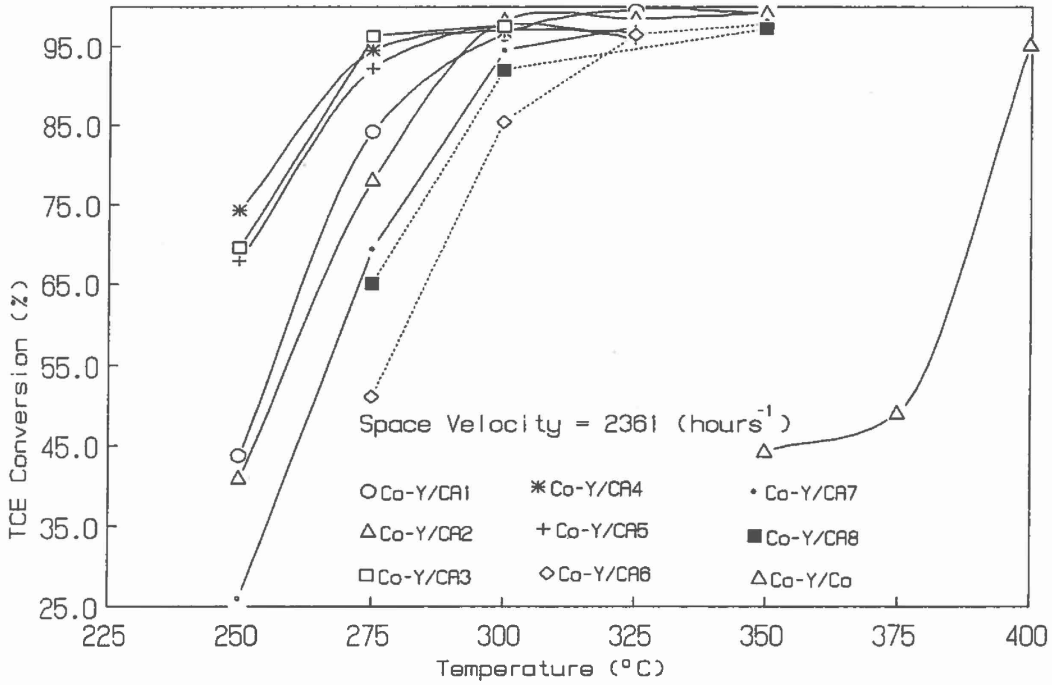

Figure 16. TCE Conversion vs. Temperature Plot with Various Catalysts

in activity could be noticed between the Co-Y/Co and the Co-Y/CA catalysts. While the Co-Y/Co produced only about 50 percent TCE conversion at 375°C, most of the Co-Y/CA catalysts showed 80 percent and above conversions from 300°C onwards. This temperature difference signified the importance of the presence of Cr_2O_3 as a catalytic agent for TCE destruction. Furthermore, comparing the TCE conversions among the Co-Y/CA6 to Co-Y/CA8 catalysts, it was found that the catalytic activity increased substantially from Co-Y/CA6 to Co-Y/CA7 and Co-Y/CA8 with an increase in Cr_2O_3 loading from 2 percent to about 14 percent.

The Co-Y/CA1 to Co-Y/CA5 catalysts, on the other hand, showed the effects of increased Co content in combination with Cr_2O_3 loading for effective TCE destruction. These five catalysts contained much less Cr_2O_3 (5.5 to 8.75 percent) than either of the Co-Y/CA7 or Co-Y/CA8 ($\simeq$ 14 percent) catalysts and yet they showed significantly higher TCE conversion under identical conditions. The primary reason for this appeared to be the higher Co content. Similar to the $MeCl_2$ results, here also the catalysts that were prepared from originally high Co containing Co-Y catalysts showed higher conversions. The Co-Y/CA3 to Co-Y/CA5 catalysts, that were prepared from Co-Y catalysts containing over 4 percent Co (expressed as Co_3O_4), showed distinctly higher TCE conversions than the rest at temperatures below 300°C. No reasonable comparisons could be made for conversions at and above 300°C since almost all the catalysts showed over 90 percent conversions in this temperature range. Among these three catalysts, the higher Co containing Co-Y/CA5 showed slightly higher (75 percent compared to 68 percent) conversion only at 250°C. At higher temperatures, the conversion results were almost identical and over 90 percent. In the case of the Co-Y/CA1 and Co-Y/CA2 catalysts, that were made from Co-Ys containing about 3 percent exchanged Co, the activity for TCE conversion was noticeably lower than the previous three catalysts. Additionally, although the conversion results were close between these two catalysts, a slightly higher conversion was obtained with the higher Cr_2O_3 containing Co-Y/CA1 (7.0 percent) than the Co-Y/CA2 (5.8 percent).

Apart from the catalyst activities for chlorinated VOC conversion, their product selectivities were also monitored as a function of changing composition. As reported earlier (27), the product spectrum of these exchanged and impregnated zeolite catalysts did not show the presence of any detectable higher chlorinated partial oxidation products and this was highly desirable. The only components detected other than the unconverted feeds were HCl, Cl_2, CO and CO_2. HCl was the major chlorine containing product while small amounts of Cl_2 were formed as a result of the Deacon reaction. Following the Deacon equilibrium, the Cl_2 concentration increased with increasing temperatures and was most noticeable at 300°C and above. Among the Co-Y/CA1 to Co-Y/CA5 catalysts, the Cl_2/HCl ratio increased from 0.01 to about 0.2 with temperature increasing from 275 to 325°C and with $MeCl_2$ as feed. With TCE, the ratio increased from

0 to about 0.17 as the temperature was increased from 250 to 300°C. Therefore, slightly higher Cl_2 formation was noticed with the higher chlorine containing TCE than $MeCl_2$, under similar temperature conditions.

Although no distinguishable trends in Cl_2/HCl ratio could be noticed as the Co concentration changed in the above catalysts, a definite increase in Cl_2 was found with increasing Cr_2O_3 concentration between the Co-Y/CA6 and Co-Y/CA7 catalysts. The Cl_2/HCl ratio obtained during $MeCl_2$ conversion with the 2 percent Cr_2O_3 containing Co-Y/CA6 varied from 0 to 0.01 with temperature increasing from 275 to 325°C, whereas the same changed from 0 to 0.05 to 0.13 with the 14 percent Cr_2O_3 containing Co-Y/CA7 catalyst (at 275, 300 and 325°C, respectively). Similarly with TCE, this ratio at 275, 300 and 325°C corresponded to 0, 0.01 and 0.03 for Co-Y/CA6 catalyst and changed to 0, 0.05 and 0.16 for Co-Y/CA7. This result indicated a definite increase in Cl_2 production via Deacon reaction with the presence of increasing amounts of Cr_2O_3.

CO and CO_2 were the only carbon-containing products detected during the oxidation of $MeCl_2$ and TCE. Though more CO than CO_2 was obtained in the product spectrum, CO_2 formation increased with increasing temperature. This was evident in the changing CO/CO_2 ratios of the catalysts. Among the Co-Y/CA1 to Co-Y/CA5 catalysts, with $MeCl_2$ as feed, the CO/CO_2 ratio decreased from about 5.5 to 4.0 to 2.5 as the temperature increased from 275 to 300 to 325°C. Again with TCE, this ratio dropped from an average of 6.0 to 3.9 to 2.5 with temperature increasing from 250 to 275 to 300°C. Therefore, at any temperature, the CO/CO_2 ratio was higher with the double carbon TCE than the single carbon $MeCl_2$ (e.g., at 275°C, 3.9 with TCE vs. 2.5 with $MeCl_2$). However, no detectable trend in the CO/CO_2 ratio was observed due to the varying Co content of the catalysts. Conversely, comparing the Co-Y/CA6 and Co-Y/CA7 catalysts, it was clear that increasing Cr_2O_3 loading did cause a drop in this ratio by producing more CO_2. The CO/CO_2 ratios obtained with Co-Y/CA6 for TCE destruction at 250, 275 and 300°C were 10.8, 6.2 and 4.5, respectively, while the same with Co-Y/CA7 were reduced to 5.7, 4.2 and 3.2. Clearly, the increased Cr_2O_3 content of the Co-Y/CA7 catalyst resulted in increased CO_2 production.

2. Discussion

The present study was undertaken to understand the effects of the exchanged Co cation and the impregnated Cr_2O_3 on the activity and selectivity of the Y zeolite in oxidation of different chlorinated hydrocarbon feeds. With this objective, several catalysts with varying loadings were prepared and tested to show the effects of the exchanged Co and the impregnated Cr_2O_3, both individually and in combination. As the results indicated, both exchanged cationic Co and impregnated Cr_2O_3 played major roles in controlling the catalytic activity and

selectivity. However, the extent of this role depended on their concentration, location, method of preparation, electronic structure, cation-oxygen bond strength, etc. Depending on these characteristics, the catalytic properties of the exchanged/impregnated Y zeolites were modified, leading to the differences in catalytic activity and selectivity for chlorocarbon oxidation.

Co Exchange: Comparing the Co-Y zeolite with the original H-Y, the most noticeable change in property appears to be the significant drop in acidity with the low level ($\simeq$ 1-2 percent) Co exchanged catalysts. This can be partly explained by the mildly acidic (pH $\simeq$ 3.3) $Co(NO_3)_2$ solution, which was used for the Co exchange. It seems possible that the initial dealumination by this solution during the exchange process caused a drop in the number of acid sites in the resulting Co-Y while increasing the strength of the remaining acid sites (Figure 13). This is further supported by the increased Si/Al ratio found with the Co-Ys (Table 8). However, apart from this mild dealumination, the size and the location of the exchanged Co ions in the low level Co exchanged Y zeolites could also have affected the acidity. It has been well documented in the literature (48, 49) that for partially exchanged Y zeolite, the metal cations and especially Co, preferentially occupy the S_1 and S_1' sites within the hexagonal prisms and the sodalite cages of the zeolite. With less than 50 percent exchange of the Y zeolite most of the exchanged cations are usually located in these smaller sodalite cages and hexagonal prisms, with almost none available in the larger supercages. However, with the Co^{2+} ions (ionic radius $\simeq$ 0.72 Å) located inside the small sodalite cages (pore diameter $\simeq$ 2.6 Å), the accessibility of the NH_3 (kinetic diameter $\simeq$ 2.6 Å) molecule to the remaining protons inside the sodalite could have been hindered. Therefore, the combination of these effects of partial dealumination and little or no available cations in the supercages along with the accessibility to the smaller sodalite cages and hexagonal prisms partly blocked, the total NH_3 adsorption in the lower level Co exchanged Y zeolites was naturally low and hence showed less acidity.

With higher Co exchange, the acidity of the Co-Y zeolites showed a significant increase. This was primarily due to the increased availability of Co^{2+} ions inside the supercages. As suggested by Poutsma et al. (48), higher Co exchange moves the cations to the S_2 sites within the supercages after filling up the smaller Sodalite cages and hexagonal prisms. As more and more cations are available in the supercages, the zeolite acidity increases by the well known (26, 48, 50) cation hydrolysis process:

$$M^{2+} + H_2O \Leftrightarrow MOH^+ + H^+,$$

which produces more mobile protons that can associate with the

framework oxygen species to produce additional Brönsted sites. Similar results of increased zeolite acidity with increasing cation content can be found in the works of Dimitrov et al., (51) and Garcia et al. (52).

As with acidity, oxygen adsorption capacity of the Co-Y catalysts also increased with increasing Co exchange. This can again be attributed to the increased availability of the Co^{2+} cations in the supercages with increasing exchange. It is known that the entrance of an O_2 molecule (kinetic dia. $\simeq$ 3.5 Å) into the sodalite cages is hindered by the small pore opening ($\simeq$ 2.6 Å) and naturally when most of the exchanged cations are clustered in the sodalite and hexagonal prisms, the oxygen adsorption is low. It has been suggested by several researchers (23, 53) that the adsorbed oxygen species exists in the form of

$$M^{n+} \cdots\cdots O^{2-} \cdots\cdots M^{n+}$$

within the zeolite matrix. Kiselev et al. (49) also discussed the cation-oxygen interactions in ion exchanged zeolites and suggested that at low degrees of exchange, the cation predominantly exists singly, whereas at higher degrees of exchange they occur in the form of the above cation-oxygen-cation bridges. Bridges of this type were previously proposed (23, 54) to explain the oxygen-cation ratios ($\simeq$ 0.5) noticed during oxygen adsorptions of several cation exchanged Y zeolites. However, in the present study the oxygen/cation atomic ratio was found to change from 0.90 (Co-Y1) to 0.67 (Co-Y2) to about 0.30 (Co-Y5 and Co-Y6) with gradual increase in the cation loading. This may suggest that in the case of lower ion-exchange, most of the oxygen was present in the form of

$$M^{n+} \cdots\cdots O^{-},$$

whereas with increasing cation availability more and more such cation-oxygen-cation bridges were formed.

Cr_2O_3 Impregnation: Cr_2O_3 impregnation is different from Co exchange in a sense that, unlike cation exchange, the metal ions that are present as anions (e.g., in chromic acid or ammonium dichromate solution) in the impregnation solution, can be incorporated within the zeolite matrix. Additionally, the impregnated metal/metal oxide is retained both inside the zeolite matrix and also on the outside (as well as on any binder material, in the case of zeolite pellets), without any framework association like the exchanged cations. In most cases, the sodalite cages and the hexagonal prisms are too small to accommodate the impregnated metal or metal oxide and consequently the whole loading occurs in the supercages. Therefore, as with the Co cations, the problem associated with location and availability due to the level of loading does not arise here and furthermore, almost all of the impregnated metal or metal oxide is accessible to the feed. In addition, impregnation can aid in

increasing metal loading in excess of the maximum exchange capacity of a zeolite and in the loading of metals for which soluble exchange salts are not easily available.

The most noticeable difference between Co exchange and Cr_2O_3 impregnation was the significant drop in the number of acid sites following Cr_2O_3 impregnation (Figures 13 and 14). The primary reason behind this appears to be the acidic nature (pH 0.085) of the CrO_3 solution that was used to obtain a well dispersed Cr_2O_3 phase. This acidic solution appeared to cause significant dealumination of the Co-Y during the impregnation process. This was evident by the increase in Si/Al ratios. With more and more dealumination, the number of acid sites dropped significantly but the strength of the remaining sites increased considerably. The dealumination process appeared to be solely dependent on the strength of the impregnating solution and, as noticed in Figure 14, the acidity of the different Co-Y/CA catalysts decreased with increasing Cr_2O_3 impregnation.

The effect of framework dealumination and possible structural loss was also evident by the decrease in surface areas of the different Co-Y/CA zeolites with increasing Cr_2O_3 loadings. However, in addition to structural loss, pore blockage by Cr_2O_3 impregnation might also have caused the apparent drop in surface area. This was inferred from the results of another study (55), which showed that by treating H-Y with solutions of HCl and CrO_3 of similar pH (0.085), lower surface areas were obtained with the Cr_2O_3 impregnated samples. Although similar XRD peak intensity losses were noticed with samples treated with the two different solutions, the lower surface area with the CrO_3 solution appeared to be a result of the combination of structural loss and pore blockage.

As far as oxygen adsorption was concerned, Cr_2O_3 impregnation actually appeared to reduce the total O_2 uptake for these catalysts taken as a group. However, this might have been the result of structural and/or surface area loss and the cation loss associated with it. The Co contents of all the catalysts were decreased following the Cr_2O_3 impregnation. However, comparing the oxygen/cation (i.e., O/Co) atomic ratios for the Co-Y/CA catalysts, the ratio was found to show an increase for almost all the cases as compared to the original Co-Y catalysts from which they were prepared. Whereas the ratio varied between 0.5 to 0.3 for the Co-Y3 to Co-Y6 catalysts, the same changed from 0.7 to 0.5 for the Co-Y/CA2 to Co-Y/CA5 catalysts. Furthermore, the oxygen/cation ratio increased to about 1.7 with the high surface area Co-Y/CA6 catalyst.

Co Impregnation: Since Cr_2O_3 impregnation substantially improved TCE conversion, Co_3O_4 impregnation was attempted to see if the higher loading and the abundance of sites would improve TCE conversion compared to the exchanged Co sites. As mentioned previously, the $Co(NO_3)_2$ solution was less acidic ($pH \simeq 3.3$) than the CrO_3 ($pH < 0.08$) solution and hence the extent

of dealumination and structural loss was significantly less with the Co-Y/Co catalyst. This was evident by the almost identical SiO_2/Al_2O_3 ratios between the original Co-Y2 and the Co-Y/Co catalysts. The acidity of the Co-Y/Co was not lower than the Co-Y2 either. However, a slight drop in surface area suggested some pore blockage during the Co_3O_4 impregnation. The unchanged oxygen adsorption further showed that the impregnated Co_3O_4 sites did not contribute significantly towards the O_2 pickup and in this respect it was less effective than either the exchanged Co sites or the impregnated Cr_2O_3 sites.

$MeCl_2$ Conversion: As the results showed, $MeCl_2$ conversion with the different Co-Y/CA catalysts increased with increasing Co content. With increasing Co exchange, it has been assumed that the Co availability in the supercages increases and consequently the acidity increases by cation hydrolysis. Therefore, $MeCl_2$ conversion appears to be related to zeolite acidity. As reported by Kiselev et al. (49), similar increases in conversion for C_2H_4 and CO oxidation, with Cu-Y and Co-Y respectively, were noticed as the cation loading was increased. They suggested that, with increasing cation availability in the supercages, better adsorption of the feed was possible and this led to increased activity. In the case of $MeCl_2$, adsorption by carbonium ion formation at the Brönsted sites seems to be possible. With increasing zeolite acidity, more sites are available for such carbonium ion formation, consequently increased adsorption of $MeCl_2$ is facilitated. As discussed earlier (26, 27), $MeCl_2$ oxidation appears to be controlled by reaction between adsorbed feed and separately adsorbed oxygen. Therefore, in addition to improving $MeCl_2$ adsorption as carbonium ions, increased cation loading also increases the oxygen adsorption capacity of the zeolite by providing more metal sites for the formation of either bridged or singly adsorbed oxygen species. This dual effect of increased $MeCl_2$ adsorption and increased oxygen availability probably results in the increased catalytic activity for higher Co loaded catalysts.

Cr_2O_3 impregnation apparently did not improve the catalytic activity for $MeCl_2$ conversion with the Co-Y/CA catalysts. On the contrary, higher Cr_2O_3 loading actually resulted in lower $MeCl_2$ conversion (Figure 15). This may suggest that acidic reactions such as carbonium ion formation and oxidation by oxygen adsorbed at nearby cationic sites is more favorable for $MeCl_2$ oxidation in the range of 250 to 350°C, than regular electrophilic type reactions of adsorption on metal oxide (Cr_2O_3) and oxidation by oxygen dissociatively adsorbed on the metal oxide. Therefore, as increased Cr_2O_3 loading causes increased dealumination and structural loss, Co content and acidity of the catalyst decrease and hence $MeCl_2$ oxidation via carbonium ion formation is also reduced. However, $MeCl_2$ oxidation by electrophilic reaction after adsorption on Cr_2O_3 and oxidation by dissociatively adsorbed oxygen probably competes with the carbonium ion type reaction, but the rate of the former is probably much less in the temperature range considered. In

fact, our previous work (27) showed that $MeCl_2$ adsorption on Co-Y/CA at 250 to 350°C was more than that with the Co-Y catalyst, even though surface area of the Co-Y/CA was lower than the Co-Y. This, in combination with the lower activity of the Co-Y/CA than the Co-Y (27), suggests that although there is considerable adsorption of $MeCl_2$ on the impregnated Cr_2O_3 sites, the $MeCl_2$ adsorbed on the acidic sites as carbonium ions is preferentially oxidized under the present reaction conditions, more readily than the $MeCl_2$ chemisorbed on the Cr_2O_3 sites.

TCE Conversion: Unlike the catalytic activity for $MeCl_2$ conversion, TCE conversion appears to be primarily controlled by the impregnated Cr_2O_3 sites. As mentioned earlier (27) and discussed in the results, both Co-Y and Co-Y/Co showed very poor activity for TCE oxidation, indicating that the cationic Co sites and the acidic sites produced by cation hydrolysis were almost ineffective for TCE conversion in the range of 250 to 350°C. However, introduction of even a small amount of Cr_2O_3 (2 percent) produces a drastic improvement in the catalytic activity of the Co-Y, as seen by comparing the Co-Y/Co and the Co-Y/CA6 catalysts. This result indicates a mechanistic difference in the catalytic oxidation of TCE as compared to $MeCl_2$.

It was shown earlier (27), that TCE adsorption on the Co-Y/CA catalyst in the range of 250 to 350°C increased almost six times compared to the Co-Y. The difference in activity for TCE oxidation, between the Co-Y/CA and the Co-Y catalyst, exactly follows this adsorption pattern. Therefore, it may be suggested that the initial adsorption of TCE on the Cr_2O_3 sites is an important step in TCE oxidation. It is apparent that in the absence of these Cr_2O_3 sites for adsorption, TCE oxidation in the Co-Y catalysts cannot proceed under the present reaction conditions. However, excess Cr_2O_3 impregnation is again detrimental for the catalytic activity. It is apparent that dealumination and structural loss associated with excess Cr_2O_3 impregnation can significantly reduce the zeolite surface area necessary for well dispersed Cr_2O_3 impregnation and thereby affect TCE conversion.

Although the acidic and cationic sites in the Co-Y zeolite appear to be quite ineffective for initial TCE oxidation steps, the acidity of the zeolite seems to play an important role when some impregnated Cr_2O_3 sites are also present. As the results showed, even after similar Cr_2O_3 impregnation, the catalysts which originally had high acidity due to high Co loading still showed higher TCE conversion compared to the lower Co loaded ones. This effect, which was more prominent at the lower temperatures (250-300°C), suggests that the acidic and cationic sites of the Co-Y zeolite probably affect the reaction only after the initial TCE adsorption has taken place at the Cr_2O_3 sites. This effect was further verified by comparing the activity and acidity of two H-Y/CA and Na-Y/CA catalysts. Both of these catalysts had about 6 percent impregnated Cr_2O_3, but, as

expected, the acidity of the H-Y/CA was significantly higher than the Na-Y/CA. For TCE oxidation, higher feed conversions were obtained with the H-Y/CA catalyst than the Na-Y/CA. Therefore, it is again evident that following the initial adsorption of TCE on the Cr_2O_3 sites, the zeolite acidic sites probably take part in the reaction, the exact nature of which is not yet certain.

SECTION IV

DEACTIVATION OF METAL-LOADED ACID CATALYSTS

A. REVERSIBLE LOSS OF ACTIVITY BY COKING

1. Results

The catalyst deactivation experiments for complete oxidation of chlorinated hydrocarbons were carried out with two primary catalysts. The first one was a modified Co-exchanged catalyst made from 1/16 inch H-Y zeolite pellets and the other was a catalyst made from 3/64 inch modified Co-Y pellets prepared by combining Co-Y powder with Silbond-H-5 binder. These two catalysts will be referred to as the modified Co-Y and the modified Co-Y/Silbond catalysts, respectively. Besides these, two other catalysts were also used during this study. These were the modified Co-exchanged 1/16 inch mordenite pellets (modified Co-M) and another set of modified Co-Y pellets with higher Co loading.

A comparison of the acidity (m moles of NH_3 desorbed/gram catalyst), BET surface areas, O_2 pickup and Co_3O_4 content of the catalysts used is shown in Table 9. Higher cobalt loading was noticed with the modified Co-Y catalyst than with the modified Co-Y/Silbond or the modified Co-M. In the case of the Co-M, smaller pores (6-8 Å) and different crystal structure could have produced the lowest Co loading, while, the lower Co loading in the modified Co-Y/Silbond pellets was partly due to the presence of the low surface area inert silica binder and partly due to lower cobalt loading of the original Co-Y powder ($\simeq$ 1 percent).

TABLE 9: COMPARISON OF PROPERTIES OF VARIOUS CATALYSTS

Catalyst	Acidity	BET	O_2 Pickup	Co_3O_4 Content
	(m mol/g)	(m^2/g)	(mg/g)	(wt%)
Mod. Co-Y	3.60	324.5	1.365	1.045
Mod. Co-Y/Silbond	3.24	456.0	1.361	0.344
Mod. Co-M	1.90	380.0	1.294	0.074
Mod. Co-Y (High Co)				1.447

The acidity results showed a slightly lower acidity with the modified Co-Y/Silbond than with the modified Co-Y. The higher silica-alumina ratio of the mordenite produced much lower acidity with the modified Co-M.

The difference in surface areas between the modified Co-Y and the modified Co-Y/Silbond pellets was primarily due to the modification process.

The first catalyst to be investigated for its deactivation characteristics was the modified Co-Y. During our previous studies (27), this 1/16 inch pelletized catalyst showed superior activity with several chlorinated VOCs ($MeCl_2$, TCE, CCl_4) for oxidation in the range of 250 to 350°C. Figure 17 shows the conversion versus time plot for the modified Co-Y catalyst used in TCE oxidation. The reaction temperature was varied from 225 to 350°C and the conversion noted over a period of 1500 minutes (25 hours). The results indicate that at 325°C and above, no appreciable decrease in TCE conversion could be noticed. However, with further lowering of temperature to below 300°C, deactivation occurred. In each case, the catalyst activity dropped from the initial complete conversion to a steady state value and the extent of this decrease increased as temperature decreased from from 300 to 225°C. Also, the time taken to attain 80 percent of the steady state conversion decreased from about 8 hours at 300°C to about 1.2 hours at 225°C, indicating that the rate of deactivation increased with reduction of temperature.

An important aspect of catalyst deactivation is whether it is reversible. Expecting deactivation by coking, the catalyst was treated in air at 450°C for 2-4 hours in an attempt to regenerate it after every deactivation experiment. Since a single batch of any catalyst pellets was used for the several deactivation experiments (instead of fresh batches for every experiment), as shown in Figure 17 and subsequent others, the catalyst always regained its original activity after such a regeneration process and produced complete conversion of the chlorinated feed at the beginning of the next experiment. Figure 18 shows a typical plot obtained during regeneration of the deactivated modified Co-Y catalyst at 450°C. Within approximately 30 minutes of beginning the oxidation at 450°C, large amounts of CO_2 and CO were obtained; no chlorinated compounds were detected. This suggests that coke or carbonaceous deposits were present on the deactivated catalyst surface, which were converted to CO_2 and CO under an oxidizing atmosphere at relatively high temperature (450°C).

The results obtained from both the deactivation and the regeneration experiments indicated that coking or formation of carbonaceous deposits inside the zeolite pores might be the cause of deactivation in the modified Co-Y catalyst. This, coupled with the difficulty of quantifying the CO_2 and CO produced during the regeneration process, led to the use of an alternative method

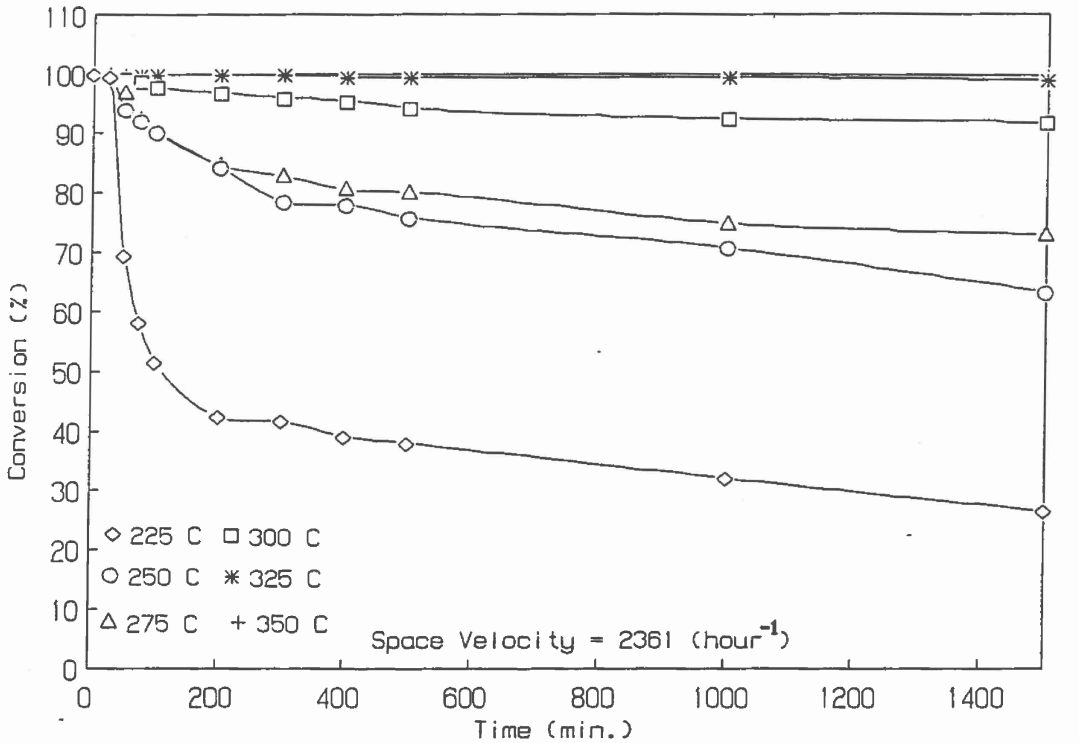

Figure 17. Deactivation of Modified Co-Y pellets during TCE Conversion at different temperatures

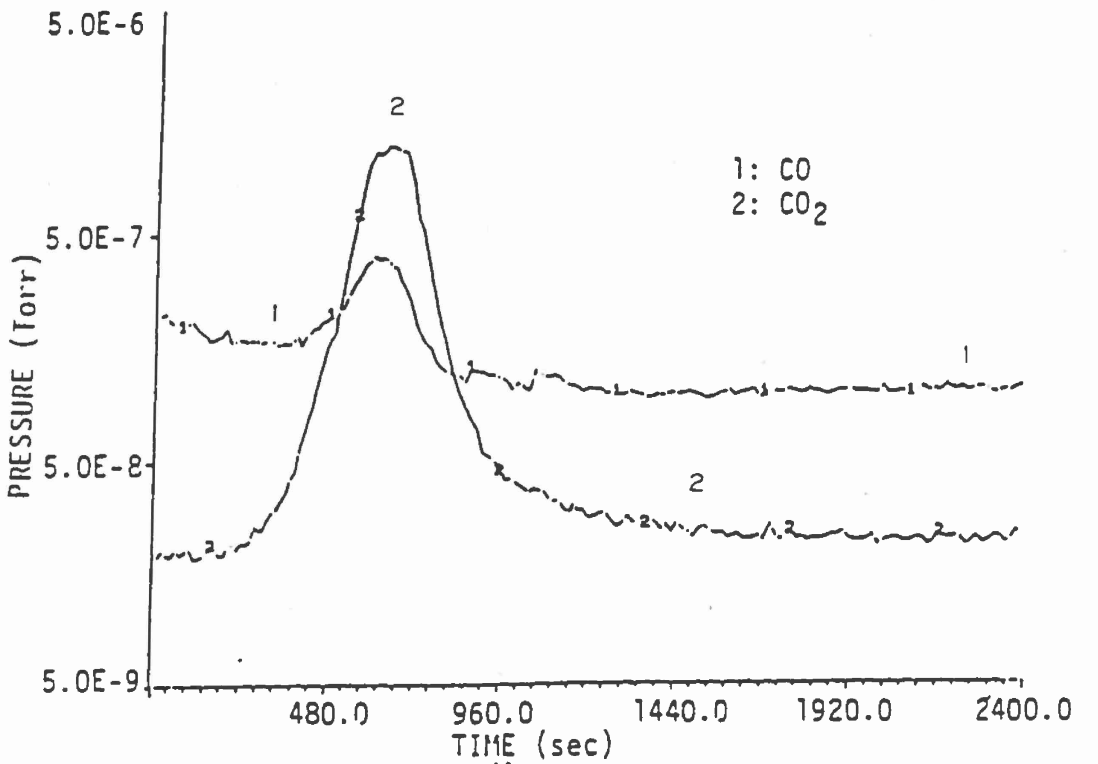

Figure 18. Product Spectrum obtained during Regeneration of Deactivated Modified Co-Y Pellets at 450 C

for quantification of the coke. Consequently, the TGA was used as a thermogravimetric reactor system for continuous monitoring of the weight change of the modified Co-Y catalyst during TCE oxidation.

Figure 19 shows the fractional weight gain (mg/g) of the catalyst during TCE oxidation at various temperatures as a function of time. At every temperature, the catalyst showed a sharp weight gain during the initial 100 minutes of the experiment. This weight gain increased with decreasing temperature from approximately 65 mg/g at 400°C to 427 mg/g at 250°C. Assuming this weight gain solely due to carbon deposition, the amount of coke deposited during TCE oxidation in the modified Co-Y catalyst appeared to increase with decreasing temperature and at 250°C was 6.5 times that at 400°C.

After characterizing the modified Co-Y catalyst for TCE oxidation, similar experiments were conducted with $MeCl_2$ feed. Figure 20 shows the conversion versus time plot for $MeCl_2$ oxidation on the modified Co-Y catalyst. As before, the modified Co-Y catalyst showed a drop in activity over 1000 minutes and the extent of deactivation became more pronounced with lowering of temperature from 350°C to 300°C. However, it appears that the rate of deactivation was lower with $MeCl_2$ than with TCE in this temperature range. TGA experiments for quantification of coking were also carried out for this modified Co-Y catalyst and are shown in Figure 21. As with the TCE experiments, coke formation increased when reaction temperature was lowered. The fractional weight gain of the modified Co-Y catalyst during $MeCl_2$ oxidation was more than doubled by decreasing the reaction temperature from 350°C to 300°C.

The comparative weight gain due to coking during oxidation of either TCE or $MeCl_2$ at different temperatures over the modified Co-Y catalyst is given in Table 10. The results clearly indicate that the total amount of coke formed at any temperature over a period of about 1000 minutes is lower with $MeCl_2$ than with TCE. For example, at 300°C, when significant deactivation could be noticed with both the feeds, total coke formation with $MeCl_2$ was about half of that formed with TCE. Conversely, when the rate of weight gain is plotted with time for the oxidation of these two compounds over the modified Co-Y catalyst (Figure 22), it is found that the rate of weight gain, assumed to correspond to coke formation, is significantly higher with $MeCl_2$ during the initial 8 or 10 minutes of reaction. During this time, the rate of weight gain goes through a parabolic profile with a distinct peak. As shown in Figure 22, the height of this peak is much greater for $MeCl_2$ than for TCE at any temperature. The value of this maximum rate of weight gain (peak value) increases with decreasing temperature. However, after this initial time period, the rate of weight gain for $MeCl_2$ oxidation decreases to a much lower value (compared to the peak) and becomes almost flat while that for TCE remains higher.

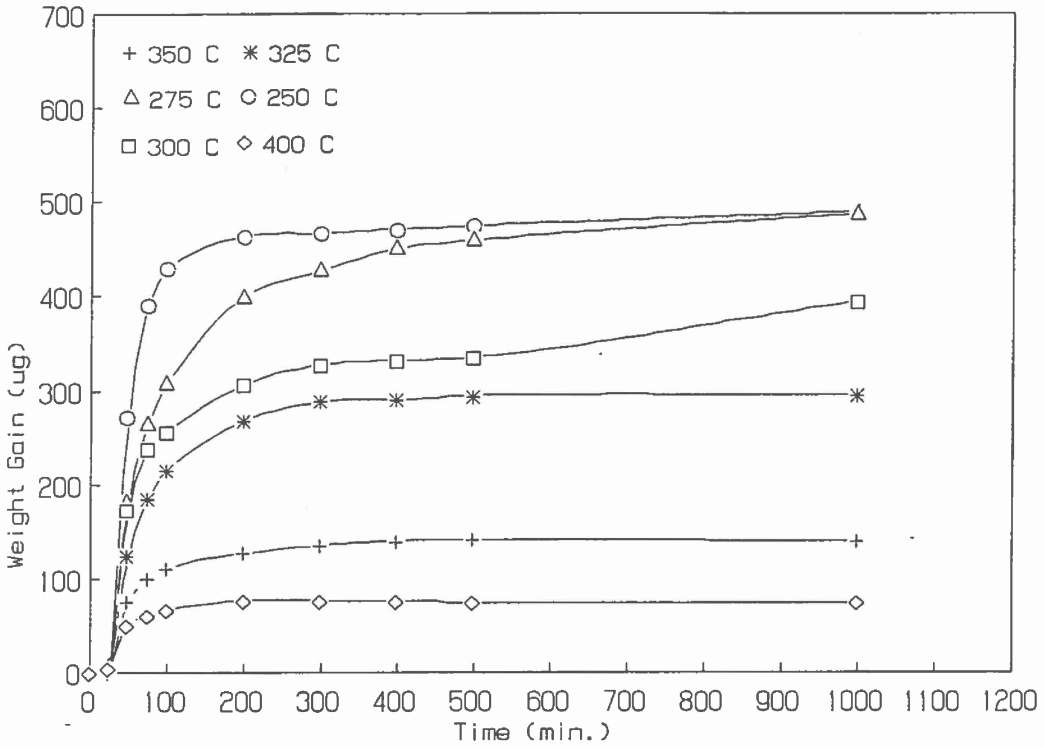

Figure 19. Coke deposition in Modified Co-Y during TCE Oxidation at different temperatures

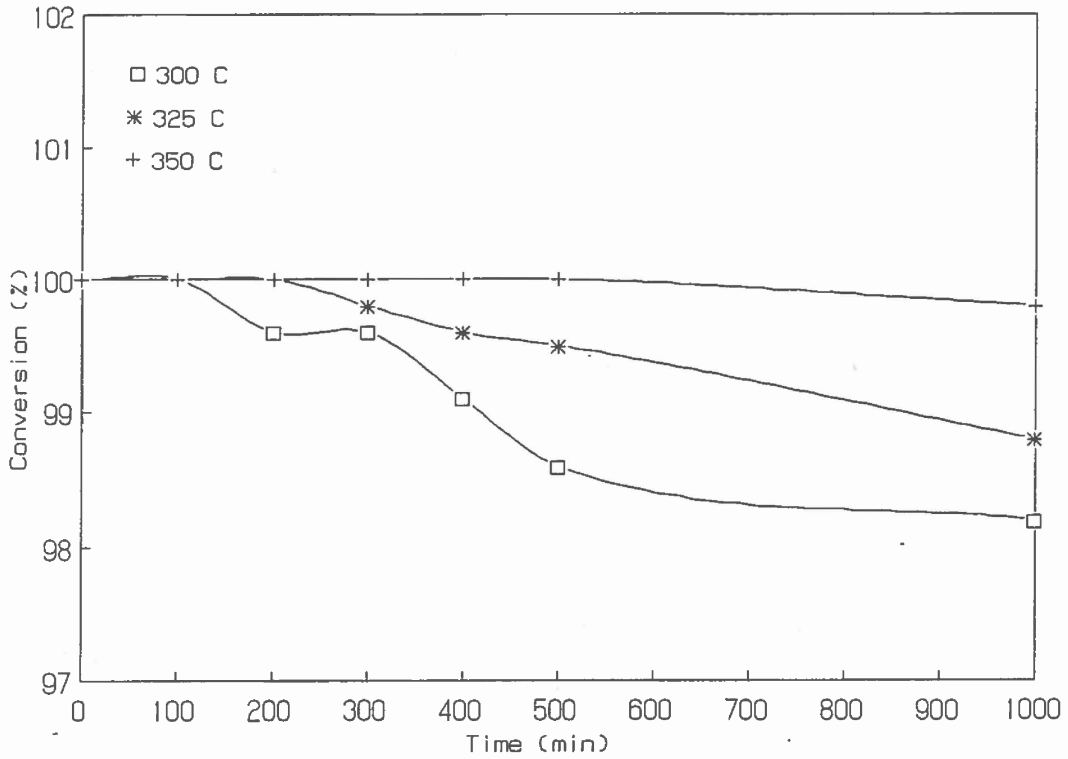

Figure 20. Deactivation of Modified Co-Y Pellets during MeCl2 Oxidation at different temperature

During this time, the rate of weight gain with TCE is significantly higher than with $MeCl_2$ and it remains so until the end.

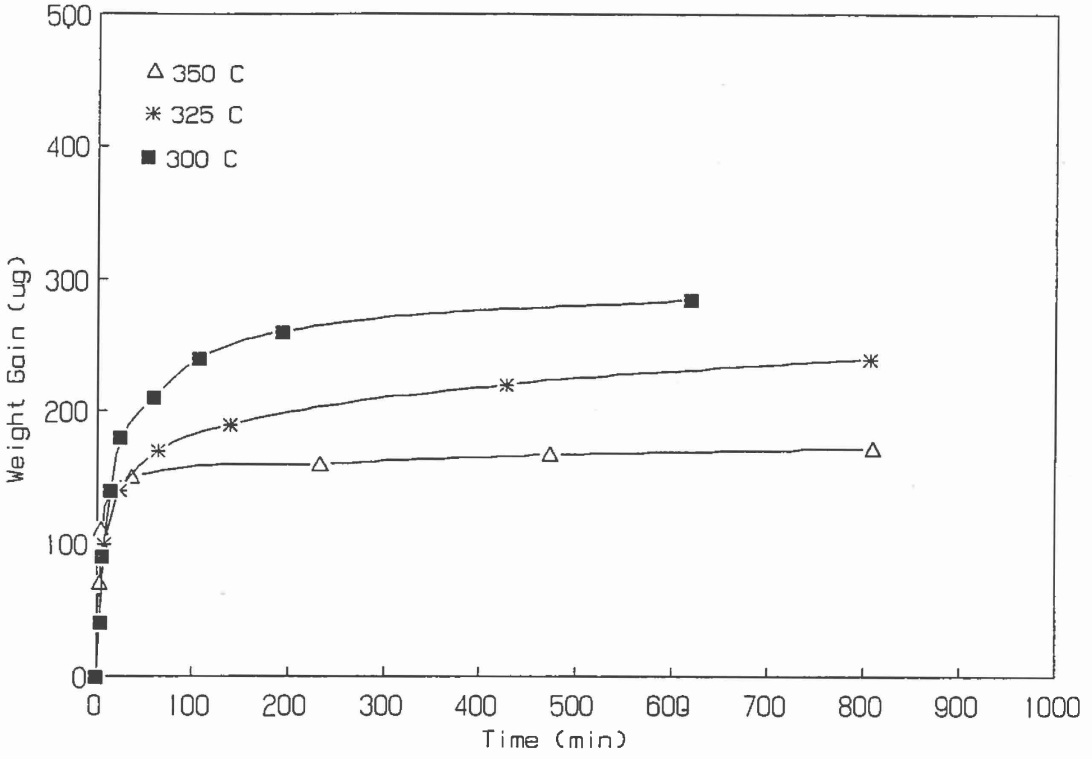

Figure 21. Coke Deposition in Modified Co-Y Pellets during MeCl2 Oxidation at different temperatures

TABLE 10: TOTAL COKE FORMATION (MG/G) IN CATALYSTS AFTER 1000 MINUTES OF CHLORINATED VOC OXIDATION

Feeds	Temperature (°C)						
	225	250	275	300	325	350	400
Modified Co-Y Catalyst							
TCE		4.715	4.709	4.086	2.847	1.351	0.709
$MeCl_2$				2.369	2.189	1.147	
CCl_4							
Modified Co-Y/Silbond Catalyst							
TCE			3.324	2.318	1.680		
$MeCl_2$				2.190	1.110	0.960	
CCl_4	1.250		0.780				

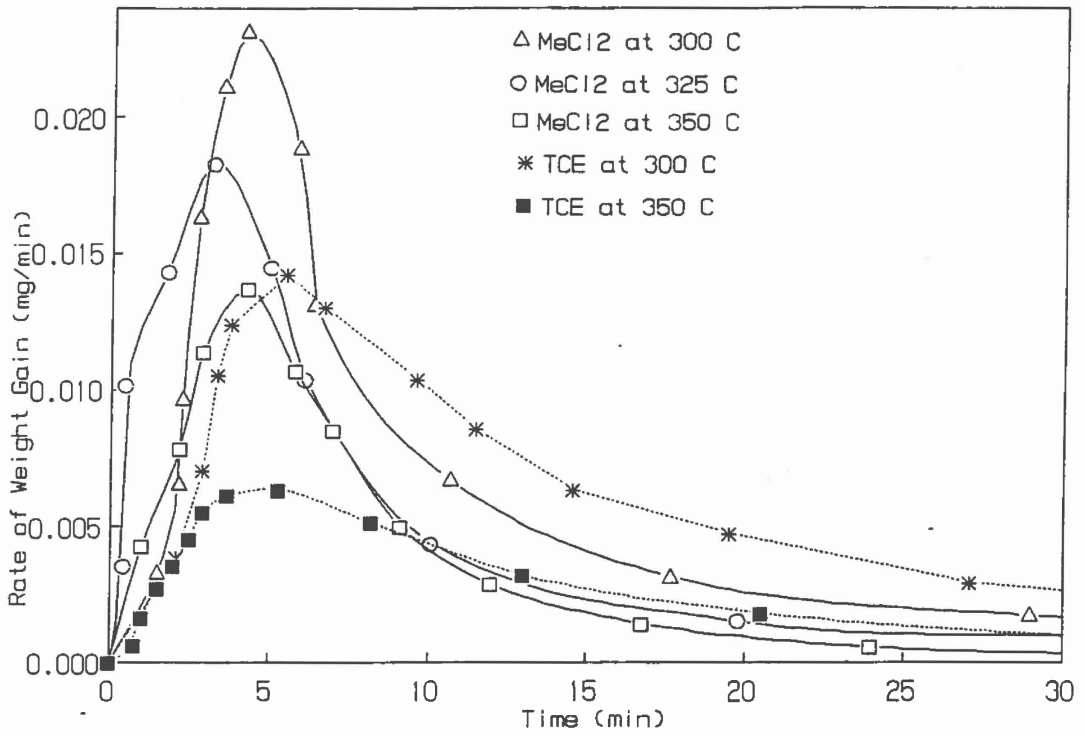

Figure 22. Rate of Weight Gain versus Time plot during Coking of Modified Co-Y pellets with TCE and MeCl2

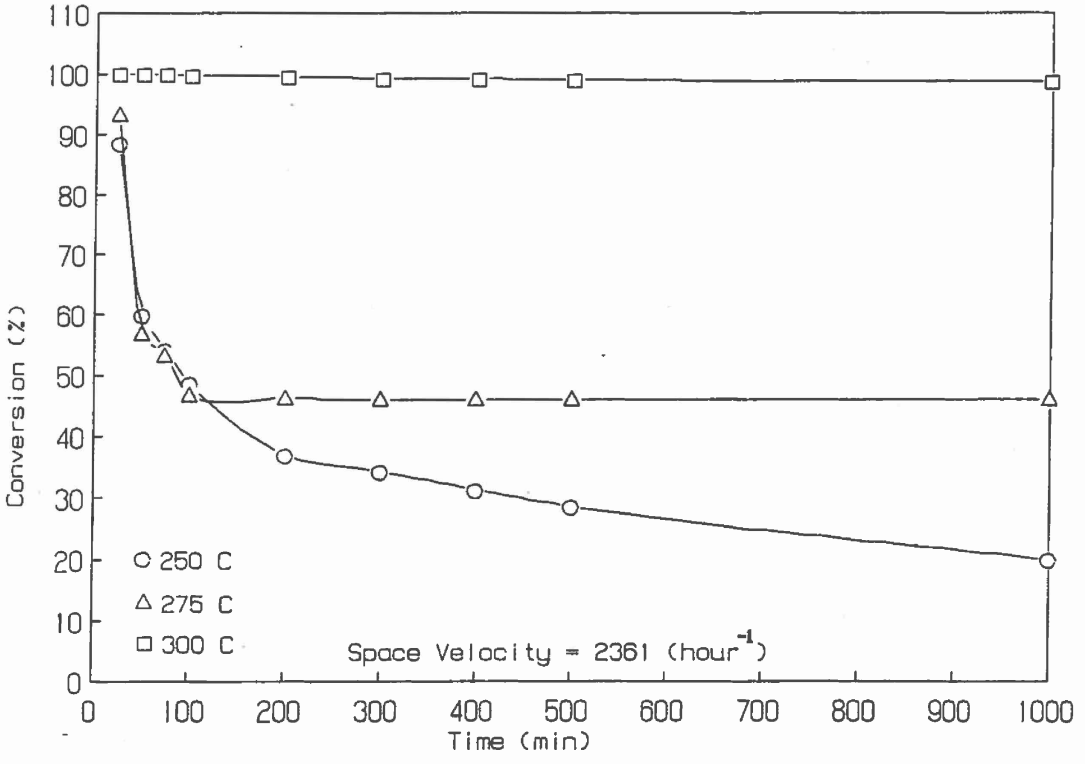

Figure 23. Deactivation of Modified Co-Y/Silbond Catalyst during TCE Oxidation at various temperatures

After completion of the deactivation experiments with the modified Co-Y catalyst, the modified Co-Y/Silbond catalyst was checked for deactivation with all three chlorinated VOCs ($MeCl_2$, TCE and CCl_4). Figure 23 shows the conversion versus time for the modified Co-Y/Silbond catalyst for TCE oxidation at different temperatures while similar plots for $MeCl_2$ and CCl_4 are shown in Figure 24. Comparing the deactivation of the modified

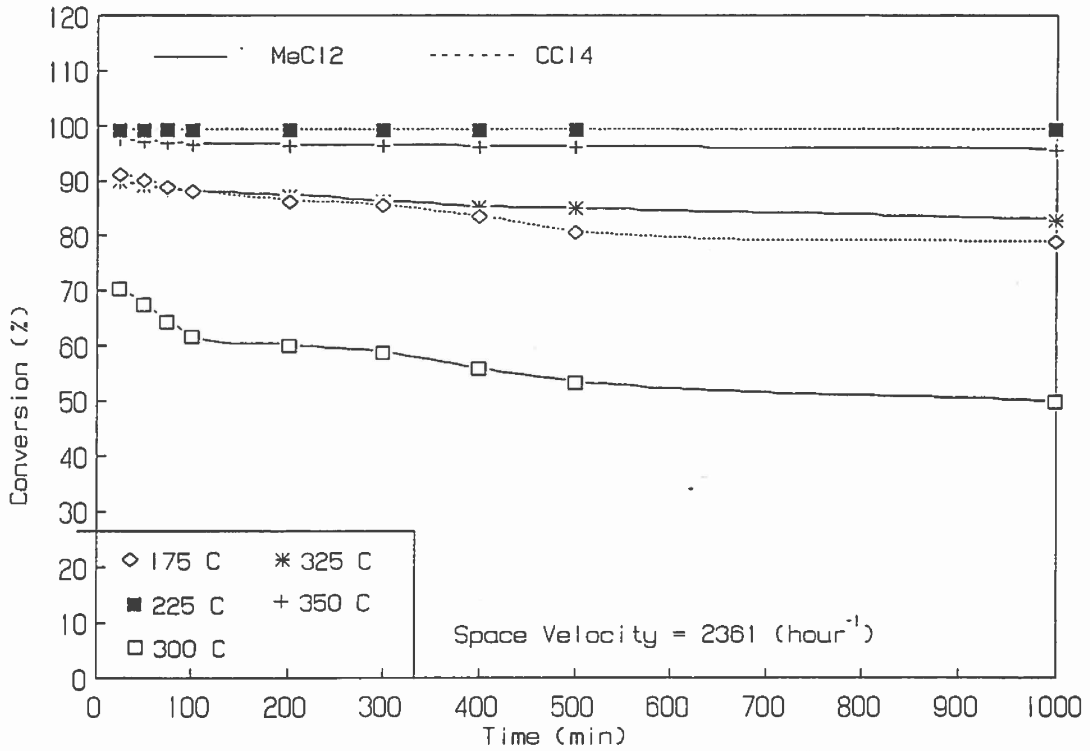

Figure 24. Deactivation of Modified Co-Y/Silbond Catalyst during MeCl2 and CCl4 Oxidation

Co-Y/Silbond catalyst among all three feeds, deactivation was negligible for CCl_4 oxidation even at a temperature as low as 225°C; noticeable deactivation was observed with CCl_4 only at 175°C. The activity of the modified Co-Y/Silbond catalyst for $MeCl_2$ oxidation was lower compared to both TCE and CCl_4, however, the rate of deactivation with $MeCl_2$ was much lower than with TCE. At 300°C, $MeCl_2$ conversion dropped from 70 percent to about 55 percent over a period of 1000 minutes whereas TCE conversion at 275°C dropped from more than 90 percent to about 50 percent over the same period.

Table 10 shows a comparison of coke formation between the modified Co-Y and the modified Co-Y/Silbond catalysts for oxidation of various VOCs. Among the three feeds, the trend in coke deposition was TCE>$MeCl_2$>CCl_4. TCE always produced maximum weight gain of the catalyst after 1000 minutes of reaction,

followed by $MeCl_2$ and CCl_4. Between the two catalysts, the modified Co-Y showed higher coke deposition with both TCE and $MeCl_2$ than the modified Co-Y/Silbond catalyst. However, comparing the rate of deactivation between the catalysts for TCE oxidation, the initial rate of deactivation was much higher in the modified Co-Y/Silbond than the modified Co-Y. For example, TCE oxidation at 275°C with the modified Co-Y/Silbond catalyst dropped from complete conversion to less than 50 percent over a period of 200 minutes while, during the same time, TCE conversion with the modified Co-Y dropped only to 83 percent. The effect of temperature on deactivation characteristics of the two catalysts was similar in both the cases. Both catalysts showed more deactivation at lower temperatures.

To investigate the effect of catalyst composition on the deactivation of the modified Co-Y, a second batch of modified Co-Y catalyst was prepared with higher Co loading (1.4 percent). This catalyst was tested for deactivation during TCE oxidation at different temperatures. Figure 25 shows conversion versus time plot for this catalyst. As with the modified Co-Y catalyst with lower cobalt loading, catalyst deactivation was more pronounced at lower temperatures. However, the rate and the extent of deactivation over a period of 1000 minutes was much higher with the higher Co-loaded modified Co-Y catalyst. Comparing Figure 17 to Figure 25, TCE conversion at 250°C with the higher Co loaded catalyst went down to almost zero within 400 minutes of operation while the lower cobalt catalyst continued to show over 65 percent conversion even after 1400 minutes of operation. This suggested a definite enhancement of coking with excessive Co exchange.

In addition to modified and metal-exchanged Y zeolite catalysts, the deactivation features of a similarly prepared mordenite catalyst were also investigated. The modified 1/16 inch Co-M catalyst pellets were used for TCE oxidation at different temperatures and the results are shown in Figure 26. It is apparent from this conversion versus time plot that the smaller pore mordenite zeolite (6-8 Å) suffered much more deactivation than the similarly treated Y under identical reactor conditions. The modified Co-M showed over 90 percent deactivation in TCE conversion at 250°C while the modified Co-Y showed less than 30 percent deactivation during the same period of time. Further, the modified Co-Y did not show any significant deactivation up to 325°C whereas the modified Co-M produced almost a 10 percent drop in TCE conversion at 325°C.

A part of the present study involved investigation of the deactivation of the modified Co-Y catalyst at 275°C at different space velocities. TCE experiments were carried out with the modified Co-Y catalyst at three different space velocities. The space velocity was varied by changing the total flow rate of the feed-air mixture while keeping the feed concentration constant. However, since the water concentration could not be kept constant over this range of space velocities,

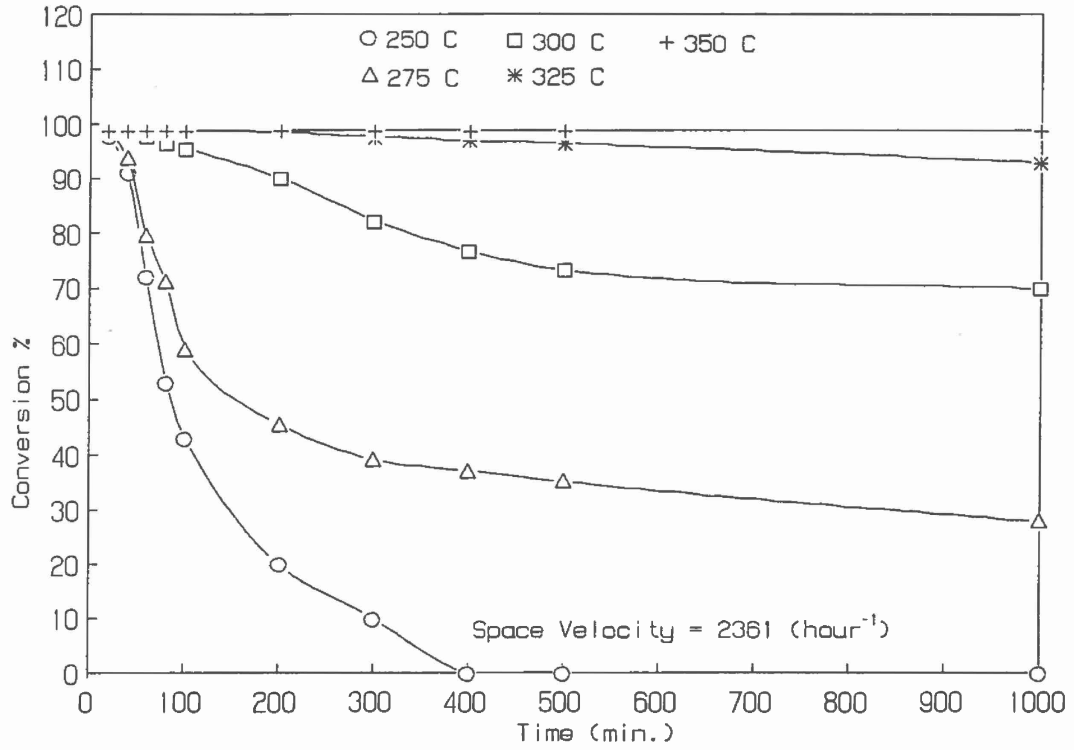

Figure 25. Deactivation of high Co loaded Modified Co-Y Catalyst during TCE Oxidation

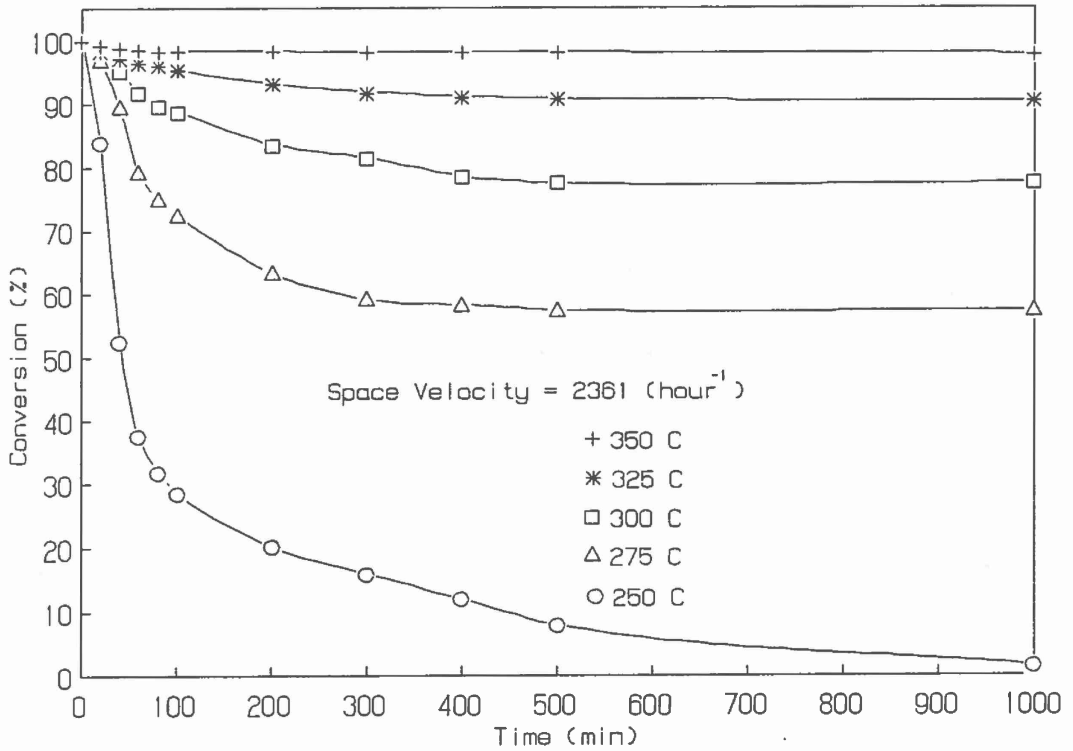

Figure 26. Deactivation of Modified Co-M Catalyst during TCE Oxidation at various temperatures

runs were carried out without water addition. Note that the space velocities were measured at the inlet conditions (25°C, 1 atm) for all the runs.

Figure 27 shows the effect of space velocity on the deactivation characteristics of the modified Co-Y catalyst during TCE oxidation at 275°C. The results indicate that, with lower space velocity (i.e., higher residence time), the rate of deactivation is lower. Conversely, experiments with higher space velocities showed faster deactivation.

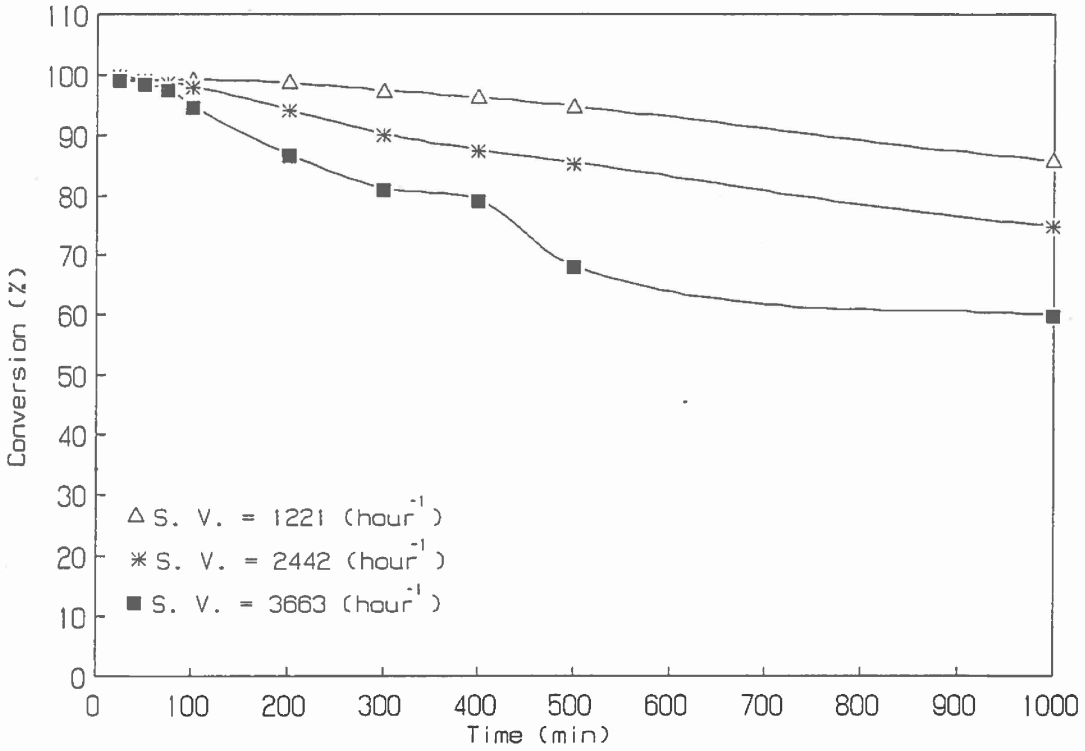

Figure 27. Effect of Space Velocity on Deactivation of Modified Co-Y Catalyst during TCE Oxidation at 275 C

The catalytic oxidation experiments during this study were carried out with a mixture of VOC feed and dry compressed air. However, it was of importance to know whether oxygen concentration played any significant part in controlling the deactivation of the modified metal exchanged catalysts. This was investigated by carrying out experiments using pure oxygen instead of air with the modified Co-Y catalyst. The TCE oxidation experiments at 275°C with the feed-oxygen mixture failed to show any improvement in the deactivation of the modified Co-Y catalyst, indicating that increased oxygen availability does not lessen the deactivation process in the concentration range examined in this study.

2. Discussion

The results showed that the modified cation-exchanged zeolite catalysts partially deactivate during chlorinated VOC oxidation. This deactivation, although it appears to be reversible, is of practical importance. The deactivation of the modified cation exchanged zeolites appears to be the result of coking within the zeolite pores. A major difference between coking in cracking reactions and chlorinated VOC oxidation is the presence of oxygen in the latter case. It is possible that the presence of oxygen reduces the extent of coking in the modified Co-Y zeolitic catalyst, which retains activity during TCE oxidation even after 25 hours of operation. However, oxygen concentration does not appear to play a controlling part in the deactivation process. Conversely, the following factors appear to influence both coking and deactivation of the modified cation exchanged zeolite catalysts during catalytic oxidation of chlorocarbons:

- Catalyst structure and composition
- Nature of VOC feed
- Reaction temperature
- Residence time

During this discussion, these factors will be individually analyzed for their effect on coking or deactivation in the present case.

As suggested by Derouane (56) and Guisnet, et al. (57-59), coking in a zeolite catalyst can deactivate it by either site blockage or by channel or pore blockage. Coking happens either by a series or a parallel mechanism:

$$A \rightarrow B \rightarrow C$$

series coking

$$A \begin{matrix} \nearrow B \\ \searrow C \end{matrix}$$

parallel coking

Here A is the feed, B is a product or intermediate and C is coke. At the onset of coking, the reaction is initiated at the catalyst active sites and forms carbonaceous deposits on the sites. As the reaction progresses, this coke molecule grows in size and gradually covers the active site and hence blocks the access of the reactants to that site. This is called site coverage. Another mechanism of deactivation is pore blockage by large molecules of coke that hinders the entry of any reactant into the zeolite cavity.

For series coking, the rate depends on the rate of formation of the coke precursor (which may be an intermediate or a reactant) which in turn depends on the rate of the primary reaction. The rate of the primary reaction in a zeolite catalyst depends on the number and strength of the acidic sites in the zeolite. This is believed to be true under either oxidizing or

reducing conditions. As suggested by Gentry et al. (17) and mentioned elsewhere (26, 27), oxidation of VOCs in the zeolite catalysts appear to be controlled by both the Brönsted acid sites and the cationic sites. The mechanism is believed to be comprised of simultaneous feed and oxygen adsorption at the protonic and the cationic sites, respectively, followed by reaction between the the two reactants adsorbed at two different sites. Further, Derouane, et al. (56) and Ghosh and Kydd (60) both reported that the Brönsted acid sites of the zeolite catalysts play an active part in coke formation. Therefore, the activity of the zeolite catalyst for coking appears to be directly related to its activity for the desired oxidation reaction.

Catalyst Structure: The two primary catalysts used for this study, modified Co-Y and modified Co-Y/Silbond, were both prepared from cobalt exchanged Y zeolite. However, the 1/16 inch modified Co-Y pellets contained almost three times more cobalt than the 3/64 inch modified Co-Y/Silbond ones. It is well known (26, 27) that higher valence cations increase the zeolite acidity by cation hydrolysis. This can be shown as:

$$Me^{n+} + xH_2O \Leftrightarrow Me(OH)_x^{(n-x)} + xH^+$$

Therefore, it could be expected that the modified Co-Y catalyst had higher acidity than the modified Co-Y/Silbond and this led to its higher activity for chlorinated VOC oxidation. As shown in Table 9, acidity results between these two catalysts supported this suggestion. Consequently, the higher acidity and hence the higher activity of the modified Co-Y catalyst, caused increased overall coking, as opposed to the modified Co-Y/Silbond. Further, the presence of less cations or active sites for the modified Co-Y/Silbond might have led to its faster deactivation by rapid site coverage unlike the higher cation loaded modified Co-Y catalyst.

Although higher Co loading in the modified Co-Y compared to the modified Co-Y/Silbond catalyst seemed to inhibit the rate of deactivation for TCE oxidation, further increase of the cobalt content (from 1.04 percent to 1.44 percent) produced excessive deactivation with the modified Co-Y catalyst. The lack of any residual activity with the higher Co loaded catalyst for TCE oxidation at 250°C after less than seven hours of operation suggested deactivation by rapid pore blockage. It is possible that the presence of the additional Co cations hindered or partially blocked the entrance of the zeolite supercages. Combined with further pore blockage by coking, this could have increased the rate of deactivation to such a point that no reactant molecule could reach any of the catalytic sites. This result indicates that the cation loading has to be optimized for reduced catalyst deactivation.

Deactivation of a zeolite catalyst by coking is also a shape selective process that depends on the zeolite pore size and inter-connectivity of channels. Guisnet et al. (57-59) reported that composition and size of coke depends on the zeolite pore volume. Since coke formation occurs inside the zeolite cavity, the extent of coking is constrained by the maximum space available inside. This causes a difference in the composition of coke formed in different zeolites such as Y, mordenite and ZSM-5. The zeolite channel structure also controls the deactivation of zeolites. Derouane (56) suggested that coke is formed more rapidly in zeolites with non-inter-connecting channels such as mordenite. This is because the active sites in mordenite are only accessible through these unidirectional channels and blockage of a channel leading to an active site by coking completely hinders access to that site. Since the channels are not interconnected, the reactant cannot reach the active site through any other channel. Conversely, in the case of zeolites such as Y, interconnected channel systems offer multiple paths to the active sites and thus coking is reduced.

Similar results were obtained by comparing the deactivation of modified Co-Y and the modified Co-M catalysts for TCE oxidation at various temperatures. The cobalt-exchanged and modified mordenite catalyst deactivated much more rapidly than the similarly prepared Y. During catalyst preparation, similar treatment with the mordenite zeolite produced much lower cobalt loading (0.07 percent) than the Y zeolite (1.04 percent). Fewer cationic sites were situated inside the zeolite pores (0.28 cm^3/cm^3) of smaller total volume than that of Y (0.48 cm^3/cm^3). Therefore, during coke formation inside the mordenite channels, pore blockage could occur faster and with a non-interconnecting channel system, no other pathway was available to the reactants. The overall result was a rapid deactivation of the modified Co-M catalyst during chlorinated VOC oxidation. In addition to that, the presence of far fewer acidic sites (Table 9), as compared to the modified Y zeolite catalysts, probably enhanced deactivation by rapid site coverage.

The coked and deactivated modified cation-exchanged Y zeolite catalysts could be easily regenerated by oxidizing in air at 450^0C for 2-4 hours. The complete regeneration of the catalyst activity after repeated deactivation experiments showed that the coke present inside the zeolite was easily accessible to oxygen and apparently did not cause any irreversible deactivation. The RGA product spectrum during regeneration (Figure 18) showed that the bulk of the coke was oxidized very quickly which may suggest that most of the coke was present inside the zeolite in such a way that it prevented the access of the sites to the reactants but was itself readily available for further reaction.

Nature of the VOC feed: Apart from the catalyst itself, the type of chlorinated feed used also appears to be a major factor in determining the extent of deactivation in the

modified cation exchanged zeolites. Comparing the different VOC reactants, it seems probable that the presence of more carbon atoms in the TCE molecule is at least partially responsible for its increased coke production and deactivation than in the others. However, the rate of coking during the TGA experiments showed higher initial rate of formation with $MeCl_2$ than TCE at any temperature. The results indicate that oxidation of the two different VOCs (and hence coke formation) may be taking place at two different types of active sites.

$MeCl_2$ is a symmetric molecule with two chlorine atoms and two hydrogen atoms bonded to a single carbon whereas TCE is an unsaturated double bonded compound with three chlorine and one hydrogen bonded to two carbon atoms. This shape, size and structural difference between these two chlorocarbons may cause a difference in the accessibility of the catalytic sites as well as the type of sites responsible for their complete conversion. In our previous study (27), it was found that although the regular Co-Y catalyst (1/16 inch pellets) produced complete conversion of $MeCl_2$ and CCl_4 at temperatures below 350°C, it was completely ineffective for TCE under the same reaction conditions. This necessitated the modification of the Co-Y. The modification process introduced an additional type of catalytic site in the Co-Y and thus complete conversion of TCE could be achieved at under 350°C, without affecting $MeCl_2$ and CCl_4 conversion. Similar results were found with other double carbon, double-bonded compounds like tetrachloroethylene (C_2Cl_4) etc. Therefore, it was apparent that the conventional protonic and cationic sites in the zeolite catalysts were not active at lower temperatures for oxidation of the double-carbon double-bonded VOCs while the additional sites introduced by modification were primarily responsible for their conversion (perhaps alone or in combination with the zeolite acidic sites).

Since $MeCl_2$ and TCE were primarily reacting at two different sites, coking during reaction with these feeds was probably also controlled by the type of sites and the mechanism. Since no conclusive data are available about the relative coking rate on the different sites, it can only be speculated that the sites responsible for $MeCl_2$ conversion (protonic or cationic or both) were prone to faster coking than the additional sites introduced by modification that enhanced TCE conversion. As these sites were gradually poisoned by coke, the coking rate dropped. Conversely, with TCE reacting at the additional sites (added by modification), the products or intermediates probably further reacted at the Brönsted sites to produce coke. The coking results along with the faster deactivation with TCE indicate that pore blockage by coke hindered access of TCE to the active sites inside the zeolite and thus deactivated the catalyst. Conversely, poisoning of the active sites by coke could have played the major role in catalyst deactivation with the smaller $MeCl_2$.

The presence of four chlorine atoms bonded to a single carbon atom in CCl_4 gives it a perfectly symmetric structure which is very similar to $MeCl_2$. However, unlike $MeCl_2$ or TCE, very low coke formation and deactivation were noticed with CCl_4. This result can be partly explained by analyzing the general composition of coke. Coke is generally regarded as a large poly-nuclear hydrocarbon with the molecular formula varying from $C_1H_{0.4}$ to C_1H_1 (61). Thus coke composition corresponds to that of a hydrocarbon with small amounts of hydrogen. It is, therefore, possible that the presence of hydrogen atoms in $MeCl_2$ and TCE resulted in coke formation during reaction with these feeds while the absence of any hydrogen in CCl_4 inhibited coking. However, apart from feed composition, coking (and hence deactivation) during catalytic oxidation of the chlorinated hydrocarbons could also have been influenced by the intermediates formed.

The possibility of reaction intermediates affecting coke formation can be determined by analyzing the product selectivity among TCE, $MeCl_2$ and CCl_4. During the deep oxidation of TCE and $MeCl_2$ with the modified Co-Y and Co-Y/Silbond catalysts, CO was produced as the major carbon containing compound. Although small amounts of CO_2 were also present in the product spectrum, the CO_2 to CO ratio with $MeCl_2$ and TCE varied from 0.21-0.60 with temperature increasing from 250 to 350°C. By contrast, no detectable CO was found during CCl_4 oxidation with the same catalysts. CO_2 was the only carbon containing product. Thus, comparing the relative coke formation (and deactivation) and product selectivity among the three chlorinated VOCs, it seems that coking in the modified cation exchanged zeolites is related to the amount of CO formed. Additional evidence towards the relationship between CO formation and catalyst deactivation by coking was provided by the higher Co loaded modified Co-Y and the modified Co-M catalysts, both of which showed more deactivation than the regular modified Co-Y. The higher Co loaded modified Co-Y catalyst produced more CO during TCE oxidation with the CO_2 to CO ratio varying from 0.10 to 0.40 as temperature was increased from 250 to 350°C. Similarly, the increased CO production noticed with the modified Co-M catalyst also appears to be related to its increased deactivation rate.

Reaction Temperature: Coke formation in the modified cation exchanged zeolites as well as rates of deactivation varied considerably with change in reaction temperatures. Decreasing the operating temperature produced more coke and hence rapid deactivation of the catalysts and vice versa. This result can be interpreted in two ways. First, the presence of oxygen during the catalytic reaction signifies that along with coking a simultaneous regeneration reaction will occur between the coke and oxygen. Part of this carbonaceous deposit will be converted to CO and CO_2 thereby reducing the extent of deactivation. However, this regeneration reaction is temperature dependent as noticed during this study and by Magnoux and Guisnet (62). Even though oxidation of carbon can begin at 250°C, the bulk of the

carbon is eliminated only at temperatures above 400°C. It is possible that as the rate of regeneration was high enough at temperatures above 325°C, no noticeable deactivation was observed with the modified Co-Y and the Co-Y/Silbond catalysts at these temperatures. Conversely, with decreasing temperatures the rate of regeneration also dropped and hence more coking and deactivation were observed.

Another way of interpreting the temperature effect is that coke formation is a parallel reaction from a reaction intermediate and decreasing temperature inhibits the desired pathway and thus more coke is produced. If the reaction can be shown as follows:

$$A \rightarrow B \rightarrow D$$
$$\downarrow$$
$$C$$

Where A is the feed, B is the intermediate, C is coke and D is the desired product, then at lower temperatures if the formation of D is inhibited, more coke will be formed from the reaction intermediate B. However, a combination of both reduced regeneration and lower rate of desired reaction products can lead to the formation of more coke at lower temperatures.

Residence Time: With increasing space velocity (decreasing conversion and residence time) the modified Co-Y catalyst showed more deactivation during TCE oxidation at 275°C. Assuming deactivation to be controlled by coke deposition, the results indicate that coke formation or formation of the coke precursor is probably an intermediate step of a series reaction. As the residence time is decreased, this series reaction cannot go to completion and consequently the concentration of the intermediate is increased causing more coke deposition. This appears similar to the series mechanism suggested previously to explain the temperature effects. If B is the coke precursor, lower residence time will reduce the rate of formation of D and hence the rate of the side reaction for coke formation may increase. Moreover, lower residence time may also reduce the rate of coke regeneration by oxygen and thus increase catalyst deactivation.

In view of the above analysis, CO may be a reaction intermediate and coke precursor. If the formation of CO from the oxidation of the VOC feed is an intermediate step, then oxidation of CO to CO_2 is perhaps the complete reaction. The increased CO production with catalysts that showed more deactivation as well as the negligible deactivation during CCl_4 oxidation (where no detectable CO was observed) may provide additional support for such a theory. Based on that, the following mechanism is postulated:

$$\{C_2HCl_3\} + 2[O] \rightarrow 2[CO] + [HCl] + \{Cl_2\} \quad (1)$$
$$[CO] \Leftrightarrow C_* \downarrow + [O] \quad (2)$$
$$[CO] + [O] \rightarrow [CO_2] + [\ ] \quad (3)$$
$$[CO_2] \rightarrow CO_2 \uparrow + [\ ] \quad (4)$$
$$[CO] \rightarrow CO \uparrow + [\ ] \quad (5)$$
$$[HCl] \rightarrow HCl \uparrow + [\ ] \quad (6)$$
$$\{Cl_2\} \rightarrow Cl_2 \uparrow + \{\ \} \quad (7)$$

Here, { } and [ ] are two different types of catalytic sites (26) on which the reactants are adsorbed. Here { } is the acidic or protonic site while [ ] is the cationic site. C_* is the coke component and production of C_* leads to the formation of coke. As suggested by Bell (63), dissociation of CO can produce elemental carbon which can polymerize to produce coke. Reaction (2) shows the reversible coking and coke regeneration reaction. The complete oxidation of CO to CO_2 is the desired series reaction. In addition to the above scheme, another path for coke formation could be by direct decomposition of the VOC feed:

$$\{C_2HCl_3\} \rightarrow \{CH_n\} + \{HCl\} + \{Cl_2\} \quad (9)$$
$$\{CH_n\} \rightarrow \{Coke\} \quad (10)$$
$$\{Coke\} + [O] \rightarrow \{H_2O\} + [CO] + [CO_2] \quad (11)$$

Here CH_n is a partially hydrogenated species that can lead to the formation of coke. It is possible that coke formation on the modified cation exchanged zeolites occurs by both of the above processes and future work will reveal further information about these mechanisms.

B. IRREVERSIBLE LOSS OF ACTIVITY BY THERMAL INSTABILITY

1. Results

In order to investigate the reasons for the irreversible deactivation of the catalysts, a new catalyst stability reactor was set up and was operated. The long term activity tests were carried out on various catalysts using TCE as the feed for up to 300 hours at 600° C. The first two catalysts tested in the stability apparatus were Silbond/CA and Chlorhydrol/CA pellets. Silbond and Chlorhydrol solutions were first dried, calcined and pelletized and then subsequently CA-impregnated for preparation of these two catalysts. Since Silbond and Chlorhydrol were comprised of SiO_2 and Al_2O_3 respectively, the objective was to check how the different support materials affected the stability of the impregnated Cr_2O_3. The results showed that the Cr_2O_3 content of the Silbond/CA catalyst dropped from 2.5 percent to 1.8 percent within the first 24 hours of operation at 600° C. This represented a loss of 25 percent of the impregnated Cr_2O_3 from the silica surface within one day. However, after 76 hours of total operation, no further Cr_2O_3 loss was detected, with the Cr_2O_3 content of the Silbond/CA remaining at 1.8 percent. By

contrast, the Cr_2O_3 content of the Chlorhydrol/CA catalyst dropped from 6.5 percent to 4.9 percent after about 92 hours of operation, showing that more deactivation time was needed for a similar 25 percent loss of impregnated Cr_2O_3 from the Al_2O_3 support. Therefore, Cr_2O_3 loss from the catalyst surface seemed to be the primary cause of deactivation of the CA-impregnated catalysts during TCE oxidation. This loss, however, was less extensive from the Al_2O_3 support than the SiO_2 based supports.

Next, the Cr-Y, the Co-Y/CA, the Cr-Y/Co and a commercial catalyst were tested for their stability during TCE oxidation at 600°C. Figure 28 shows how the TCE conversions at 275°C with these catalysts changed during the deactivation at 600°C. It seems apparent that the Cr-Y and the Cr-Y/Co with Cr as exchanged sites were more stable than the Co-Y/CA with the impregnated Cr_2O_3 sites. Conversely, the commercial Cr_2O_3 catalyst, which had Cr_2O_3 impregnated on alumina, showed good activity and was very stable (>90 percent after 400 hours of operation) during its deactivation study. Though the Co-Y/CA showed a drop in activity after about 75 hours of operation, the Cr-Y did not show any deactivation until 200 hours. After almost 300 hours of operation at 600°C, the Cr-Y still showed 70 percent TCE conversion at 275°C, while the Co-Y/CA showed only 50 percent conversion. The Cr-Y/Co showed a small decrease in activity after 125 hours of operation but maintained its stability later. Since it has been found that the Cr sites are primarily responsible for TCE oxidation, the rapid deactivation of the Co-Y/CA signified faster loss of the impregnated Cr_2O_3 sites than the exchanged Cr sites in the Cr-Y. Additional catalysts are currently being evaluated in this apparatus.

The chromia content of all the catalysts was determined using the XRF and is plotted as a function of deactivation time in Figure 29. The commercial Cr_2O_3 catalyst showed a rapid drop in its chromia content as the deactivation proceeded. Also, it had a very high initial chromia content when compared to the other catalysts. The chromia contents of the other three catalysts namely, Co-Y/CA, Cr-Y and Cr-Y/Co were constant over the period of deactivation.

2. Discussion

From the results of the Silbond/CA and Chlorhydrol/CA long term deactivation studies it was confirmed that there was definitely a loss in the chromia content of the catalyst which caused the deactivation. Also the rate of loss of chromia in the Silbond/CA was more than that in the Chlorhydrol/CA.

Both the Cr-Y and the Cr-Y/Co catalysts which had chromia in the exchanged form showed good activity and were quite stable. The Co-Y/CA catalyst showed a significant loss in activity, suggesting that there might have been a loss of the impregnated chromia. But the chromia content of this catalyst did not drop significantly. Though the commercial Cr_2O_3 catalyst showed good activity and stability, the rate of chromia loss in

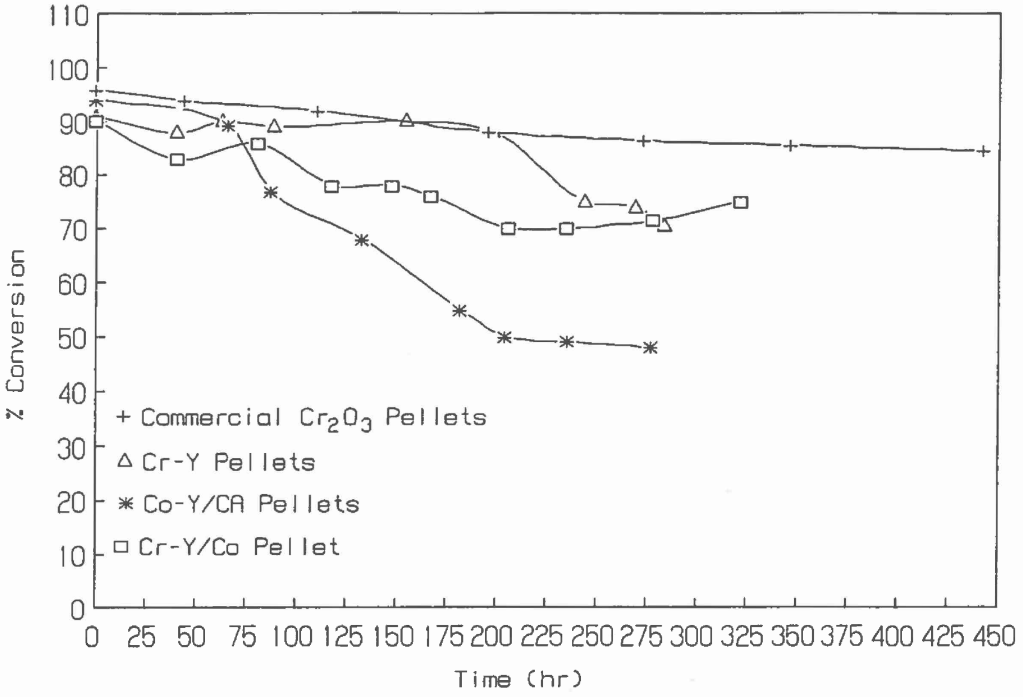

Figure 28. Stability of Catalysts for TCE Conversion at 275 C after Aging at 600 C

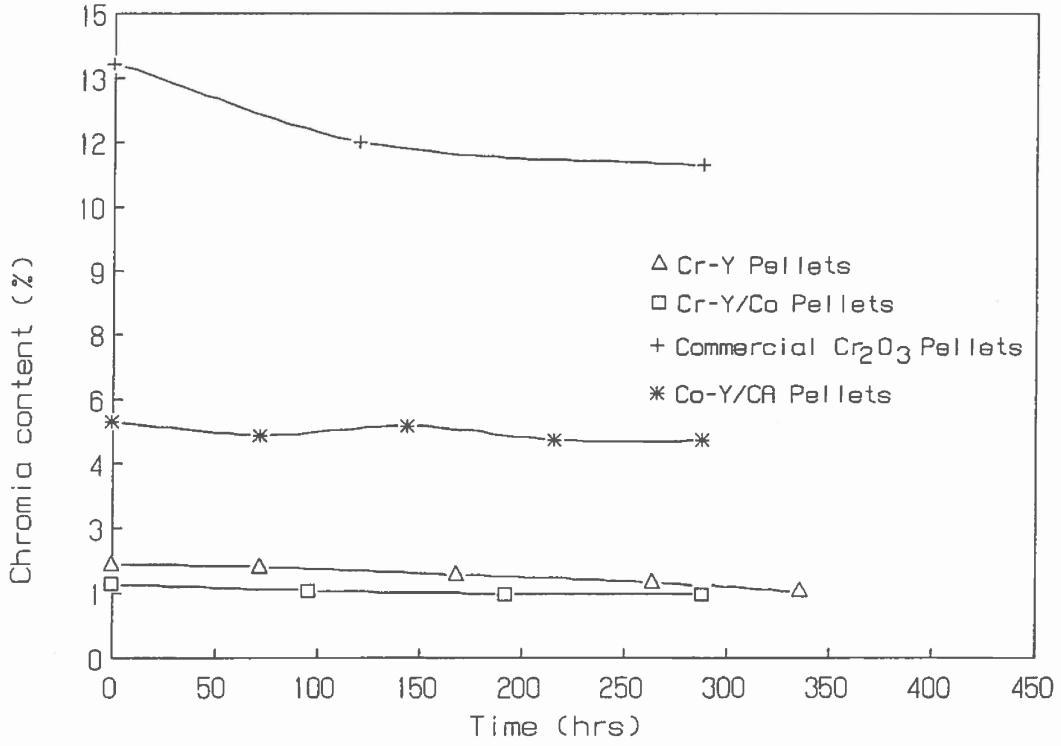

Figure 29. Chromia content of different Catalysts after Aging at 600 C

this catalyst was the most. This aided the reasoning that it was the impregnated chromia and not the exchanged chromia that was removed from the catalyst during the deactivation.

Another reason for the loss of activity in the Co-Y/CA catalyst was the fact that the crystallinity of the catalyst was reduced, resulting from the treatment of the catalyst with a highly acidic solution of chromic acid during the impregnation of chromium. Also, during the long term test, sintering of the catalyst could happen, resulting in the formation of agglomerates of chromium on the surface of the catalyst, thereby considerably reducing the dispersion of the chromium on the catalyst surface. This explains the fact that even though no loss in chromium content was observed with the Co-Y/CA catalyst, the activity of the catalyst dropped significantly.

SECTION V
CONCLUSIONS

The primary thrust of this research project has been the discovery, development and understanding of zeolite based catalysts for the oxidative destruction of halogenated VOCs.

A set of general conclusions covering the scope of our results is listed below. Detailed results may be found in appropriate sections of this report.

1. Cation exchanged/impregnated zeolites represent moderate cost, active, selective, stable catalysts for oxidative destruction of chlorinated VOCs.

2. Zeolites offer many degrees of freedom in catalyst development, including pore size, acidity, nature and levels of exchange/impregnating cations, ets.

3. The use and relative success of zeolites for a deep oxidation process (destruction of CVOCs) is novel since they are primarily employed under reducing conditions.

4. The combined process of both exchange and impregnation developed herein yields a zeolite catalyst with high activity for both single and multiple carbon CVOCs.

5. Combinations of Cr and Co cations during zeolite processing give the most stable and active catalysts for CVOC destruction.

6. Large-pore zeolites (type-Y) are preferred in this application in order to minimize diffusional limitations.

7. Total acidity and strength, as well as O_2 pickup and feed pickup of the modified zeolites, are good predictors of catalytic activity for CVOC destruction.

8. At a space velocity of $\simeq$ 2500 hr^{-1} and temperatures of about 350^{0}C, several of the developed exchanged/impregnated zeolite catalysts are capable of destroying a variety of one and two-carbon CVOCs at 98 percent or better conversion levels.

9. Under the above conditions, no detectable higher CVOC products are formed.

10. These catalysts can deactivate reversibly over time by coke formation at low temperatures, or irreversibly by loss of cation, framework crystallinity, or dispersion at higher temperatures.

11. The activity of the zeolite catalysts for coking appears to be directly related to its activity for the desired oxidation reaction.

12. In general, for the catalyst formulations studied here, the higher the CO rate of production appeared to be related to an increased deactivation rate.

SECTION VI
RECOMMENDATIONS

The end goal of this research has been to develop catalysts which are highly active, selective and stable during deep oxidation of CVOCs. To that end we have investigated the use of modified zeolites (exchanged and impregnated) as catalysts, and have produced several low cost highly active candidates.

It is recommended that investigation of these zeolite catalysts continue in three specific areas: catalyst stability, selectivity and toxicity.

Stability at high temperature needs improvement in order to minimize loss of activity with time. This can most likely be brought about by modifying catalyst preparation techniques or choosing an alternate cation.

Selectivity of Cr-containing catalysts shows some product tendency towards CO and Cl_2 which should be minimized. Addition of co-catalysts (other cations or transition metal oxides) may be the best technique for adding alternate sites to the catalyst surface.

The toxicity of chromium as a waste material is sufficiently high as to make it of some concern for safe disposal of spent catalyst. A substitute for chromium or at least a means of significantly reducing Cr content should be further investigated.

It is further recommended that the most promising catalysts developed during this research be tested in the field under prototype conditions using vapors from an actual CVOC contaminated ground water source as a feed. Both short term (2 days) and long term (2 months) tests for catalyst activity, selectivity and stability should be undertaken at that time.

REFERENCES

1. Bond, G. C. and Sadeghi, N., "Catalyzed Destruction of Chlorinated Hydrocarbons," J. Appl. Chem. Biotechnol. 25, 241 (1975).

2. Gonzales, R. D. and Nagai, M., "Oxidation of Ethanol on Silica Supported Noble Metal and Bimetallic Catalysts," Appl. Catal. 18, 57 (1985).

3. Cullis, C. F. and Williatt, B. M., "Oxidation of Methane over Supported Precious Metal Catalysts," J. Catal. 83, 267 (1983).

4. Natsukawa, K. and Yasuda, K., "Oxidation of Organic Solvent Vapors on Pt-Catalysts Contaminated with Paint Components," Atmos. Environ. 13, 335, Environ. Prot. Eng. 10, (1979).

5. Mendyka, B. and Rutkowski, J. D., "Study of Effect of Hydrochloric Acid on the Activity of Platinum Catalysts," Environ. Prot. Eng. 10, 5 (1984).

6. Pallazolo, M. A., Steinmetz, J. I., Lewis, D. L. and Beltz, J. F., "Parametric Evaluation of Volatile Organic Compounds-Hazardous/Toxic Air Pollutants Destruction via Catalytic Incineration," EPA-600/2-85-041, NTIS No. PB85-191187, April 1985.

7. Tichenor, B. A., and Pallazolo, M. A., in "AIChE 1985 Annual Meeting, November 10-15, 1985", Paper No. 496.

8. Pallazolo, M. A., Jamgochian, C. L., Steinmetz, J. I. and Lewis, D. L., "Destruction of Chlorinated Hydrocarbons by Catalytic Oxidation," EPA-600/2-86-079, NTIS No. PB87-1011234/GAR, September 1986.

9. Spivey, J. J., "Complete Catalytic Oxidation of Volatile Organics," Ind. Eng. Chem. Res. 26, 2165 (1987).

10. Manning, M. P., "Fluid Bed Catalytic Oxidation: An Undeveloped Hazardous Waste Disposal Technology," Hazard. Waste 1(1), 41 (1984).

11. Weldon, J. and Senkan, S. M., "Catalytic Oxidation of Volatile Organics," Combust. Sci. Technol. 47, 229 (1986).

12. Danals, R., "Reaction Mechanisms of Chlorinated Methanes over KCl/V_2O_5 Catalyst," M. S. thesis, University of Akron, 1989.

13. Mugalinskii, F. F., Guseinzade, E. M. and Mamedov, B. P., "Problem of Complete Oxidation During Oxidative Chlorination," Oxid. Commun. 7(34), 235(1984).

14. Golodets, G. I. ,"Heterogeneous Catalytic Reactions Involving Molecular Oxygen", Elsevier, Amsterdam/New York, 1983.

15. Guisnet, M., Gnep, W. S., Bearez, C. and Chevalier, F., "Catalysis by Zeolites"(B. Imelik et al., Eds.), p. 77, Amsterdam, 1980.

16. Mochida, I., Hayata, S., Kato, A. and Seiyama, T., "Catalytic Oxidation over Molecular Sieves Ion Exchanged with Transition Metal Ions in the Oxidation of Propylene and Ethylene," J. Catal. 23, 31(1971).

17. Gentry, S. J., Rudham, R. and Sanders, M. K., "The Catalytic Properties of Zeolites Containing Transition Metal Ions. III. Propylene Oxidation," J. Catal. 35, 376(1974).

18. Suzuki, M., Tsutsumi, K., Takahashi, H. and Saito, Y., "Activity of Highly Dispersed Transition Metal Oxides Formed in Y-Zeolites for Toluene Oxidation," Zeolites, 8, 387(1988).

19. Park, S. and Lunsford, J. H., "Oxidation of 2-Propanol over Cobalt-Y Zeolites," Inorg. Chem. 26, 1993(1987).

20. Lee, H. and Kevan, L., "Catalytic Oxidation of Propylene on Cu(II) Location (M)X and Y Type Zeolites Where M=Na, K, Ti and Ca: Observation of Cu(II) Migration by Electron Spin Resonance During Reaction," J. Phys. Chem. 90, 5781(1986).

21. Tsuruya, S., Tsukamoto, M., Watanabe, M. and Masai, M., "Ethanol Oxidation over Y-Type Zeolite Ion-Exchanged with Copper(II) and Cobalt(II) Ions," J. Catal. 93, 303(1985).

22. Aparicio, L. M., Ulla, M. A., Millman, W. S. and Dumesic, J. A., "Characterization and Catalytic Studies of Y-Zeolites Co-Exchanged with Iron and a Second Polyvalent Cation," J. Catal. 110, 330(1988).

23. Kubo, T., Tominaga, H. and Kunugi, T., "Oxidation of Carbon Monoxide over Transition Metal Ion-Zeolite Catalysts," Bull. Chem. Soc. Jpn. 46, 3549(1973).

24. Wolford, T. L., "Selective Conversion of Chlorinated Alkanes to Hydrogen Chloride and Carbon Dioxide," United States Patent 4,423,024(1983).

25. Johnston, E. I., "Low Temperature Catalytic Oxidation of Chlorinated Compounds to Recover Chlorine Values using Chromium-Impregnated Supported Catalysts," United States Patent 3,989,807(1976).

26. Chatterjee, S. and Greene, H. L., "Oxidative Catalysis of Chlorinated Hydrocarbons by Metal-Loaded Acid Catalysts," J. Catal. 130, 76 (1991).

27. Chatterjee, S., Greene, H. L. and Park,Y. J., "Comparison of Modified Transition Metal Exchanged Zeolite Catalysts for Oxidation of Chlorinated Hydrocarbons," J. Catal., 138, 179 (1992).

28. Chatterjee, S., Greene, H. L., "Effects of Catalyst Composition on Dual Site Zeolite Catalysts used in Chlorinated Hydrocarbon Oxidation," has been accepted, J. Applied Catal.

29. Chatterjee, S., Greene, H. L. and Park, Y. J., "Deactivation of Metal Exchanged Zeolite Catalysts during Exposure to Chlorinated Hydrocarbons under Oxidizing Conditions," Catalysis Today, 11, 569(1992).

30. "Ion Exchange and Metal-Loading Procedure", Linde Molecular Sieves Catalyst Bulletin, 1988.

31. Desai, F., "Catalytic Oxidation of the Pyrolysis Products of Polystyrene-Based Ion Exchange Resins," M. S. thesis, University of Akron, 1985.

32. Wichterlova, B., Jiru, P. and Beran, S., "Chromium Ions within Zeolites. Part I. Infrared, Electron Spin Resonance and Temperature-Programmed Reduction Studies of the Valence States of Chromium Ions," J. Chem. Soc., Faraday Trans. 1, vol. 79, pp 1573(1983).

33. Tempere, J. F., Bozon-Verduraz, F., Delafosse, D. and Cornu, O., "A Kinetic Study of the Oxidation of Cerium Ions in an X Zeolite," Mat. Res. Bull. 12, 871(1977).

34. Bailar, J. C., et al., Eds.,"Comprehensive Inorganic Chemistry", Vol. 4, Pergamon, Elmsford, NY, 1973.

35. Lee, E. F. T. and Rees, L. V. C., "Calcination of Cerium(III) Exchanged Y Zeolite," Zeolites, 7, 446(1987).

36. Jerocki, B., Golebiowski, S., Grochowska, M., Hofman, L. and Rutkowska, M., "Catalytic Activity of Molecular Sieves," Int. Chem. Eng. 13(2), 201(1973).

37. Mortier, W. J., "Zeolite Electronegativity Related to Physicochemical Properties," J. Catal. 55, 138(1978).

38. Petunchi, J. O. and Hall, W. K., "Studies of a CuY Zeolite as a Redox Catalyst," J. Catal. 80, 403(1983).

39. Breck, D. W.,"Zeolite Molecular Sieves", Wiley-Interscience, New York, 1974.

40. Chu, C. T-W., and Chang, C. D., "Isomorphous Substituion in Zeolite Frameworks. 1. Acidity of Surface Hydroxyls in [B]-, [Fe]-, [Ga]- and [Al]-ZSM-5," J. Phys. Chem., 89, 1569 (1985).

41. Dzwigaj, S., Haber, J., and Romotowski, T., "IR Study of Acid Centers in Type NaM-Y Zeolites (M=H, Mg, Co)," Zeolites, 3, 134 (1983).

42. Noller, H., and Vinek, H., "Coordination Chemical Approach to Catalytic Oxidation Reactions," J. Mol. Catal., 51, 285 (1989).

43. Weast, R. C., et al., Eds., "CRC Handbook of Chemistry and Physics," 66th Edition, CRC Press, Inc., Boca Raton, 1986.

44. Bose, D., and Senkan, S. M., "On the Combustion of Chlorinated Hydrocarbons. 1. Trichloroethylene," Combust. Sci. Technol., 35, 187 (1983).

45. Rao, M. B., and Jenkins, R. G., "Molecular Dimensions and Kinetic Diameter for Diffusion for Various Species," Carbon, 25(3), 445 (1987).

46. Mourits, F. M., and Rummens, F. H. A., "A Critical Evaluation of Lennard-Jones and Stockmayer Potential Parameters and of some Correlation Methods," Can. J. Chem., 55, 3007 (1977).

47. Fevrier, D., Mignon, P., and Vernet, J. L., "Reactivity of Some Halogenated Alkanes on 13X Molecular Sieve," J. Catal., 50, 390 (1977).

48. Poutsma, M. L., in "Zeolite Chemistry and Catalysis", ACS Monograph 171 (Ed: Rabo, J. A.), 1976.

49. Kiselev, V. F. and Krylov, O. V., in "Adsorption and Catalysis on Transition Metals and Their Oxides", Springer-Verlag, 1989.

50. Ward, J. W., "The Nature of Active Sites on Zeolites. XII. The Acidity and Catalytic Activity of Transition Metal Y Zeolites," J. Catal. 22, 237 (1971).

51. Dimitrov, Kh, Tabet, M. and Bezukhanova, Ts., "Catalytic Activity regarding Toluene Conversion of Zeolites containing Hydrogen," Dokl. Bolg. Akad. Nauk 33(6), 795 (1980).

52. Pietri De Garcia, E., Goldwasser, M. R., Parra, C. F. and Leal, O., "Oxidative Dehydrogenation of Cyclohexane over Cobalt-Exchanged Y-Zeolites," Appl. Catal. 50(1), 55 (1989).

53. Aparicio, L. M. and Dumesic, J. A., "Kinetic Modeling Studies of Transition Metal-Exchanged Zeolites as Catalysts for Redox Reactions," J. Mol. Catal. 49(2), 205 (1989).

54. Garten, R. L., Delgass, W. N. and Boudart, M., "A Mössbauer Spectroscopic Study of the Reversible Oxidation of Ferrous Ions in Y Zeolite," J. Catal. 18, 90 (1970).

55. Chatterjee, S. and Greene, H. L., "An Investigation of the Effects of the Acidic Nature of Impregnation Solutions on the Properties of VOC Oxidation Catalysts," submitted to Ind. Eng. Chem. Res., (1992).

56. Derouane, E. G., in "Catalysis by Acids and Bases" (B. Imelik, et al. Eds.), Studies in Surface Science and Catalysis, vol. 20, Elsevier, Amsterdam, 1985, pp. 221.

57. Guisnet, M., Magnoux, P. and Canaff, C., in "Chemical Reactions in Organic and Inorganic Constrained Systems" (R. Setton, Ed.), NATO Series C 165, Reidel, Dordrecht, 1986, pp. 131.

58. Guisnet, M., Magnoux, P. and Canaff, C., in "New Developments in Zeolite Science Technology", Proceedings, 7th International Zeolite Conference (Y. Murakami, et al. Eds.), Kodansha Ltd., Tokyo, 1986, pp. 701.

59. Magnoux, P., Cartraud, P., Miguard, S. and Guisnet, M., "Coking, Aging and Regeneration of Zeolites. II. Deactivation of HY Zeolite during n-Heptane Cracking," J. Catal., 106 (1987) 235.

60. Ghosh, A. K. and Kydd, R. A., "A Fourier-Transform Infrared Spectral Study of Propene Reactions on Acidic Zeolites," J. Catal., 100 (1986) 185.

61. Hughes, R., "Deactivation of Catalysts", Academic Press Inc. (London) Ltd., 1984.

62. Magnoux, P. and Guisnet, M., "Coking, Aging and Regeneration of Zeolites. VI. Comparison of the Rates of Coke Oxidation of HY, H-Mordenite and HZSM-5," Appl. Catal., 38 (1988) 341.

63. Bell, A. T., in "Catalyst Deactivation" (Petersen, E. E. and Bell, A. T. Eds.), Chemical Industries, vol. 30, Marcel Dekker, Inc., New York, 1987, pp. 235.

64. Greene, H L. and Chatterjee, S. U. S. Patent (Pending).